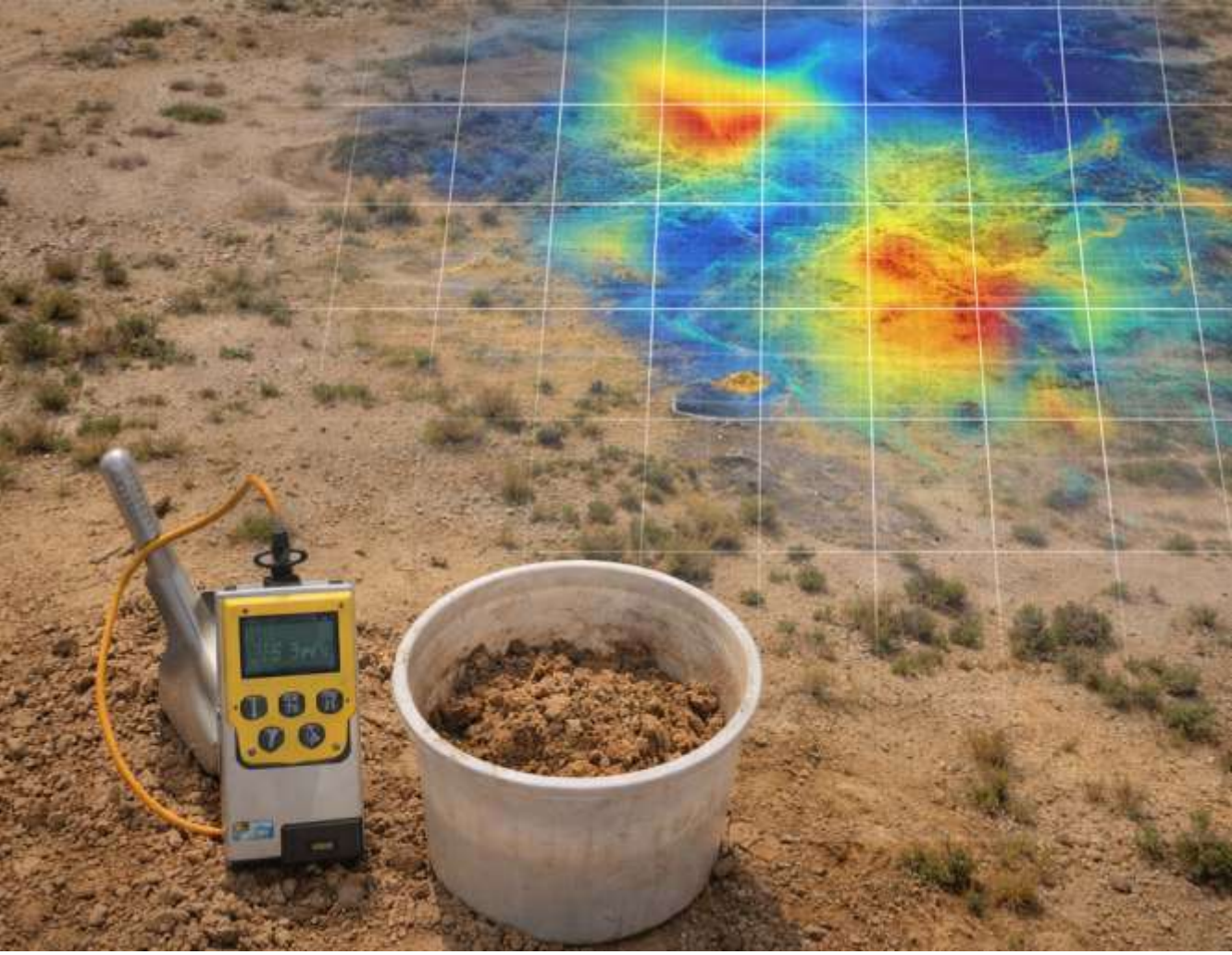

Natural Radionuclide Distribution Mapping in Soils

A Case Study of Al-Najaf and Kufa Regions in Iraq

Lubna Abdulrasool Mahdi Al-Asadi
Ali Abid Abojassim Al-Hamidawi

DeepScience

Natural Radionuclide Distribution Mapping in Soils: A Case Study of Al-Najaf and Kufa Regions in Iraq

Lubna Abdulrasool Mahdi Al-Asadi

University of Kufa, Faculty of Science, Department of Physics, Al-Najaf, Iraq

Ali Abid Abojassim Al-Hamidawi

University of Kufa, Faculty of Science, Department of Physics, Al-Najaf, Iraq

DeepScience

Published, marketed, and distributed by:

Deep Science Publishing, 2026
USA | UK | India | Turkey
Reg. No. MH-33-0658412
www.deepscienceresearch.com
editor@deepscienceresearch.com
WhatsApp: +91 7977171947

ISBN: 978-93-7185-020-9

E-ISBN: 978-93-7185-213-5

https://doi.org/10.70593/978-93-7185-213-5

Citation: Al-Asadi, L. A. M. & Al-Hamidawi, A. A. A. (2026). *Natural Radionuclide Distribution Mapping in Soils: A Case Study of Al-Najaf and Kufa Regions in Iraq*. Deep Science Publishing. https://doi.org/10.70593/978-93-7185-213-5

TABLE OF CONTENTS

PREFACE

The radiological properties of soils represent an important factor for the investigation of the natural background radiation and possible environmental and health hazards. Soils play a role as the main reservoir of naturally-occurring radionuclides, such as uranium (U), thorium (Th), potassium (K) and radium, & their progeny, which are responsible for the external and internal exposure to radiation. The spatial distribution of these radionuclides is not identical, being significantly influenced by geological formations, soil type, and environmental characteristics, so radiological mapping becomes a very important tool regarding environmental characterization and radiation protection.

In this book, a part is dedicated to the principles, methods, and practice of radiologic mapping of soil in limited regions. It gives a round-up of the state-of-knowledge on specific aspects of soil radionuclide transfer following accidents, such as dynamic approaches to model soil transfer both in real and laboratory conditions, data analysis methods used in investigating soil radioactivity, and dynamic model testing. The focus has been on the linking of specific radiological measurements with geospatial devices, primarily Geographic Information Systems (GIS), to allow visualization and interpretation of the spatial distribution of radionuclides and their associated radiological hazards.

The motivation for this research comes from a rising demand of good baseline data on soil radioactivity, particularly in places with limited environmental monitoring infrastructure. Not only do they represent an added value to the scientific knowledge of natural radiation, but a useful tool for environmental management, territorial planning, and public health decision making. Such maps are important for characterization of the high-radiation areas as well as providing guidelines on possible risks to the population and non-human biota.

The intended book users of the present work are researchers, environmental scientists, health physicists, geologists, and post graduate student in the fields of environmental radioactivity and spatial analysis. It will also be useful as a guide for regulatory bodies and radiation monitoring professionals dealing with environmental protection. On the other hand, in terms of practical contribution, it is hoped that by integrating theory with practice-based case studies, this paper will also help promote the development of radiological assessment and the usage of soil mapping as a tool for environmental safety and sustainable development.

ABSTRACT

The present study aims at measuring the natural radioactivity of background radiation (Dose rate), gamma emitters (Uranium-238, Uranium-235, Thorium-232, and Potassium-40), and alpha emitters (Radon-222, Radium-226, and Uranium-238) in soil samples collected from two cities, Najaf and Kufa at Al-Najaf governorate. Many techniques have been used, such as Alert INSPECTOR Dosimeter, gamma-ray spectroscopy with NaI(Tl) its dimension 3"× 3", CR-39 of TASTRAK analysis system, and RAD-7 detector, as well as radiological hazard index due to gamma and alpha emitters of samples, are determined. Then, the Geographic Information System (GIS) technique is used to map most main results.

The results using the dosimeter are shown that the average value of Dose rate (D), Annual Average Effective Dose (AAED), and Excess Lifetime Cancer Risk (ELCR) due to the natural background in soil samples for Kufa city are 0.127±0.005 μSv/h, 1.12±0.04 mSv/y and (3.90±0.15) $\times 10^{-3}$, respectively. While, the average values of D, AAED, and ELCR for Najaf city are 0.121±0.004 μSv/h, 1.06±0.03 mSv/y, and 3.73±0.12, respectively.

The results using NaI(Tl) detector are shown that the average value of specific activity in Kufa city for (^{238}U, ^{235}U, ^{232}Th, ^{40}K) are 6.2±0.74 Bq/kg, 278.10±19.43 Bq/kg, 6.41±0.82 Bq/kg, and 278.10±19.43 Bq/kg, respectively. While, the average value of specific activity in Najaf city for (^{238}U, ^{235}U, ^{232}Th, ^{40}K) are 18.01±1.24 Bq/kg, 0.83±0.44 Bq/kg, 13.36±0.91 Bq/kg, and 256.86±12.23 Bq/kg, respectively.

The results using the CR-39 detector are shown that the average value of the radon concentration in the tube's airspace (C), the radon concentration in the sample (C_{Rn}), The radium content in the sample (C_{Ra}), and uranium concentrations (C_U) for Kufa city are 14.1±1 Bq/m^3, 895 ± 74 Bq/m^3, 0.028±0.008 Bq/kg, and 0.048±0.008 ppm, respectively. While, the average value of the C, C_{Rn}, C_{Ra}, and C_U for Najaf city are 16.10±3.166 Bq/m^3, 684.92± 140.5 Bq/m^3, 0.029±0.0058 Bq/kg, and 0.036±0.0072 ppm, respectively.

It is found that the highest values of D and AAED due to background radiation in all samples under study are lower than the average worldwide limits of 0.247 μSv/hr and 2.4 mSv/y according to UNSCEAR 2008, respectively. As well as, the specific activity of ^{238}U, ^{232}Th, and ^{40}K are lower than worldwide according to UNSCEAR 2008, except some samples have ^{40}K larger than worldwide. In comparison, the results of alpha emitters in all present study samples are less than the world average levels. At the same time, all radiological parameters due to gamma emitters in most samples in Kufa and Najaf cities are within possible limit according to the radiation protection report UNSCEAR2000, UNSCEAR2008, OECD and ICRP1993. On other hand, the radiological parameters due to alpha emitters in all samples in Kufa and Najaf city, are within possible limit.

Next step, many correlations between detectors are made between three techniques for all areas under study (Kufa and Najaf): first dosimeter and NaI (Tl) detectors, second NaI (Tl),

and CR-39 detectors, and third CR-39 with RAD-7 detectors. The study has proved a high correlation factor for all the present study samples. This is evidence that the soil samples under study are original and affected by Goegical area and filtration. Thus the correct sequence of the uranium-238 basket can be achieved. Also, a good association between the Uranium-238 and Radon -222 would be considered statistically significant, but there is a weak association for all sites in the present study between radon-222 with thorium-232 and potassium-40; no one found the relation between radon-222 with thorium-232 series inside and potassium-40 from another side. Also, a good relationship between passive and active techniques.

At last, the study results are safe compared with the permissible values globally, except for some area that needs future studies.

Keywords : Soil, Radioactive nuclide, Dosimeter, NaI(Th), CR-39, Radiological Risks, Kufa, Najaf.

INTRODUCTION

Living kinds are faced radiation both from natural and artificial sources. Nature participates in about 82 percent. As for the industrial, medical, and consumer sources, the participation reaches 18 percent[1]. The earth is constantly influenced by ionizing radiation from outer space. This is called cosmic radiation. This radiation and others from similar sources contribute to what is known as background radiation [2]. The terrestrial nuclides include natural series and non-series such as uranium, thorium, actinium, and potassium. In the environment, Natural radionuclides are found in all elements in relying amounts. They exist in the water, air, animal and vegetarian food, soil, and the human body [3]. (NCRP) and (UNSCEAR) posted in a letter referenced by their, "the most important source of radiation exposure is natural radiation in the environment "[4]. Humans are exposed to significant levels of inside and outside radiation daily without being aware of it.

Radionuclides enter the human body by ingesting contaminated water and food, as well as inhaling polluted air. It may also enter via wounding [3]. Either outside exposure comes from human contact with contaminated soil and air. Gamma-ray and radon are the most dangerous elements in nature, and it poses a threat to the ecological balance and human health[5]. The dangers of human exposure to radioactive nuclides and toxic elements come from ingestion and inhalation. Exposure to high levels of radiation could reason actual damage to the human body and can cause death. Al-Najaf governorate as decoration of Iraq has craved desirable environmental promiscuity to save of the Golf wars took place on it, exceptionally Separation wars I and II in distinction 1990 and 2003[6]. The uranium enters the construct of the atomic weapons, and weapons of gather nullification are used in these wars.

Uranium and its progeny have a repulsive effect on familiar people, which is classified as a hazard in this way. Soil is considered an essential and necessary primary resource for life and food production. The existence of natural radioactivity in soil results in inside and outside exposure to humans [7]. Natural radioactive materials stand for the largest donating of radiation doses received by human beings, where the natural radioactivity is found in almost all soil types of although the concentrations vary greatly [4]. Therefore, the study of radionuclides in soil samples becomes very important due to their radiological hazards on the humans. The motivation of the thesis is to measure and draw maps of natural radioactivity for background radiation, gamma and alpha emitters in soil samples collected from Najaf and Kufa cities, Al-Najaf governorate, Iraq. These samples are measured using different nuclear techniques that

available in nuclear laboratory such as dosimeter, NaI(Tl), SSNTD (CR-39), and RAD-7 detector.

1.1 The Basic Theory of Radioactivity

The radioactive elements that can be found in nature are classed as cosmogenic or terrestrial[8]. Radioactivity is a process in which atoms release small, energetic particles or waves during a breakup. Radiation occurs when an atom decays or is fusing, when a chemical reaction occurs, when hot objects are ignited, and when gases are excited by an electric current.

In addition to the common forms of radiation we encounter in our bodies, such as ^{14}C and ^{40}K, several processes can cause them to emit radiation[9]. Radiation sources include natural and manufactured sources.

1.1.1 Natural Radioactive Sources

There are three types of natural radioactive sources which are cosmic radiation, Terrestrial Radiation, and Internal Radiation. Cosmic radiation is made out of incredibly high-energy particles (up to 1018 eV) and is, for the most part, protons (87%), with some bigger particles (alpha radiation 13%). A vast level of it originates from the outside of our solar system and is saved all through space. A portion of the essential, enormous radiation evolves from our sun, created amid sun-based flares [10]. The truth is that the nuclear weapons and nuclear power industries contribute less than 0.3% to our population's radiation exposure, in addition to medical and consumer products that contain manufactured radiation (e.g., X-rays, T.V.s, smoke detectors, etc.).A constant background of natural radiation is continuously emitted into the population; on average, natural radiation is the most significant risk to humans. Natural sources of background radiation can be categorized into four major categories: radionuclides, cosmic rays, and terrestrial and internal sources [11].

1.2.2 Manufactured Radiation Sources

The most critical source of artificial radiation exposure to the overall population is from therapeutic methodology by a wide margin, for example, indicative X-rays, nuclear drugs, and radiation treatment. Individuals in the open are exposed to radiation from shopper items, for example, tobacco (polonium ^{210}Po), building materials, burnable powers (gas, coal), ophthalmic glass, T.V.s, iridescent watches and dials (tritium), air terminal X-rays frameworks, smoke indicators (americium), street development materials,

electron tubes, fluorescent light starters, lamp mantles (thorium), and so on[12]. People who occupationally exposed in different ways depending on their jobs and the sources in the place which they work. Dosimeters, pocket-sized equipment that quantifies radiation exposure, are used to carefully monitor these people's exposure to radiation[13][14].

1.3 Radioactivity in Soil

On a universal scale, radionuclide elements play essential roles. These elements are present in the atmosphere, water, plants, and soil and, in different ways, contaminate the environment—relationships between three main components: water, vegetation, and dirt. Figure (1.1) outlines the process of radionuclides being incorporated into the soil until humans finally absorb them. During fallout times when cows graze and eat grass from the pasture, the most severe contamination occurs [15].

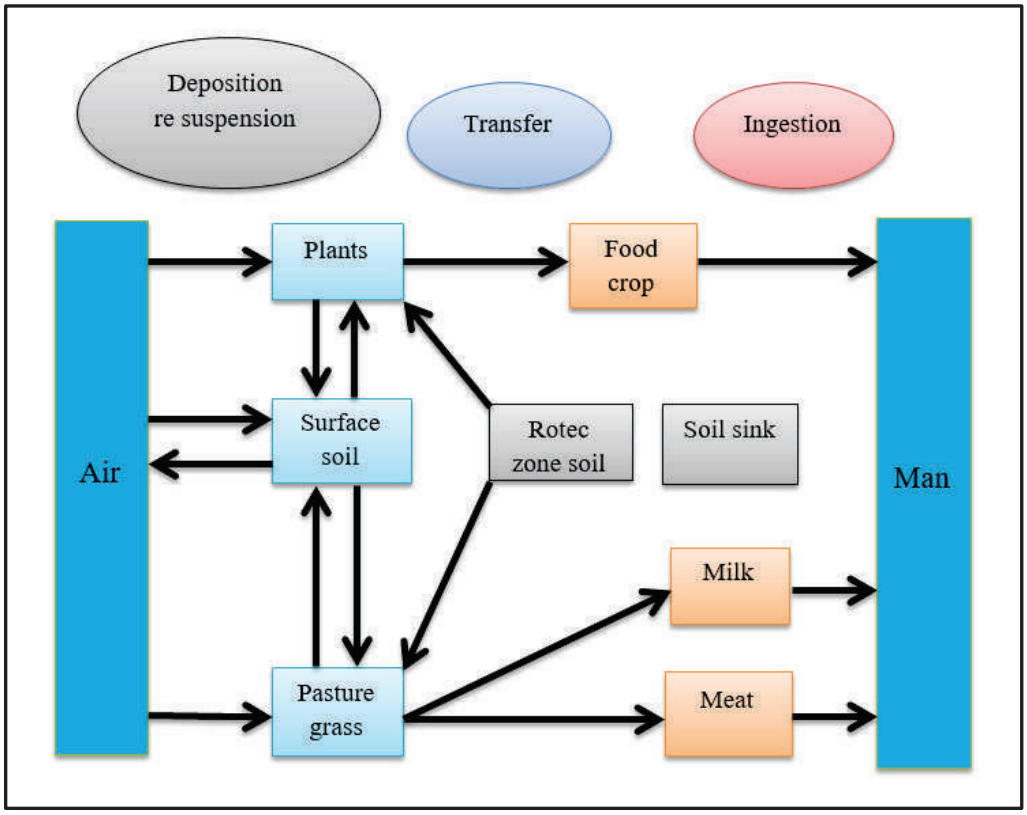

Figure (1.1): A typical collection of routes created by a radiation source exposed to the air as it passes through the environment[15].

The average international inside dose from radionuclides (other than radon and its decay products) is 0.29 mSv, with 0.17 mSv from ^{40}K and 0.12 mSv from the ^{238}U and ^{232}Th series and 12 mSv from ^{14}C[16].

Cosmic rays and terrestrial gamma rays are the two significant natural sources of outside radiation exposure to humans. Terrestrial gamma rays are basically due to radionuclides related to uranium, thorium series, and singly occurring potassium in the earth's crust. The distributions of ^{238}U, ^{226}Ra, ^{232}Th, and ^{40}K in soils are influenced by the radionuclide distribution in the rocks from which they originate, as well as the ways that concentrate the soil. The most important source of terrestrial gamma radiation levels is soil, as it contains trace amounts of terrestrial radionuclides, the concentrations determined by the geology of each place throughout the world [17].

It represents the center of all the different organisms of plants, microbes, and animals, which is undoubtedly an essential feature. Whenever food is produced, the soil is a vital part of the process; therefore, any effect on the soil, harmful to the soil, or pollution of the soil impacts all of the life connected to it and the human who lives on it [18]. Soil is composed of minerals and organic matter, water, and air arranged in a complex physical and chemical system to provide plants with a mechanical foothold and meet their nutritional requirements[19]. Normal movement in the convergence of ^{40}K, ^{238}U, and ^{232}Th in different sorts of soil and evaluated consumed portion in the air (1 m) over topsoil, Table (1.1) [20].

Table (1.1): Average activity concentrations of, ^{238}U, ^{232}Th and ^{40}K in different types of soil and estimated absorbed dose [20].

Type of soil	Average Activity Concentration (pCi g^{-1})			Absorbed dose rate in air (μrad h^{-1})
	^{40}K	^{238}U	^{232}Th	
Serozem	18	0.85	1.3	7.4
Gray - brown	19	0.75	1.1	6.9
Chestnut	15	0.72	1.0	6.0
Chernozem	11	0.58	0.97	5.1
Gray forest	10	0.48	0.72	4.1
Sodpozolic	8.1	0.41	0.60	3.4
Podzlic	4.0	0.24	0.33	1.8
Boggy	2.4	0.17	0.17	1.1
World average	10	0.7	0.7	4.6
Typical range	3-20	0.3-1.4	0.2-1.3	1.4-9

1.4 Geographic Information System

A geographic information system (GIS) is a computer program that captures, stores, queries, analyzes and displays large datasets. The spatial analysis describes the location and the characteristics of spatial features. A geographic information system (GIS) comprises technology, software, data, people, and an organization. GIS grew in popularity in the 1980s, thanks to the introduction of personal computers (PCs) and graphical user interfaces. GIS is necessary for many industries, including resource management, emergency planning, criminal analysis, public health, land records management, precision farming, and many others [21].

From a software perspective, a GIS is a computer program capable of storing, editing, processing, and displaying maps using geographic data and information. Environmental

Systems Research Institute is among GIS software providers. Regardless of manufacturer, all GIS software includes a database management system that can handle and integrate two types of data: geographical and attribute data. A computer, memory, storage devices, scanners, printers, Global Positioning System (GPS) units, and other physical components make up a GIS' hardware. Assume the machine is connected to a network. In such an instance, the network can be clarified as an essential part of the GIS because it allows us to share data and information that the GIS consumes as inputs and produces as outputs [22]. Flowchart below describes the composition of the GIS system [23].

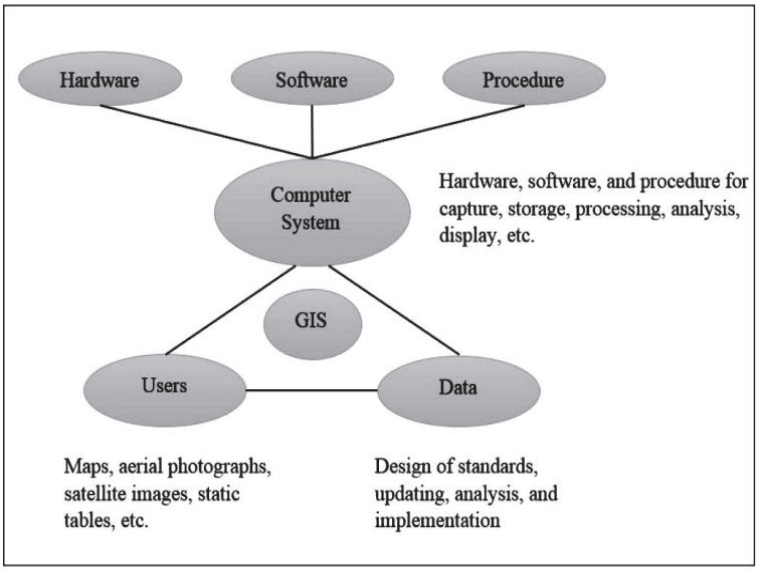

Figure (1.2): Component of GIS system [23]

1.5 Review of Previous Studies

Literature surveys are classified into four types according to the technique used to measure natural radioactivity as follows:

1.5.1 Previous Studies of NaI(Tl)

No.	Author, Year, and Reference	Country	Results
1	H. Mutuk & et.al,2013 [24]	Turkey (Bafra Kizilirmak Delta)	The average of activity concentrations of ^{238}U, ^{232}Th, and ^{40}K are (37.2+2.8, 33.7+3.1, and 413.0+59.8) Bq/kg, respectively.
2	B.A.Almayahi & et.al , 2014 [25]	Iraq (Najaf/Najaf sea)	The mean specific activity of radionuclides are within (IAEA) except two samples.
3	L. A. Najam & et.al ,2015[26]	Iraq (Mosul/Nineveh)	The results ^{226}Ra, ^{214}Pb, ^{232}Th and ^{40}K ranged from 17.02 to 40.98 Bq/kg, 8.46 to 16.00 Bq/kg , 11.22 to 32.65 Bq/kg and from 206.51 to 509.56 Bq/kg, respectively.
4	L. Sahin & et.al,2016[27]	Turkey (Kütahya)	The results obtained are compared within the limits of values obtained in other cities of Turkey.
5	R. L. Njinga &et.al,2016[28]	South Africa (Tudor Shaft mine environs)	The average activities of three nuclides are 271.96 ± 3.59 Bq/ kg, 47.65 ± 3.69 Bq/kg, and 87.17 ± 5.19 Bq/kg, respectively.
6	I. H. Kadhim &et.al2016[29]	Iraq (Karbala/ Touirij region)	The average activity potassium (245.1),Uranium (30.96-5.86) Bq/Kg (19.45)Bq/Kg, and thorium (24.47) Bq/Kg.
7	A. manjeet &et.al2017[30]	India (Panipat city)	The activity concentrations are for Uranium (14.82 ± 0.26 -42.82 ± 0.84 Bq/kg), Thorium (12.94 ± 0.32 - 43.48 ± 0.96 Bq/kg), and potassium (238.05 ± 0.28 - 348.50 ± 0.95 Bq/kg).
8	E. F. Salman &et.al2019[31]	Iraq (Babylon Governorate)	The results of ^{238}U, ^{232}Th, ^{235}U and ^{40}K are all within international limit
9	A. A. Ibraheem &et.al2018[32]	Saudi Arabia (Asir region)	Average activity for ^{226}Ra, ^{232}Th and ^{40}K in range of 38.2 ± 0.1–44.1 ± 0.1, 23.49 ± 0.20–41.9 ± 0.2 and from 182.5 ± 1.0 to 251.5 ± 1.3 Bq Kg^{-1} respectively.
10	B. Lyngkhoi et.al2018[33]	India (District of Megha-laya)	AEDE (outdoor) is 80.0 μSv y^{-1}. The average AGDE is found to be 429.8 μSv y^{-1}. ELCR is 0.280 × 10^{-3}
11	M. K. Muttaleb et.al2018[34]	Iraq (Maysan)	(D_r), (R_{eq}), (E_{eff}), (AEDE), (ELCR), (I_γ), and (H_{ex}) and (H_{in}) hazard indices are calculated. Which is located within limits allowed by the (IAEA).
12	A.M. Al-Qararaha et.al 2019[35]	Jordan (Tafila governorate)	The average concentrations of ^{238}U, ^{226}Ra, ^{232}Th, ^{40}K and ^{137}Cs are 23.6 ± 3.1, 23.3 ± 0.7, 16.7 ± 1.0, 234.1 ± 9.85 and 5.4 ± 0.3 Bq kg^{-1}, respectively.
13	O.A. Oyebanjo et.al2019[36]	Nigeria (Ikorodu metropolis)	Activity concentration for ^{40}K, ^{238}U and ^{232}Th in soil samples ranged from 14.84±1.07 $BqKg^{-1}$ to 82.01±5.54 $BqKg^{-1}$, 0.029±0.05 $BqKg^{-1}$ to 7.65±0.9 $BqKg^{-1}$ and 1.68±0.14 $BqKg^{-1}$ to 3.93±0.28 $BqKg^{-1}$.

14	S. R. Yousif et.al2019[37]	Iraq (Badra Oil Field Project)	The averages of specific activity for ^{238}U, ^{232}Th and ^{40}K are 24.7 Bq/kg, 13.6 Bq/kg and 538.9 Bq/kg respectively.
15	N. Maden et.al2020[38]	Turkey (Gümüşhane)	(AEDE), (H_{in}, H_{ex}) and (ELCR) uranium, thorium and potassium are estimated.
16	E.Pudjadi et.al2020[39]	Indonesia (Botteng Utara village area)	This present work shows that area under study has high background radiation exposure from primordial radionuclides activity.
17	C.C. Mbonu et.al2020[40]	Nigeria (Orlu, Imo State)	The study shows that the regions under study are relatively safe for human live.
18	M. Zubair et.al2020[41]	India (Sijua Dhanbad)	The computed values are deemed to be safe for the environment and public health in the study area because they are substantially below the 1 mSv. y^{-1} limit.
19	L. A. Najam et.al2020[42]	Iraq (Ancient Mosul)	The specific activities of three radionuclides are compared with those reported from other countries and worldwide on average.
20	P. Lamichhane et.al2021[43]	Nepal (Kathmandu valley)	The overall findings indicate no radiological threat to the population's health in the study area.
21	S. F. Alhous et.al2021[44]	Iraq (Najaf/ Al Rahmah area)	The specific activity of the ^{226}Ra, ^{232}Th and ^{40}K nuclei are below IAEA.
22	A. A. Ibrahim et.al2021[45]	Iraq (Karbala/ Faculty of Agriculture (Al-Husseineya site) and Faculty of Medicine (Al-Mothafeen site)	Most results are within an acceptable level, as defined by OCDE, UNSCEAR, and ICRP.
23	I. Akkurt et.al2022 [46]	Turkey (Istanbul)	Activity concentrations of natural radionuclides ^{40}K, ^{226}Ra, and ^{232}Th are measured in soil samples collected from Çekmeköy-Istanbul using gamma ray spectroscopy technique with NaI (Tl) detector.

1.5.2 Previous Studies of SSNTD (CR-39)

No.	Author, Year, and Reference	Country	Results
1	M.S. Karim et.al2012[47]	Iraq (Al-Anbar/ (Ameria-AL-Falluja,AL-Garma,Rawa,AL-Habania,AL-Saqlawia)	The highest and lowest average alpha particle concentration in soil samples are (4.79 ppm) and (1.26 ppm) respectively.

2	S. S. Shafik et.al2014[48]	Iraq (Al-Anbar/ Al-Fallujah)	The natural uranium (U) concentration different from one region to another Each piece is taken from three different depths, 15, 30, and 45 cm, to study the distribution of U in soil.
3	K. H. Abass et.al 2015[49]	Iraq (Babylon/ (Al-werdeiaa, Al-seiahy, Al-Thewrae, Al-muhendisen, Al-keliss, Nadeer))	The results demonstrate that the radon gas concentration in all soil samples is below the (ICRP) agency's authorized level.
4	S. S. Fleifil et.al2016[50]	Iraq (Basrah)	The study further shows that 39 surface soil samples have boron below the detection limit.
5	A. A. Abojassim 2017[51]	Iraq (Najaf)	The values of C, Ra, C_{Rn}, AED and U_c in samples are below the limits of the world average .
6	H. N. Azeez et.al2018[52]	Iraq (Ainkawa)	The reference level of (WHO) and well below of U.K. (NRPB) and European Commission Recommendation Level of 200 Bq/m^3.
7	K. M. Thabayneh 2018[53]	Palestine (Bethlehem region)	The results reveal that radon concentrations and dosages are below the ICRP's allowable level.
8	A. Elzain et.al2019[54]	Sudan (Halfa Aljadida area)	A comparison between the results and other findings is related to each other. The results certainly show that the area under study is safe.
9	M. H. Kheder 2019[55]	Iraq (Bartella)	All of the test samples fall within the acceptable limits of radium content of 370 Bq/kg and radon exhalation of 57600 mBq/m^2 /hr (OECD).
10	Malik H. Kheder etl 2019[56]	Iraq (Al-Hamdaniya)	All matters of the samples under the test are below the allowed limit and worldwide average value.
11	W. M. Shakir et.al2019[57]	Iraq (Baghdad University Campus- AL-Jadiriyah)	The findings of this investigation revealed that radon emissions are below the recommended levels, allowing the region to be used for future human dwellings and other activities.
12	D.A. Salim et.al2019[58]	Iraq (College of Education, Ibn Al- Haitham buildings)	Except for two samples F1 and F2, the values of CR-39 are within the range allowed internationally by (ICRP), which is (200-300)Bq/m^3.
13	S. Ş. bal et.al2020, [59]	Turkey	In this study, the values of radon gas analyzed in the soil from monitoring stations with different topics (i) Station I ,(ii)Station II and (iii) Station III .
14	H. S. Mustafa et.al2020[60]	Iraq (Bartella)	The results obtained of the deductible mathematical method and actual experimental are close to each other.

15	M. G.Al Gharabi et.al2020[61]	Iraq (Al-Diwaniyah)	In all the examined soil samples, Radon concentrations within the acceptable value of 600 Bq/m^3, according to ICRP and IAEA.
16	E. F.Salman 2021[62]	Iraq (Kifl)	Radon concentration is measured by passive technique based on SSNTD (CR-39) detectors at different locations in Kifl. The results show that the radon concentration 205 to Bq/ m^3. The results concentration of radon in this good work agreement with radon concentration levels recommended by the (ICRP)"

Below some of previous and recently studies of dosimeter and RAD-7.

1.5.3 Previous Studies of RAD-7

No.	Author, Year, and Reference	Country	Results
1	A. K. Hasan et.al2011[63]	Iraq (Najaf)	The results obtained indicate that the region has background radioactivity levels within the natural limits.
2	A. A. Abojassim et.al2012[64]	Iraq (Kufa)	The concentrations values of radon and thoron are well below the acceptable levels.
3	R. Mehra et.al2014[65]	India (Hamirpur district)	AED limit is lower the recommended reference level (3 mSv y^{-1} to 10 mSv y^{-1}) of the world organizations.
4	R. Avikumar et.al2015[66]	India (Chitradurga district)	The results showed the radon values in the soil-gas of Chitradurga district are low (< 0.8 kBq/m^3) enough to categorize them under low radon risk areas (viz., 10 kBq/m^3).
5	Y. M. Z.Al-bakhat et.al2017[67]	Iraq (Al-Tuwaitha Nuclear Site)	The results from this study shows that the region has background radioactivity levels within the natural limits
6	M. A. Hassan et.al2018[68]	Iraq (Bghdad)	Identify locations with significant levels of contamination, a map depicting the distribution of radon concentrations in chosen areas is created.
7	A. A. Sharrad et.al2019[69]	Iraq (Samawa)	The radon in soil gas are measured using a continuous radon monitoring device RAD-7. Radon concentrations and (AED) due to inhalation is estimated and found to be within the international values.
8	M. O. Isinkaye et.al2020[70]	Nigeria	The mean activity concentration of ^{226}Ra and ^{222}Rn are within the world average value of 35 Bq kg^{-1} as reported by UNSCEAR and WHO respectively.

1.5.4 Previous Studies of Dosimeter

No.	Author, Year, and Reference	Country	Results
1	I. Yashodhara et.al2011[71]	India (Gogi region)	The ambient gamma absorbed dose rate and activity are varied and under the international recommendation.
2	S.Monica et.al2016[72]	India (Kollam district)	The mean indoor and outdoor are higher than 0.48 mSv y^{-1} and (ELCR) indoor and outdoor are larger, compared with resulting worldwide average 0.25×10^{-3}.
3	A. H. Alasadi et.al2016[73]	Iraq (Najaf/Agriculture and Science Faculities)	The indoor rate of an AED is found to be greater than 1mSv/y, which is the recommended dose limit for the general public, while the outdoor is according to specific limit.
4	S. P. Gautam, et.al2020[74]	Nepal (Mahendra Cave area)	The measurements of background radiation dose rate and average annual effective dose rate are within the recommendations limits.
5	P. O.Olagbaju et.al2021[75]	Nigeria (Ijebu-Ife)	The resulting of AED is below the UNSCEAR, 2000 maximum allowed limit for the general population of 1 mSv/y, as well as the (BDL), which are lower than the UNSCEAR, 2000 average values of 400, 35, and 30 Bq/kg for ^{40}K, ^{226}Ra, and ^{232}Th, respectively.

2.1 Introduction

Humans have been exposed to ionizing radiation from natural sources for as long as they have existed on the earth, yet human activities can alter the exposure. In addition, throughout the last century or two, new artificial sources of exposure have emerged. For most people, natural background radiation accounts for the majority of their overall radiation exposure. The simplest example is living in houses, some vegetables and fruits are commonly used in markets, soil in building, and enhancing materials such as medicinal plants for making purposes[16]. The measurements of gamma background radiation differ according to the purpose [76]. External exposure is mostly caused by γ -emitting primordial radionuclides, primarily radioactive potassium (^{40}K) and the radioactive series of uranium (^{238}U) and thorium (^{232}Th), whereas internal exposure is primarily caused by radon (^{222}Rn) and its decay products in the ^{238}U series[77].

A significant contribution to nathe tural exposure of humans is due to radon noble gas. (^{222}Rn) and ^{220}Rn are the gaseous radioactive products of the decay of the radium isotopes ^{226}Ra and ^{224}Ra, respectively. The γ-emitting decay products of ^{222}Rn are lead (^{214}Pb) and bismuth (^{214}Bi), which are found in radioactive secular equilibrium with radium (^{226}Ra) only if sealed to stop radon from escaping, while the decay products of ^{220}Rn are ^{212}Pb and ^{212}Bi, which are found in radioactive secular equilibrium with ^{224}Ra only if sealed to stop ^{220}Rn from escaping[78].

2.2 Nuclear Series

Radionuclides are unstable form of nuclides that disintegrate spontaneously into different daughter nuclides in order to achieve stable nuclide. They occur naturally in ground water through contact with rocks or soils that have naturally occurring radioactive materials(NORMs). Some radionuclides, such as the primordial nuclides of uranium-238, thorium-232, and potassium-40, which have been present since the beginning of time and are often referred to as naturally occurring radionuclides and materials in which they are present, deserve special consideration due to the threat they may pose as environmental pollutants when they undergo radioactivity[79]. Figure (2.1) shows transitions for the three radionuclide[80].

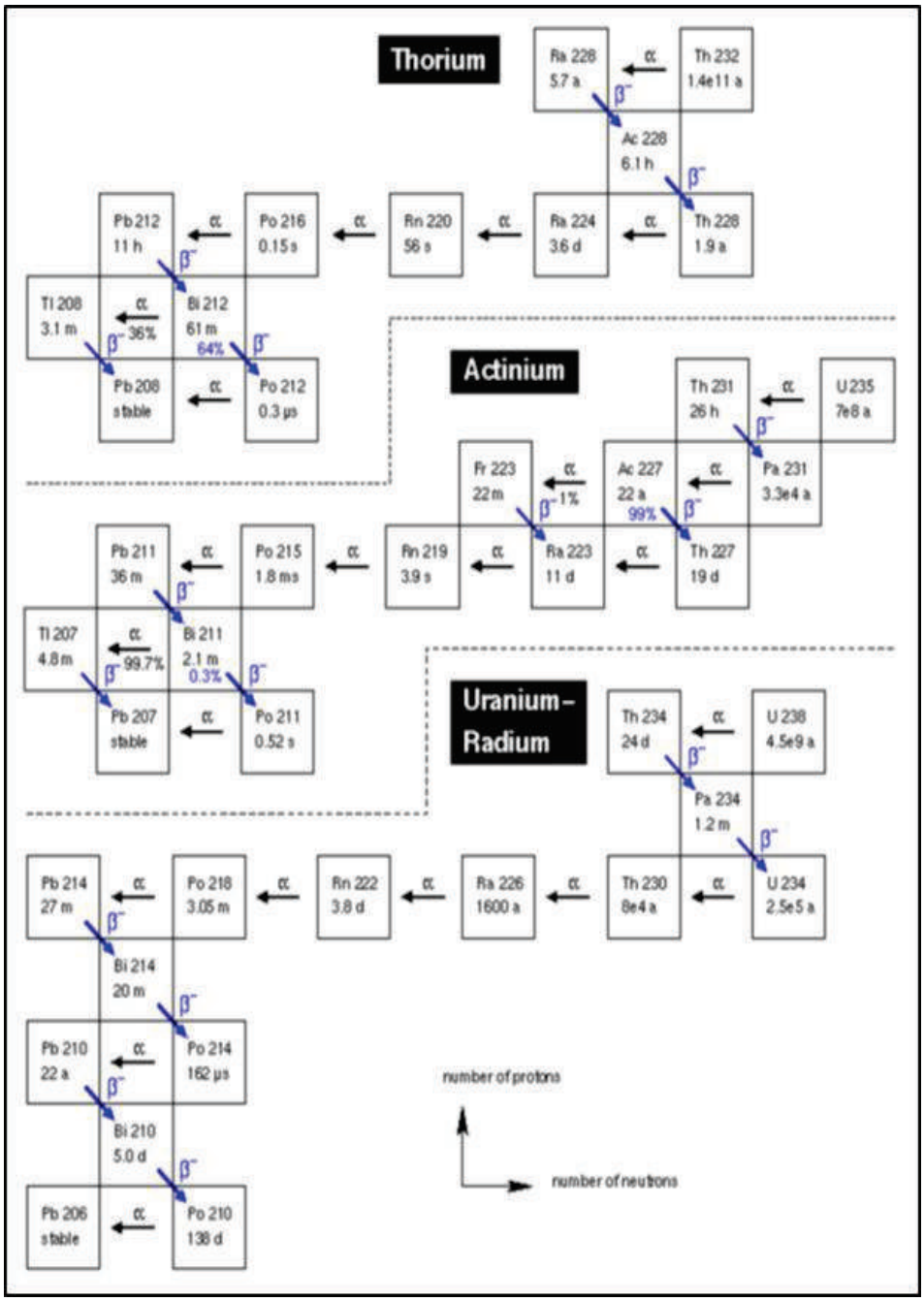

Figure (2.1) Transitions for the three radionuclides [80]

2.2.1 Uranium (^{238}U)

The most essential element in nature is uranium. It has mass numbers of 234, 235, and 238 so is found in at least three isotopic forms. This series begins with 238U nuclei (half-life 4.49×10^{9} years) and gradually is converted into ^{206}Pb, stable nucleus through sequences of alpha and beta particles emission. Since nuclides have very long half-life, this chain is still present today. This decay series includes the ^{226}Ra which has half-lives of 1600 years and chemical properties clearly different from those of Uranium ^{226}Ra decay into ^{222}Rn[81].

2.2.2 Thorium (^{232}Th)

Thorium is discovered by “Berzelins”. This series begins with Th-232 nuclei (half life $1.39x10^{10}$ y) and ends with Pb-208 stable isotope[82] . Thorium poisoning can lead to malignancies of the lungs, pancreas, liver, bones, and kidneys. As previously stated, naturally occurring radioactive elements in the environment account for 87 percent of human exposure to radiation.[83].

2.2.3 Potassium (^{40}K)

Natural Potassium has 3 isotopes: ^{39}K, ^{40}K and ^{41}K. Only ^{40}K has natural gamma radiation, and its quantity in nature is 0.012 percent of all potassium in the earth's crust, with a half-life of $1.28x10^{9}$ years (10). Figure (2.2) shows Potassium-40 decay scheme. During decay, ^{40}K creates two daughter isotopes, ^{40}Ca and ^{40}Ar, which emit beta and gamma radiation [84].

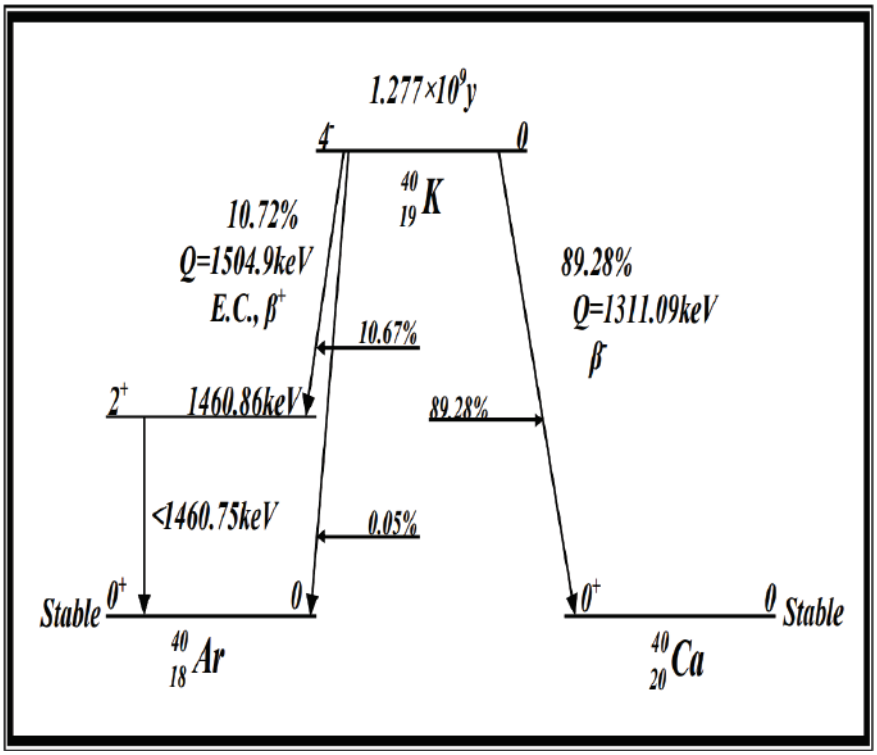

Figure (2.2): Decay scheme of Potassium-40 [84]

2.3 Interaction of Gamma ray with Matter

Gamma radiation induces ionization in the atom as it passes through Matter mainly due to interaction with electron, and only significant thickness of dense material such as steel or lead can provide adequate shielding[85]. Photoelectric absorption, Compton scattering, and pair formation are the three main ways gamma rays interact with materials. Gamma- ray, in the course of photoelectric absorption, in a one interaction loses all the energy The likelihood of this process is very highly reliant on gamma-ray energy E_γ (hν) and atomic number Z as show in figure (2.3a). Compton scattering is the mechanism in when a free or weakly bound electron meets with a gamma-ray ($E_\gamma >> E_b$), in which E_b represents the binding energy in the atom for electrons and passes part of its energy to the electron Gamma- ray loses only portion of its energy as show in figure (2.3b). In one interaction In a single pair-production interaction, all of the energy in a gamma ray can be lost. Nevertheless, an electron-positron pair will be produced by gamma -ray with at least (1.022 MeV) of energy as show in figure (2.3c)[86].

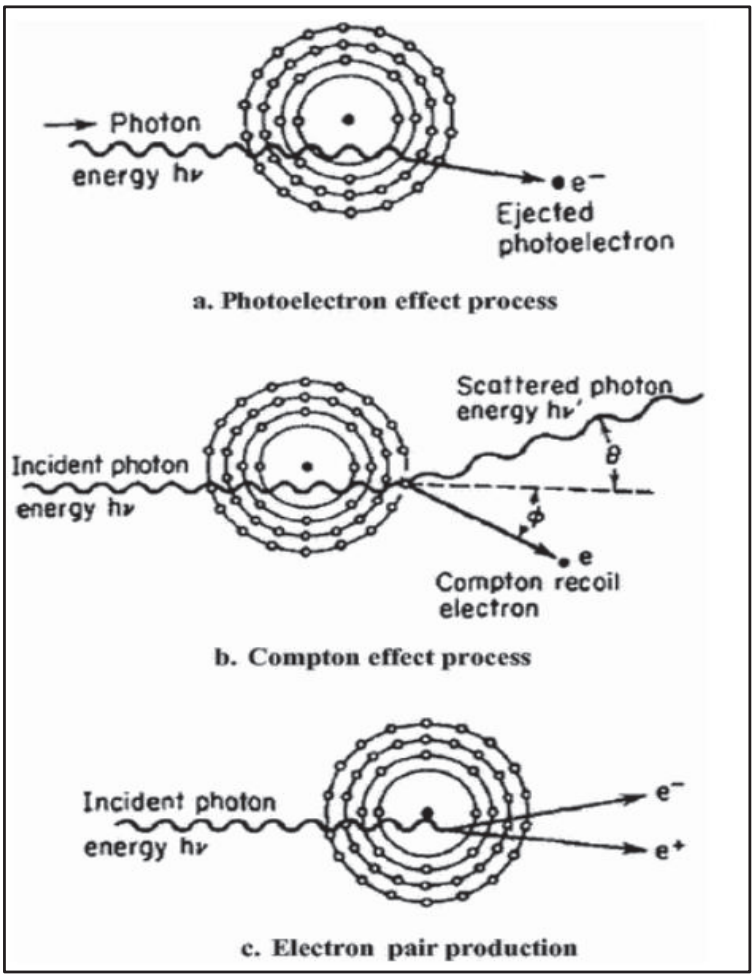

Figure(2.3) Three processes of interaction of gamma-ray with matter [86]

2.4 Radon Gas

Radon is classified as a noble gas. As a result, it is thought to have no affinity for other chemical elements. Its solid disintegration products, on the other hand, have high affinity with the materials in their surroundings. Polonium, bismuth, thallium, and lead are among the deadly progeny of radon, making it the second leading cause of lung cancer after smoking. From ^{238}U, ^{232}Th, and ^{235}U found in the Earth's crust, radon (^{222}Rn), thoron (^{220}Rn), and action (^{219}Rn) are three naturally occurring isotopes of radon [87]. The most important isotope of radon is (^{222}Rn) it's half-life is($t_{1/2}$= 3.82 days) and can move substantial distances from its point of origin[88].

As a result, when evaluating risk factors from radon exposure, only (^{222}Rn) is commonly considered a health hazard. There are no radon sinks, and only trace amounts of the gas escape to the stratosphere, according to estimates [89].

2.4.1 Physical and Chemical Properties of Radon

Radon is a radioactive gas that is colorless, tasteless, and odorless. It is also non-flammable. As a result, human senses are unable to perceive it. It has a melting point of (-70) degrees Celsius and a boiling point of (-60.8) degrees Celsius. As a noble gas, radon has the maximum density of (9.96) kg/m^3 and is nearly seven times more dense than air. As a result, it has a better capacity to travel easily through soil, air, and other media [90].

2.4.2 Radon Decay

The risk of radon arises from the fact that, when radon decays in the air its daughters are solids and when they are inhaled deposited on the inner surfaces of the lungs. Figure (2.4) given decay chains of ^{222}Rn[91].

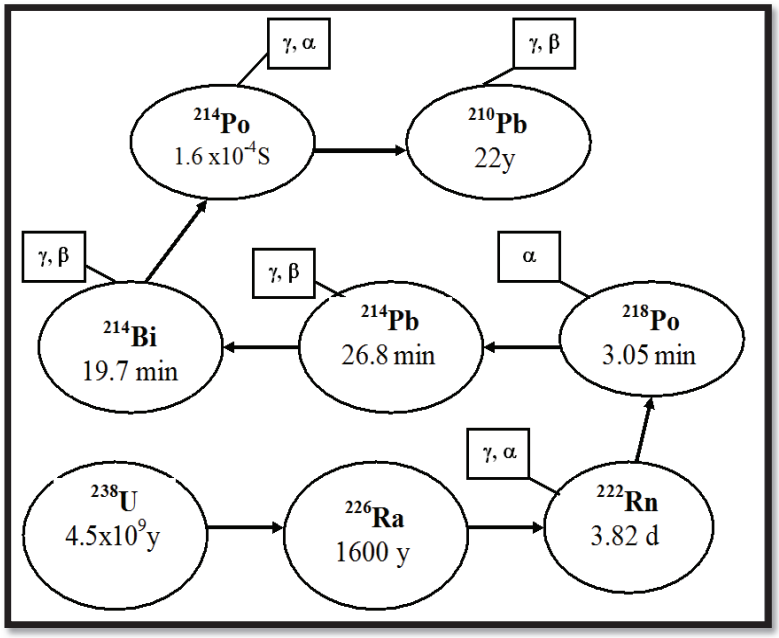

Figure (2.4) Radon-222 decay chart [91].

2.4.3 Radon Sources

Over several decades, our understanding of radon sources and transit pathways has progressed. High levels of radon are discovered in households and drinking water from dug wells in the 1950s. Initially, the main worry regarding radon in water is the health repercussions of drinking it.

The major health danger of radon in water is later revealed to be inhalation of radon emitted indoors. Due to the usage of alum shale1 with higher quantities of radium, radon emission from construction materials is discovered to be a concern in some places by the mid-1970s. By 1978, residences with indoor radon concentrations that are not linked to well water conveyance or radon emission from construction components had been observed. The most common source of indoor radon is shown to be soil gas penetration. In most cases, other sources, such as construction materials and well water, are less important. The contribution of different radon sources varies between countries and even regions. The following mechanisms may be considered[92]:

- Pressure-driven soil gas infiltration.
- Emanation of radon from building materials.
- Water transport of radon.

Measurements of radon in tap water, natural water, and soil are valuable in uranium and thorium exploration. It's also critical to locate radon-rich locations. The ability to identify distinct places of construction purposes and develop new buildings requires knowledge of radon levels in soil. Radon emission and exhalation from soil and construction materials are also a concern: It's helpful to identify radon sources in building materials and soils [93].

2.5 Radioactive Equilibrium

Decay series occur when all radionuclides decompose, at the same rate in equilibrium. There are three different types of equilibrium: Secular equilibrium, No equilibrium, and transient equilibrium depending on whether the half-life of the parent is larger or smaller than the half-life of the daughter[94].

2.5.1 Secular Equilibrium

A (secular equilibrium) usually occurs when a radionuclide has a substantially "longer" half-life than the others in the series ($A_P = A_D$) daughter activity is equal to parent activity [95].

$$\lambda_D \gg \lambda_P \quad (t_{D\,1/2} \ll t_{P1/2}) \qquad (2-1)$$

$$A_D / A_P = 1 \qquad (2-2)$$

2.5.2 Transient Equilibrium

Transient Equilibrium When the (half-life) of the parent of the radionuclide is longer than the daughter's half-life, transient equilibrium occurs .The daughter's activity will increase until the activity of the parents exceeds, then the daughter will be dissolved in the half-life if the parent has the same half-life. The daughter's activity is ($A_2 = \lambda_2 N_2$) and accumulates steadily over time,($e^{-\lambda\,2t}$) became negligible with respect to ($e^{-\lambda\,1t}$) then we will get[96]:

$$A_2 = \lambda_2\, \lambda_1\, N_1\, e^{(-\lambda t)} / (\lambda_2 - \lambda_1) \qquad (2-3)$$

2.5.3 No Equilibrium

No equilibrium occurs. If the half-life of the parent is less than the half-life of the daughter .The daughter's activity will increase and Parent activity decreases[97].

2.6 Health Effects of Radiation

The biological effects of radiation may be divided into two categories based on the relationship between the responses (symptoms or effects) and the dosage (or quantity of radiation absorbed). Stochastic effects are the first type of biological effect. Deterministic effects are the second type of biological effect. Stochastic effects are those that have higher likelihood of occurring with increasing dosage but they have the same severity [97] .Example; skin cancer and sunlight. The probability of getting skin cancer increases with increasing exposure to the sun. Deterministic Effects are those that get more severe as the dose is raised. Take, for instance, sunburn. The sunburn will be more severe the more you are exposed to the sun and the greater the 'dosage' of sunlight you receive [98]. The biological effects of radiation on living cells can occur by indirect or direct effect, as show in figure (2.5).

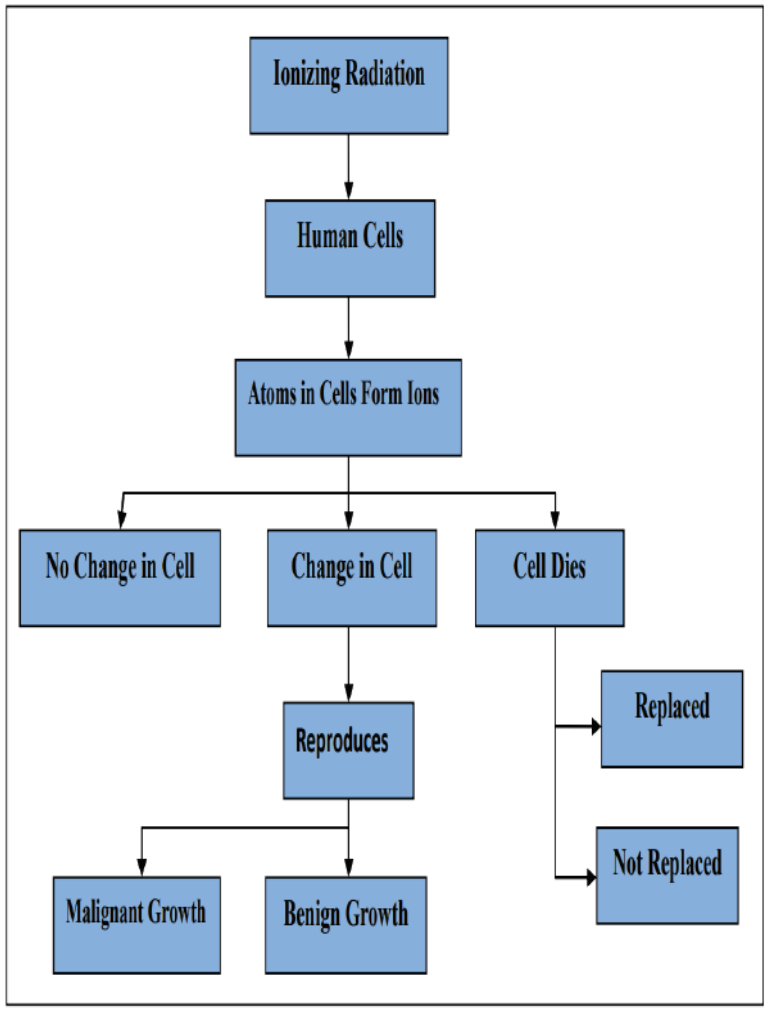

Figure (2.5) Biological effect of radiation [98].

The direct effect occurs when the ionizing radiation causes excitation in the same molecule, where deposited and absorbed radiation directly affect DNA molecules by the primary radiation, the direct ionization in the target tissue of atoms in DNA molecules via the Compton interactions and photoelectric effect is the result of energy absorbing it. If this ingested energy is adequate to expel electrons from the molecule, bonds are broken, which can break one DNA strand or both[98].

When the ionizing radiation is absorbed in water molecule in the human body, indirect effects occurs and produces short-life chemically reactive products that react with other molecules in other sites in the body[99].

The effect of nuclear radiation on human body causes many diseases[100]:

1-Cancer disease: that exposes to nuclear radiation causes no injury to the various cancerous diseases and depend on amount of radiation does and area to which the radiation exposed.

2-Eye lens opacity: the eye lens is a very sensitively area to nuclear radiation in general and neutrons particular lead to permanent damage to the eye lens that may be lead to loss of vision.

3-Infertility: there is evidence indicating that reproductive organs are subjected to certain doses of radiation, leading to a person infected with infertility.

4- Death to be exposed to radiation doses and low does not alone constitute major impact on human health until it has been exposed to these doses for a long period extending over years the immunity weakens the body against disease and lead to death.

2.7 Nuclear Detectors

Nuclear detection is used in several domains of activity from the physics researches, the nuclear industry, the medical and industrial sectors, the security etc. The particles of interest are the α, β, X, γ and neutrons[101]. One of the most crucial considerations for anyone who operate with or near radiation is being aware of the amounts of radiation present. This is generally performed through the use of several types of radiation detectors. A basic awareness of the many types of detectors available and how they function will help you pick the ideal detector for the job at hand as well as maximize the benefits of using that detector [102].Figure(2.6) shows Tree diagram of the relationship between types and classification of most common particle detectors[103].

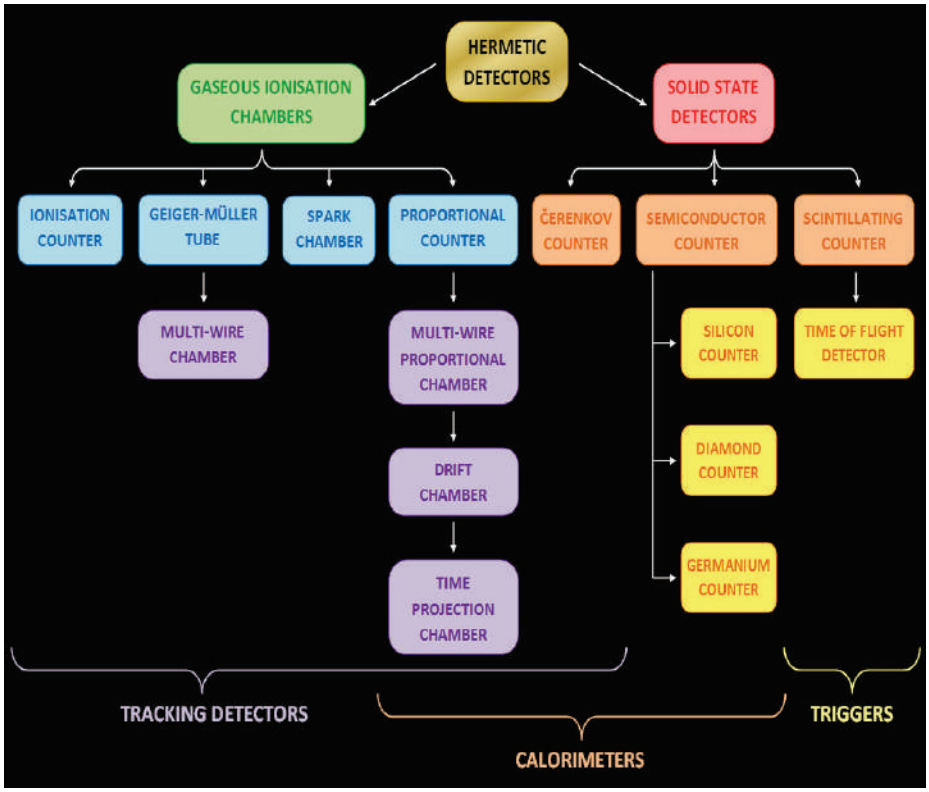

Figure(2.6) The link between the types and classifications of the most common particle detectors depicted in a tree diagram [103].

Depending on recent work, many detectors had been used: dosimeter detector, scintillation detectors (NaI/Tl), solid state nuclear track detector/(CR-39) and semiconductor detector /(RAD-7).

2.7.1 Dosimeter Detector

A radiation dosimeter is a device, instrument, or system that measures or analyzes exposure, absorbed dose, or equivalent dose, or their temporal derivatives (rates), or related quantities of ionizing radiation, either directly or indirectly. A dosimetry system is a combination of a dosimeter and a reader. The process of determining the value of a dosimetric quantity experimentally utilizing dosimetry instruments is known as measurement [104].

Figure (2.7) Portable radiation alert Inspector dosimeter[105]

The value of dosimetric quantity represented as the product of numerical value and an appropriate unit is the outcome of a measurement. The dosimeter must have at least one physical characteristic that is a function of the measured dosimetric quantity and that can be utilized for radiation dosimetry with correct calibration in order to operate as a radiation dosimeter. Figure (2.7) Dosimeter Detector[105]. Radiation dosimeters must possess numerous desired features in order to be helpful. In radiotherapy, for example, precise information of the absorbed dosage to water at a given site and its geographical distribution, as well as the ability to calculate the dose to a patient's organ of interest, are critical. Accuracy and precision, linearity, dosage or dose rate dependency, energy response, directional dependence, and spatial resolution are all desired dosimeter qualities in this context [104].

2.7.2 Scintillation Detectors

The first solid material to be used as a particle detector is a scintillator. The amount of light produced in the scintillator is very small. It must be amplified before it can be recorded as a pulse or in any other way.

The amplification or multiplication of the scintillator's light is achieved with a device known as the photomultiplier tube (or phototube). Its name denotes its function: it accepts a small amount of light, amplifies it many times, and delivers a strong pulse at its output.

Amplifications of the order of 10^6 are common for many commercial photomultiplier tubes. Apart from the phototube, a detection system that uses a scintillator is no different from any other (Figure 2.8). The operation of a scintillation detector may be divided into two broad steps[106]:

1. Absorption of incident radiation energy by the scintillator and production of photons in the visible part of the electromagnetic spectrum

2. Amplification of the light by the photomultiplier tube and production of the output pulse.

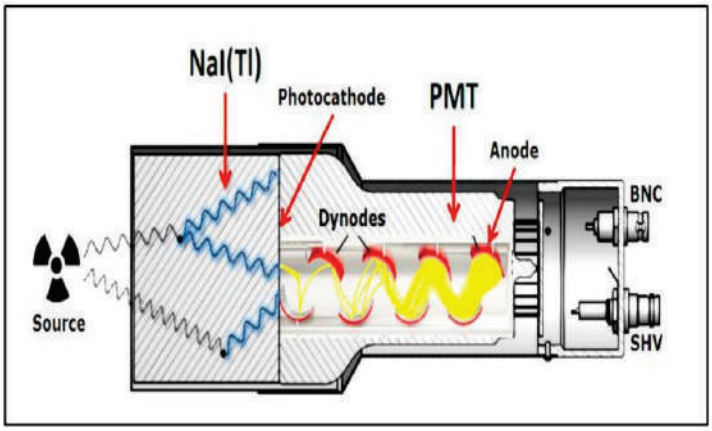

Figure (2.8) A detection system using a scintillator(NaI/Tl)[106]

2.7.3 Solid State Nuclear Track Detectors

Since its discovery in 1958 by (Young, 1958; Silk and Barnes, 1959), the technique now generally known as Solid State Nuclear Track Detection (SSNTD) has, over the last few decades, become a popular and well established method of measurement in a large number of fields involving different aspects of radioactivity or nuclear interactions.

The basic simplicity of its approach and the inexpensive cost of its components, together with the enormous flexibility of its various applications—as will become obvious in the following—are the reasons for its widespread use [107].Figure (2.9) shows a construction of SSNTD[108].

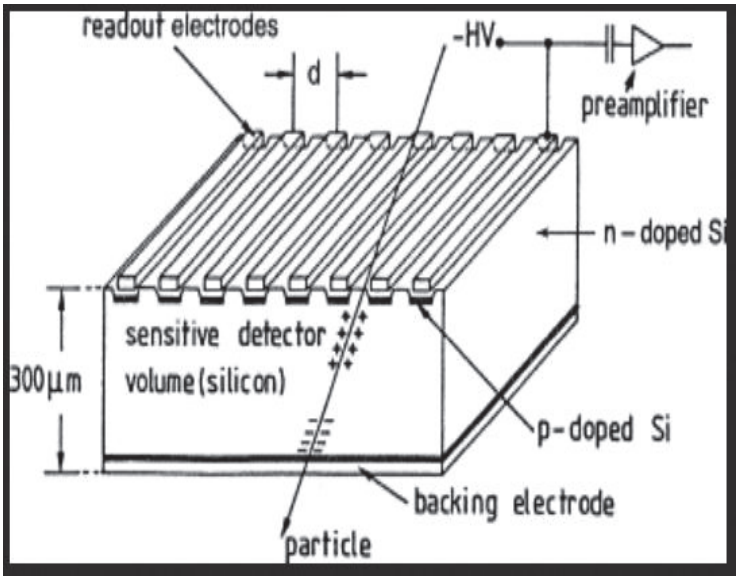

Figure (2.9) Construction of SSNTD[108].

SSNTDs (solid state nuclear track detectors) are commonly employed in a variety of scientific sectors. The basis of these detectors is based on their capacity to detect and record charged particles as latent tracks, which will become visible under the optical microscope after adequate chemical etching in all scientific domains . The operation of the solid-state nuclear track detector is based on the fact that when a heavy charged particle travels through a medium, it causes widespread ionization of the substance [109].

Through the process of ionization, nearly all the molecules nearest to his direction become ionized by an alpha particle. Fundamentally, a numbers to the additional chemicals processes that can be caused by the ionizing phase are involved in the formation of free chemicals radical and other chemical compounds that the drilling method then produces. This compromised region is called a latent trail[110].

2.7.4 Rad-7 Detector

The DURRIDGE RAD-7 uses a solid state alpha detector. A solid state detector is a semiconductor material (usually silicon) that converts alpha radiation directly to an electrical signal. The RAD7's internal sample cell is a 0.7 liter hemisphere, coated on the inside with an electrical conductor.A solid-state, Ion-implanted, Planar, Silicon alpha detector is at the center of the hemisphere. The high voltage power circuit charges the inside conductor to a potential of 2000 to 2500V, relative to the detector, creating an electric field throughout the volume of the cell.

The electric field propels positively charged particles onto the detector. One important advantage of solid state devices is ruggedness. Another advantage is the ability to electronically determine the energy of each alpha particle. This makes it possible to tell exactly which isotope (polonium-218, polonium-214, etc.) produced the radiation, so that you can immediately distinguish old radon from new radon, radon from thoron, and signal from noise. This technique, known as alpha spectrometry, is a tremendous advantage in sniffing, or grab sampling, applications ,figure (2.10) shows basic point of RAD-7[111] .

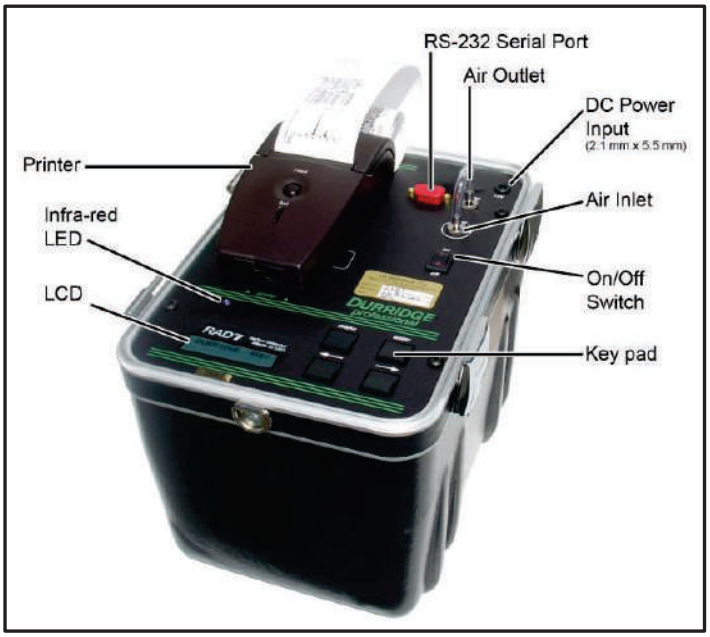

Figure(2.10) The Durridge RAD-7 [111]

3.1 Introduction

This chapter discusses the crucial stages (materials and procedures) that are followed to examine the soil samples obtained from various places in Najaf and Kufa, sample collection, sample preparation, and measurement systems NaI(Tl), The CR-39 detector, as well as a theoretical consideration, are employed in this investigation (see Figure 3.1). Also, it uses GIS technology for mapping specific activity and radiological radiation parameters for all samples under study.

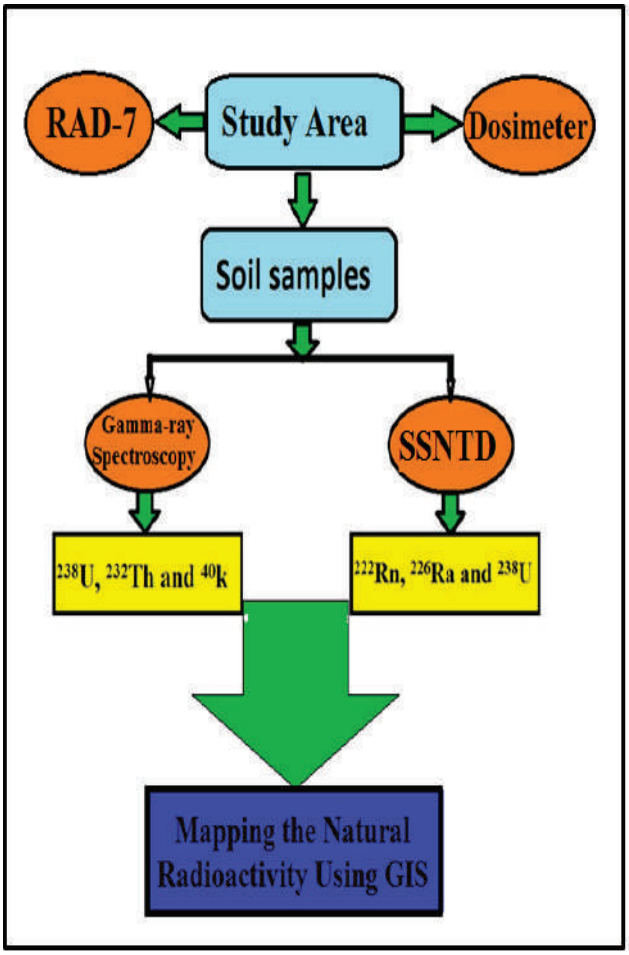

Figure (3.1): A schematic diagram of the main parts of the current study.

3.2 Area of Study

Najaf city, one of the provinces in southern Iraq, lies on the edge of Iraq's western plateau southwest of Baghdad, about 161 kilometers away [112]. It is located near the Euphrates River, 182 km southeast of Baghdad, latitude 32 ° 01'44 "north, longitude 44 ° 27'57.89" east [113] .The city of Najaf is one of the most important administrative centers in the holy city of Najaf. The city of Al-Haydariyah lies in the north of Al-Najaf at a distance of (40 km), and the city of Kufa lies in the east of Al-Najaf at a distance of (10 km), and adjacent to it from the southeast is located the city of Al-Manazira at a distance of (25 km), while the course of the Euphrates River lies on its western side. The city overlooks the Najaf sea depression. The area of the city is about (183 km^2) as part of its master plan for 2018.

The city is located on a high hill that forms part of the edge of a desert plateau with sandy rocks. From the southeast side, this hill overlooks the Bahr al-Najaf depression, while it overlooks from the north and northwest sides on a spacious space represented by the Wadi al-Salam cemetery, its eastern side is represented by the sloping land towards the city of Kufa, while its western side is barren lands represented by the eastern section of the western hill. The study area is characterized as a mixed gypsum desert, or sandy or sandy mixture, and sometimes covered by a layer of gravel, and because of its characteristics, it is exposed to air discharge processes as a result of multiple erosion factors [114].

The Kufa district is located about (8.99) km eastern of AL-Najaf, it positioned geographically (44020'0"–44037'30"E and 31058'30"–32012'30" N)[115].In this location, it is one of the cities located in the southwestern part of Iraq. The city of Kufa is located in the eastern side of Najaf Governorate, and it is located on the western side of the Kufa Shatt, which is an important branch of the Euphrates River, which is the important water resource in it. As it is an important urban center for Najaf Governorate. It is bordered on the north by Al-Kifl (Babylon Governorate) with a distance of (20 km), and in the east by Al-Abbasiya, with a distance of (5 km), and from the west the center of Najaf city, and from the south by Al-Manathrah district with a distance of (12 km), It is far from the city of Baghdad (160 km), from the city of Hilla (50 km), from the city of Karbala (78 km), and from the city of Diwaniyah (65 km).With regard to the climate, the city of Kufa falls within the characteristics of a hot, dry desert climate[116].

The sub-districts under the district of Kufa are the sub-district of Al-Abbassiya and the sub-district of Al-Huriya. As it is known, soil represents recent deposits. It covers large areas of the study area, and the constituents of these sediments are detrital materials of clay,

silt, and sand, as these sediments are a source of gravel, sand, and clays. They are also a source of groundwater bodies.

The Quaternary Period sediments are divided into four categories: gravel deposits on river terraces, flood plain sediments, irrigation channels sediments, depression deposits consisting of thin layers of sand-clay silts, and dry marsh deposits comprised of clay, mud, and organic materials[117].Figure (3.2) shows area of study for both Najaf and Kufa .

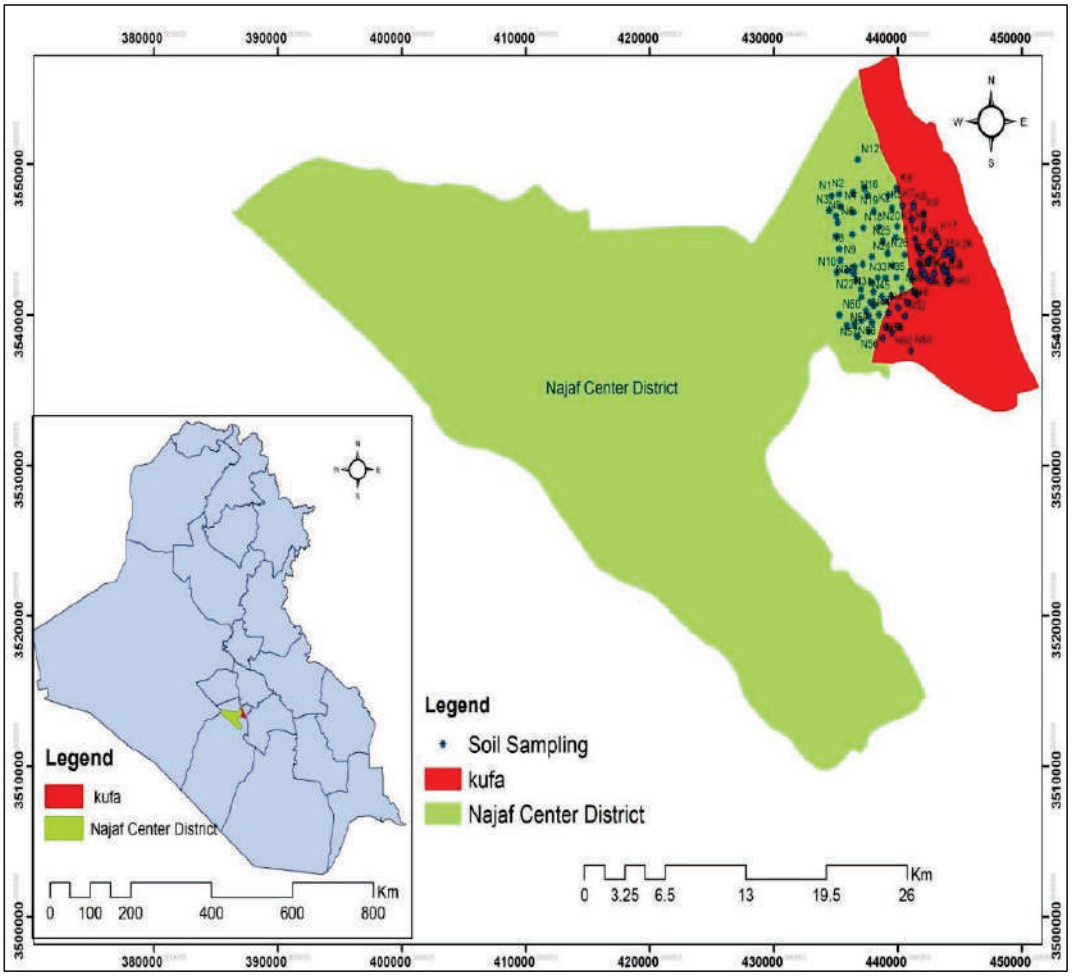

Figure (3.2) Najaf Governorate Area.

3.3 Collection and Preparation of Samples

Five hundred samples are collected from the cities of Najaf and Kufa, and then the average is taken for every five samples from the same area in one sample, so the number of samples became one hundred sample to be studied in this research. Sixty samples of them are collected from AL –Najaf city and forty of them are collected from Kufa city during February and March 2021 at a depth of (10-15) cm from the ground surface in order to estimate the natural radioactivity and radiological hazrdsindex of gamma and alpha emitters. The sample locations are determined of coordinates using "Global Positioning System." GPS is a satellite navigation system used to determine the ground position of an object see figure (3.3).

Figure (3.3) Global Positioning System.

The collected specimens are moved to mark sealed polyethylene bags and taken to the advanced radiation detection and measurement laboratory in the physics department, faculty of science, university of Kufa. The sample codes, locations, and coordinates are shown in Tables (3.1) and (3.2) for Najaf and Kufa area respectively, as well as figure (3.4) and figure (3.5) show the study area for Najaf and kufa respectively.

Table (3.1) Names and locations with Coordinates of Soil samples of Najaf.

Sample code	Name of Samples	Coordinates	
N1	Alnidaa-1	32°03'53.6"N	44°18'26.5"E
N2	Alnidaa-2	32°03'57.1"N	44°18'51.2"E
N3	Alnidaa-3	32°03'24.0"N	44°18'22.6"E
N4	Alnidaa-4	32°03'29.9"N	44°18'54.9"E

Next

N5	New Almilad	32°03'12.7"N	44°18'42.8"E
N6	Almilad	32°02'55.4"N	44°18'46.5"E
N7	Alnasor banzen station	32°02'28.7"N	44°18'42.9"E
N8	Alnasor mohandseen	32°02'01.3"N	44°18'50.9"E
N9	Abotalib	32°01'33.8"N	44°18'55.6"E
N10	Alrahma-1	32°01'08.3"N	44°18'45.4"E
N11	2 Alrahma-	32°01'12.9"N	44°19'18.2"E
N12	Algahdeer village	32°05'13.0"N	44°19'48.3"E
N13	Almakrama-1	32°04'00.5"N	44°19'33.1"E
N14	2 Almakrama-1	32°03'18.8"N	44°19'33.9"E
N15	Alaskari-1	32°04'10.0"N	44°20'10.6"E
N16	Alaskari-2	32°03'54.2"N	44°20'19.1"E
N17	Aljameea(Alresalah-1)	32°02'30.0"N	44°19'33.0"E
N18	Aloroba (Alresalah-2)	32°02'46.0"N	44°20'05.2"E
N19	Alwafaa (Alhindiya homes)	32°03'21.1"N	44°20'36.9"E
N20	Alshohadaa	32°02'48.9"N	44°20'53.8"E
N21	First gari (Alnafot)	32°01'22.8"N	44°19'38.5"E
N22	Second gari (Alatibaa)	32°01'05.8"N	44°19'37.0"E
N23	Second gari	32°01'26.3"N	44°20'03.6"E
N24	Alsalam	32°01'42.9"N	44°20'30.6"E
N25	Aljamea-1	32°02'16.4"N	44°21'05.0"E
N26	Aljamea-2	32°01'51.3"N	44°21'19.3"E
N27	Alolamaa	32°00'51.9"N	44°19'46.0"E
N28	Alhussein	32°00'32.7"N	44°19'59.0"E
N29	Alayubeen (Alhanana)	32°00'15.4"N	44°20'01.0"E
N30	Alkarama	32°00'47.8"N	44°20'28.9"E
N31	Alseha	32°00'27.7"N	44°20'34.7"E
N32	Algahdeer	32°00'57.6"N	44°20'48.2"E
N33	Alforat	32°00'58.4"N	44°21'14.2"E
N34	Aladala-1	32°01'26.4"N	44°21'34.3"E
N35	Aladala-2	32°00'59.5"N	44°21'47.1"E
N36	Alsaad	32°00'06.1"N	44°20'27.0"E
N37	Abokahled	31°59'47.2"N	44°20'12.4"E
N38	Almoalmeen	31°59'36.5"N	44°20'24.7"E

Next

N39	Imam Mahdi	31°59'22.1"N	44°20'33.3"E
N40	Almuthana	31°59'57.1"N	44°20'38.0"E
N41	Adan	31°59'39.2"N	44°20'55.7"E
N42	Aliskan	32°00'20.5"N	44°21'03.3"E
N43	Alishtiraki	32°00'08.8"N	44°21'15.5"E
N44	Alhawraa (Alswaq)	31°59'43.8"N	44°21'24.2"E
N45	Alameer-1	32°00'21.4"N	44°21'31.8"E
N46	Alameer-2	32°00'36.2"N	44°22'05.3"E
N47	Alzahraa	31°59'55.5"N	44°21'53.5"E
N48	Alqadisiya	32°00'06.4"N	44°22'22.2"E
N49	Alansar-1	31°59'14.3"N	44°21'17.7"E
N50	Alansar-2	31°59'01.4"N	44°21'34.4"E
N51	Alsinaeya (alharafeen-1)	31°59'13.0"N	44°21'57.6"E
N52	Alsinaeya (alharafeen-2)	31°59'36.7"N	44°22'15.5"E
N53	Alkudos-1	31°58'23.3"N	44°22'32.9"E
N54	Alkudos-2	31°58'47.8"N	44°21'04.1"E
N55	Scientific city	31°59'04.1"N	44°20'26.1"E
N56	Alshorta	31°58'53.3"N	44°19'49.2"E
N57	Aljodaydat-1	31°59'25.4"N	44°20'01.2"E
N58	Aljodaydat-2	31°59'19.2"N	44°19'39.5"E
N59	Aljodaydat-3	31°59'14.0"N	44°19'18.0"E
N60	Old city	31°59'38.2"N	44°18'54.6"E

Table (3.2) Names and locations with Coordinates of Soil samples of kufa.

Sample code	Name of Samples	Coordinates	
K1	Maysan 1	44°21'21.5"E	32°03'59.5"N
K2	Maysan 2	44°21'33.1"E	32°03'30.5"N
K3	Maysan 3	44°21'50.4"E	32°02'51.7"N
K4	Alwat Alfahal 1	44°21'47.7"E	32°04'13.8"N
K5	Alwat Alfahal 2	44°22'06.1"E	32°03'37.2"N
K6	Alwat Alfahal 3	44°22'34.3"E	32°03'06.6"N
K7	Alzarga 1	44°22'38.1"E	32°03'39.6"N
K8	Alzarga 2	44°22'39.7"E	32°03'34.6"N
K9	Alzarga 3	44°23'10.0"E	32°03'20.0"N
K10	Middle Euphrates Center	44°21'46.0"E	32°02'28.2"N
K11	Kufa University 1	44°22'13.7"E	32°01'49.7"N
K12	Kufa University 2	44°22'30.3"E	32°01'12.1"N

Next

K13	Alsahla	44°22'44.8"E	32°02'22.6"N
K14	Palm Street area	44°23'11.4"E	32°02'53.1"N
K15	Alaskari	44°22'51.3"E	32°02'07.0"N
K16	Alsehilia 1	44°23'31.9"E	32°02'17.0"N
K17	Alsehilia 2	44°23'51.1"E	32°02'29.1"N
K18	Almutanabi	44°23'02.2"E	32°01'54.4"N
K19	Aljamea	44°23'45.8"E	32°02'00.1"N
K20	Aljomhoria	44°24'22.6"E	32°01'56.2"N
K21	Aljdaidaat	44°24'33.2"E	32°02'01.1"N
K22	Alshorta	44°23'00.7"E	32°01'30.3"N
K23	Kenda 1	44°23'24.2"E	32°01'33.5"N
K24	Almolimeen	44°23'29.9"E	32°01'42.8"N
K25	Alwakaf	44°24'13.2"E	32°01'50.1"N
K26	Alrashadiya	44°24'37.8"E	32°01'50.7"N
K27	Industrial District 1	44°22'34.9"E	32°00'56.3"N
K28	Industrial District 2	44°22'40.1"E	32°00'32.6"N
K29	Almatar	44°22'51.3"E	32°00'24.7"N
K30	Tamoz	44°23'04.7"E	32°01'14.3"N
K31	Kenda 2	44°23'15.0"E	32°01'07.9"N
K32	Maytham Altamaar 1	44°23'23.6"E	32°00'57.3"N
K33	Maytham Altamaar 2	44°23'42.9"E	32°01'10.4"N
K34	Alsafeer	44°24'11.8"E	32°01'23.4"N
K35	Alkareeat	44°24'39.0"E	32°01'48.3"N
K36	Alforat 1	44°24'12.1"E	32°01'16.5"N
K37	Alforat 2	44°24'30.6"E	32°01'02.6"N
K38	Role of cement plant	44°23'36.6"E	32°00'52.9"N
K39	Alsadar –Third 1	44°24'21.2"E	32°01'14.8"N
K40	Alsadar –Third 2	44°24'31.5"E	32°01'03.0"N

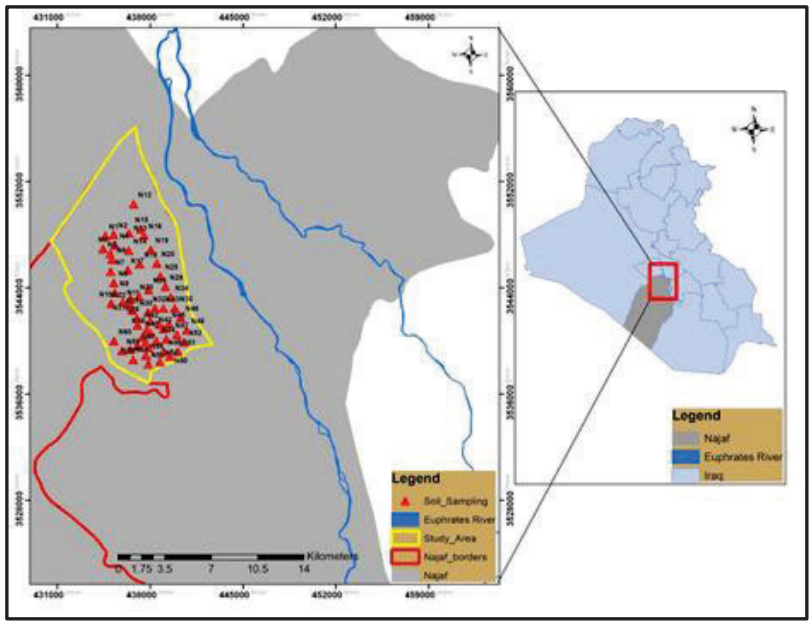

Figure (3.4): Najaf study area.

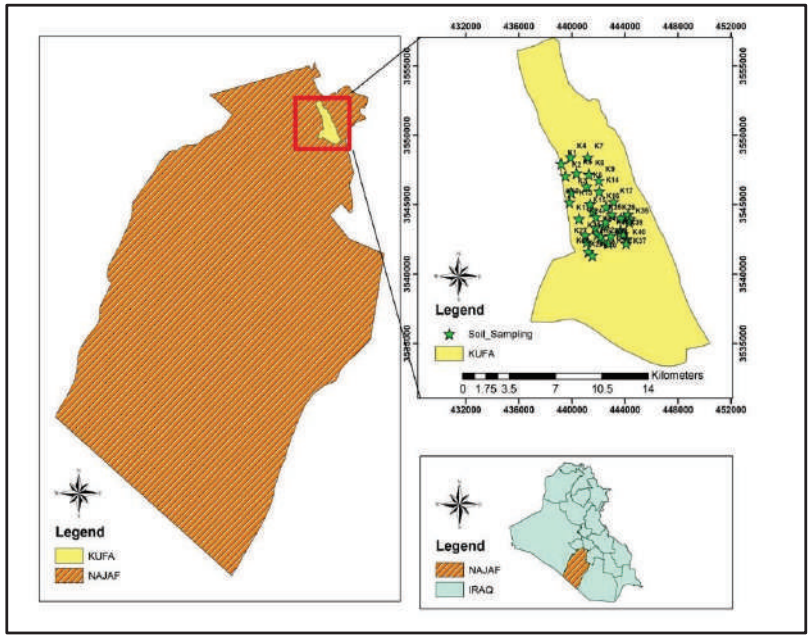

Figure (3.5): Kufa study area.

The samples are set for analysis following the procedure of drying, and keeping them moisture-free by putting them for (30-60) minute in an oven at 100˚C , Figure (3.5) to ensure that moisture is completely removed.

Figure (3.6) Oven used in the study.

The samples are mechanically crushed using electric mill of micro soil grinded to reach a suitable homogeneity, Figure (3.7) and figure (3.8).

Figure (3.7): Electric mill.

Figure (3.8) Preparation samples.

To make the sample air-free completely, the latter is pressed on by the light cap of the marinelli beaker. The respective net weights are measured and recorded with a high sensitive digital weighting balance with a percent of ±0.01%. Later, around (1kg) of each sample of Najaf and Kufa area is packed in a standard marinelli beaker that is sealed for one month hermetically and dry weighted to get homogeneity figure (3.8), while (200gm) sample of Najaf and kufa area saved in a cup of precise dimension for three months, figures (3.9) and (3.10) show all saved samples.

The samples are stored for one month and three months under normal laboratory conditions. This time is necessary to get a radiological equilibrating to the samples, before counting the concentration of natural radioactive material for the samples.

Figure (3.9) Saved samples of Najaf.

Figure (3.10) Saved samples of Kufa.

3.4 Detection System

This study uses four detection measurement: Alert INSPECTOR Dosimeter, NaI(Tl) scintillation detector , solid state nuclear track detector (SSNTD) and radon-thoron detector (RAD-7).

3.4.1 Alert Inspector Dosimeter

The Radiation Alert Inspector is a hand-held, microprocessor-based radiation detector that detects potentially harmful ionizing alpha and beta particles and gamma and x-ray radiation, has a four-digit, LCD digital display of millirem (mR) per hour, and function indicators . This radiation detector can detect low levels of the four main types of ionizing alpha and beta particles and gamma rays and x-rays over automatic operational ranges. The radiation detector has a 2" halogen-quenched, uncompensated Geiger Mueller (GM) tube with a narrow, mica end window for sensing ionizing radiation.

A radiation symbol on the front label marks the center of the detector. It is used for surveying naturally occurring radioactive material (NORM) contamination, gross wipe counting, contamination inspection of packages, equipment, and people, regulatory reviews, and low energy radionuclide detection[75].

One hundred of soil samples are collected from different locations of Najaf and Kufa. Each soil sample is preserved in a plastic pouch, classified, and numbered according to its collected site. One kg of soil samples is measured background radiation directly without any preparation for ten minutes and repeated for three times for each sample, as show in figure (3.11).

Figure (3.11) Measurement of samples by dosimeter.

3.4.2 NaI (Tl) Detection System

The scintillation detector is illustrated in Figure (3.12). It consists of an Alpha Spectra, Inc.-12I12/3 scintillation detector with a crystal diameter of (3"×3"), a high voltage power supply (the voltages used in the research are 778 volts), a preamplifier, an amplifier provided by Alpha Spectra, Inc.-12I12/3 through an interface. It's coupled to a 4096- Chapter Three Materials and Methods 40 channel multi-channel analyzer (MCA) and an ADC (Analog to Digital Converter) unit (ORTEC –Digi Base). Finally, the spectral data are immediately sent to the laboratory's computer.

Gamma-ray detectors have an incredible sensitivity. The counting room will be surrounded by and contain radioactive particles due to the presence of natural radioactivity (back ground radiation) that found in laboratory materials, so it is important to use the same of these studies shielding's. Figure (3.13) shows how the ORTEC cylindrical chamber supports and protects the detector.

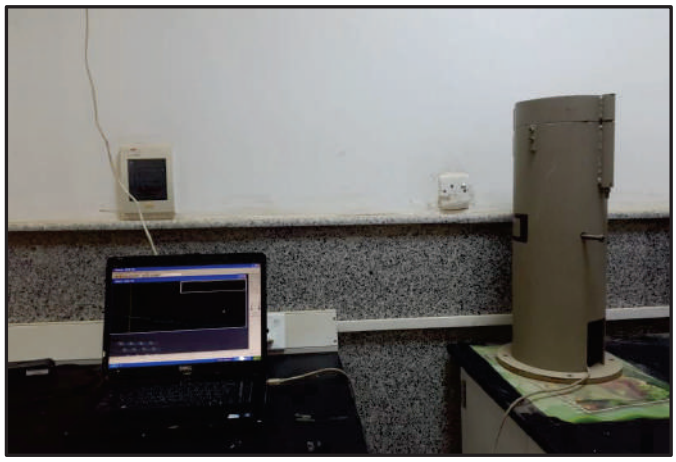

Figure (3.12) The scintillation detector system.

Figure (3.13): Shielding chamber of the detector (ORTEC, made in USA).

3.4.2.1 Energy Calibration for NaI (Tl) Detector

Energy calibration is the relation of energy of gamma- ray absorbed by detector (photo peak) to the channels that corresponding it [118]. As shown in Table (3.3), the energy of this detector is calibrated using a number of predefined -ray sources "Gamma Source Set" (^{137}Cs, ^{60}Co, ^{22}Na, ^{54}Mn, and ^{152}Eu) from the IAEA (Model RSS–8) as show in figure (3.14).

Figure (3.15) obtains the energy calibration curve. The relationship between gamma energy and number of channel is obtained and it showed a straight line with excellent correlation (0.96%) . This relationship can be represented mathematically by the following equation:

Energy (KeV) = 0.2208 × Channel No. - 10.109 ……. (3-1)

Table (3.3) Properties of radioactive sources used in the present study.

Source	Energy (KeV)	Activity (µci)	Serial number	Production date	I_γ %
Co-60	1173.24	1	IRS-141	1/1/2009	99.9
	1332.5	1			99.88
Na-22	511	1	IRS-139	1/2/2009	181
	1274	1	IRS-139	1/2/2009	99.95
Cs-137	661.66	1	IRS-126	1/1/2009	85.21
Mn-54	834	1	IRS-128	1/1/2009	100
Eu-152	1407	0.9	IRS-149	1/11/2009	24
	1112	0.9			16.4
	1085.8	0.9			10
	964	0.9			17.3
	778.9	0.9			15.2

Figure (3.14) Gamma- ray standard sources used in the study.

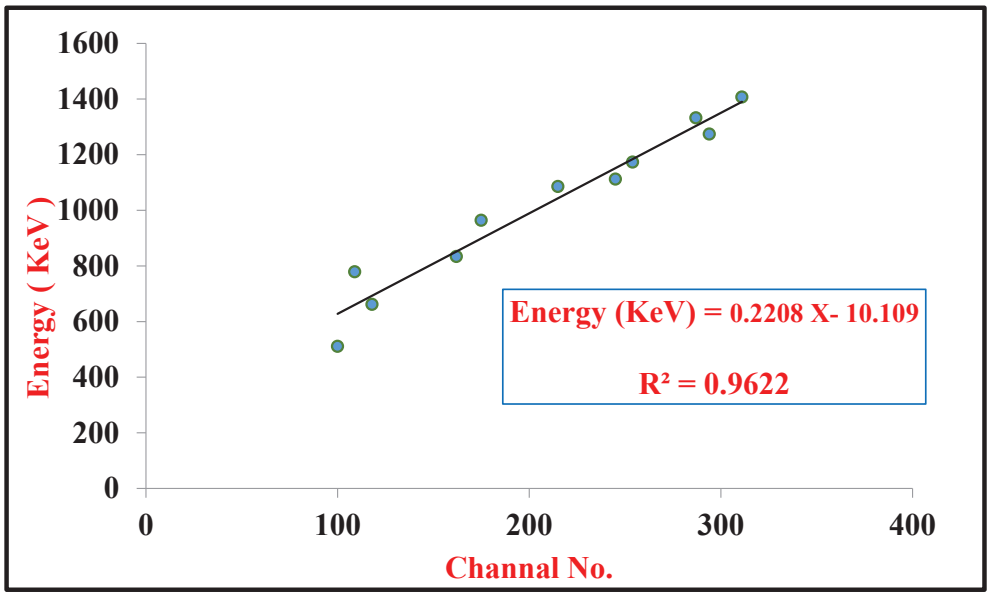

Figure (3.15) Energy calibration curve of NaI(TI) 3"×3".

3.4.2.2 Efficiency for NaI (Tl) Detector

Detection efficiency (ε) can be defined as the ratio of count rate of radiation between recorded to detected by the detector, which can be calculated in the present study using equation (3-2)[119].

$$\varepsilon = \frac{C}{A \times I\gamma \times t} \times 100\ \% \quad \ldots\ldots\ldots (3-2)$$

Where, (C) is net area (under photo peak), (A) is the activity in unit (Bq or Ci) of the stander source at measurement of time , (I_γ) is the probability of gamma-ray emitted and (t) is time of collection of spectrum, with one notice that (A) can often be computed by equation (3-3)[119].

$$A = A_0\ e^{-\lambda \times \Delta t} \qquad \ldots\ldots\ldots (3-3)$$

Where (A) is the source's activity (Bq) at time (t), (A_o) is each source's starting activity (Bq) at time to, (λ) is the rate of deterioration, and Δt (Δt= t-t_o) is the time of decay between the product of the stander source (t_o) and time at time measurement (t).

As shown in Figure (3.16), five distinct sources are used to calibrate the variation in absolute photo-peak detector efficiency with gamma-ray energy: ^{137}Cs, ^{60}Co, ^{22}Na, ^{54}Mn, and ^{152}Eu. Based on data in figure (3-16) the efficiency of ^{238}U (^{214}Bi; 1765 keV), ^{232}Th (^{208}Ti; 2614 keV), and ^{40}K (^{40}Ar; 1460 keV) .

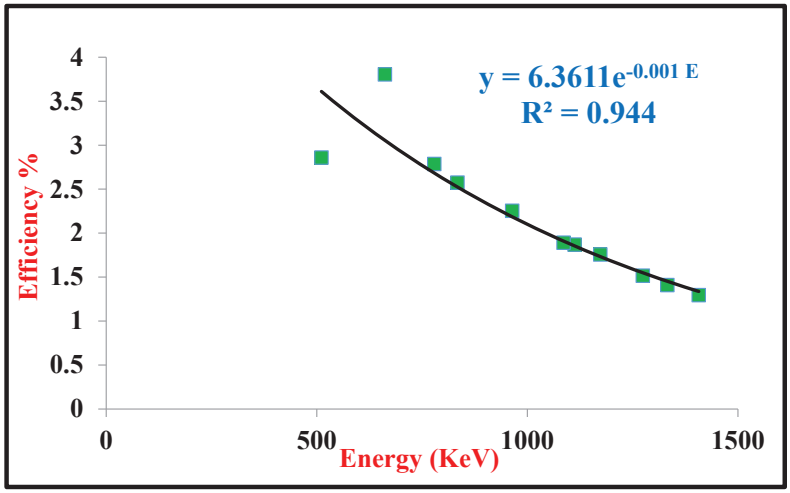

Figure (3.16): The curve of efficiency for NaI(Tl) detected in present study.

3.4.2.3 Resolution for NaI (Tl) Detector

The energy resolution (R) of a detector refers to its capacity to distinguish between two peaks with a small energy difference .The following equation can be used to calculate resolution[119]:

$$R = \frac{FWHM}{C} \times 100\ \% \ldots\ldots\ldots (3-4)$$

Where 'FWHM' is the full width at half maximum for the photo peak of a gamma rays source's spectrum, and 'C' is the channel number at the gamma peak's centroid[118]. The value of R in this study is (7.4 %) ^{137}Cs with standard source energy 661.66 KeV, figure illustrates (3.17).

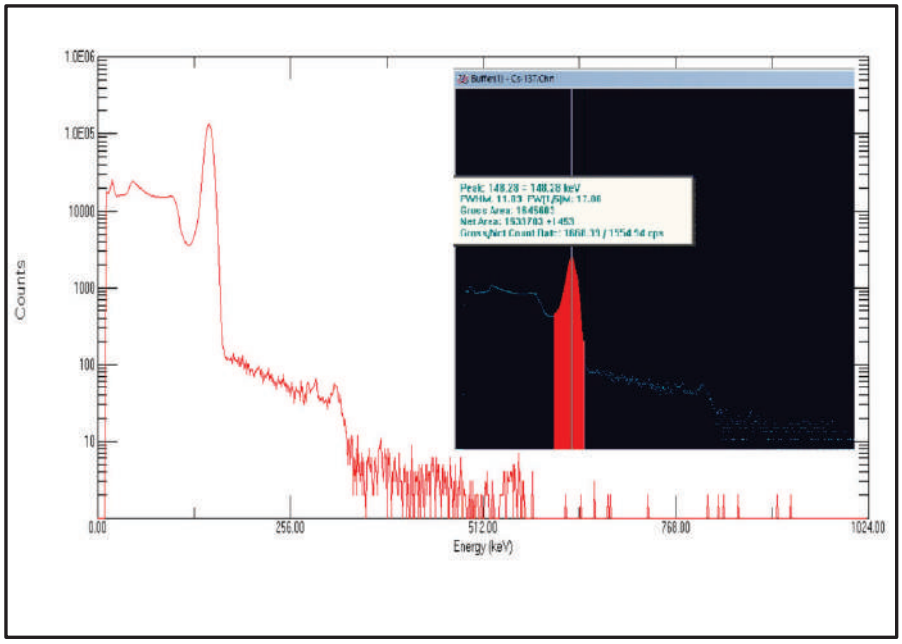

Figure (3.17): Spectrum of ^{137}Cs using (Maestro-32).

3.4.2.4 Background and Samples Measurement

The net zone under the comparing photograph tops is determined in the energy range by subtracting check because of background sources from the net zone of a specific top by utilizing MAESTRO-32 information examination bundle. The background range estimated by utilizing capacity empty (1L) polyethylene plastic marinelli. Due to the poor resolution of NaI(TI) detector, at low gamma energies which haven't well-isolated photo-peaks, containers on the indicator and checking in the meantime for the sample estimations[120]. In this manner, the measuring of the specific activity (Bq/kg) activity concentrations is possible at well-separated photopeaks high energies as that acquired in our outcomes from the gamma beams produced by the progenies of (^{232}Th) and (^{238}U), which are in common harmony with them while (^{40}K) is assessed specifically by its gamma-line of 1460 keV (^{40}Ar). Hence, the specific activity of (^{238}U) is determined using the gamma-lines 1765 keV (^{214}Bi). Similar results have been calculated of (^{232}Th) are identified using the gamma-ray lines 2614 keV (^{208}Ti), as shown in figure (3.18)[121].

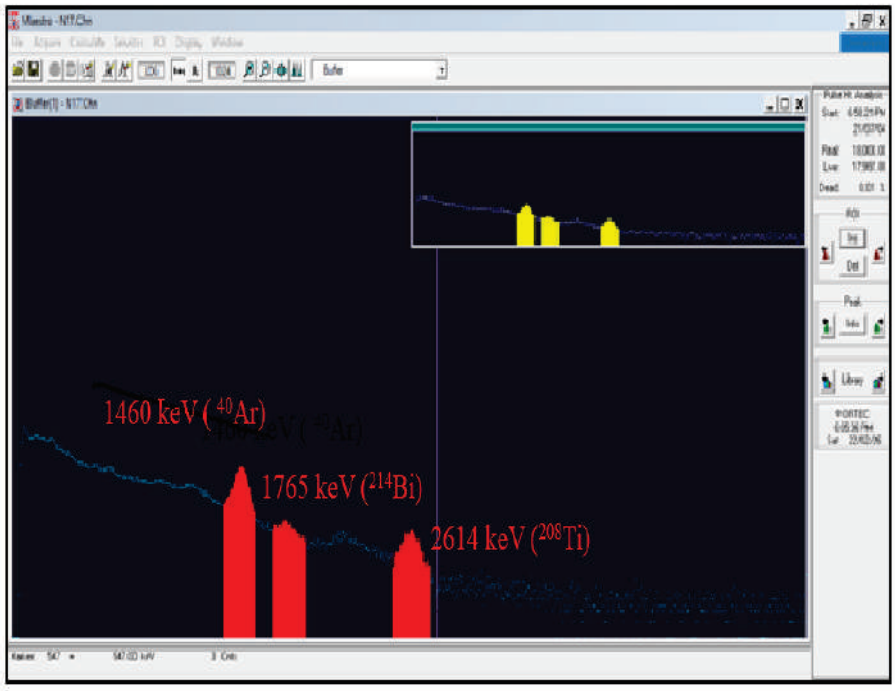

Figure (3.18): MAESTRO-32 software.

3.4.3 CR-39 Track Detector

The collection and processing of ornamental materials samples utilized in the track methodology are identical to that employed in the NaI(Tl) approach. Each sample are assigned a unique code in order to differentiate them. TASTRAK Analysis System, Ltd., UK: TASTRACK sold the detector CR-39 ($C_{12}H_{18}O_7$). A CR-39 detector sheet had dimensions of (2.5cm × 2.5cm), a thickness of (1mm), and a code for each sheet that suited the TASL image system (figure 3.19). The sheet has a density of almost 1.3 gm.cm $^{-3}$.

Figure (3.19): CR-39 detector (TASTRAK, made in UK).

3.4.3.1 Sample Container

The sample name and storage date are inscribed on the sealed plastic cans, which have dimensions of (12 cm) high and (6 cm) in average diameter. The plastic container utilized in this investigation is shown in Figure (3.20). The detectors (CR-39) are adhered to the upper section of the containers using adhesive tape, and the containers are subsequently filled with ornamental materials samples of varying thickness (h=3 cm), as well as the distance between the sample and the detector (L=9 cm), as illustrated in figure (3.21). To prevent Radon gas from escaping out, the containers' covers are fastened with a layer of adhesive tape. In the present study the samples are kept in nuclear laboratory of University of Kufa, Faculty of Science, Department of physics for 120 days. The current investigation uses a long-term irradiation approach. After the irradiation period has ended, the detectors are removed from the containers and the chemical etching procedure begins.

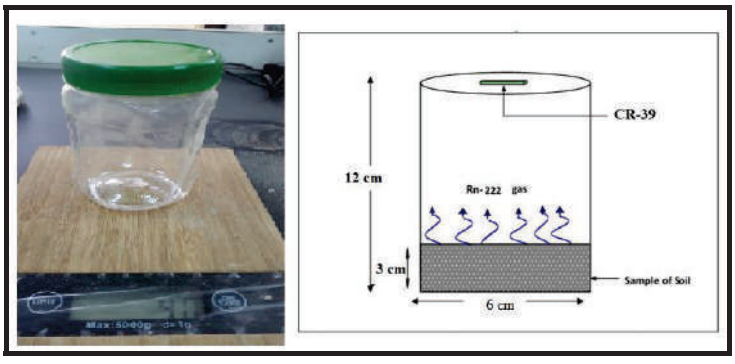

Figure (3.21) A plastic container that used in present study.

3.4.3.2 Chemical of Etchant Solution

Sodium hydroxide (NaOH) solution is made by dissolving (100) gm of (NaOH) in (0.4) Litter of pure water using the equation[122]:

$W = W_{eq} \times N \times V$ ….. (3 – 5)

Where W denotes the weight of NaOH required creating the specified normalcy, W_{eq} is weight equivalent for NaOH, N denotes the normalcy, and V is distilled water volume as in figure (3.21).

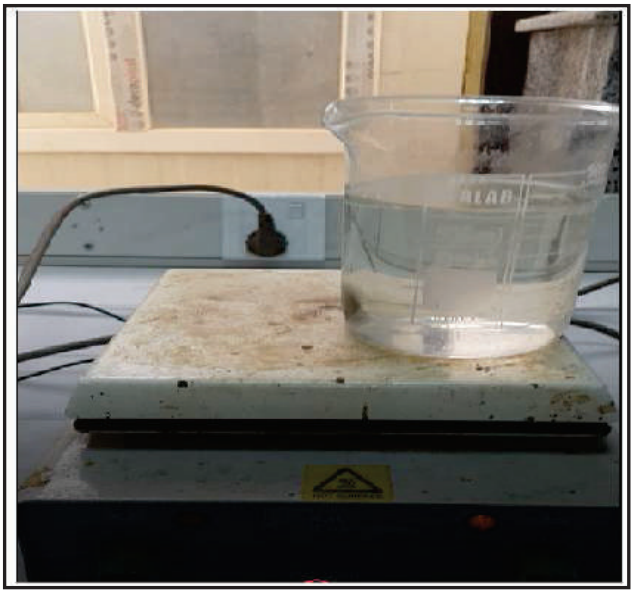

Figure (3.21): Magnetic stirrer (HP-3000, made in USA).

CR-39 detectors are placed in a solution of NaOH at 6.25 N and put Pyrex in a HH-1 electrical water bath and it is fix its at 98˚C within one hours as shown in figure (3.22a), then the slides are fixed in iron ties in special nippers and lower them into the chemical solution that has been prepared as in the figure (3.22b). Finally, the detectors are taken out of the solution and thoroughly cleaned with distilled water before being dried with soft tissue paper as in figure (3.22c).

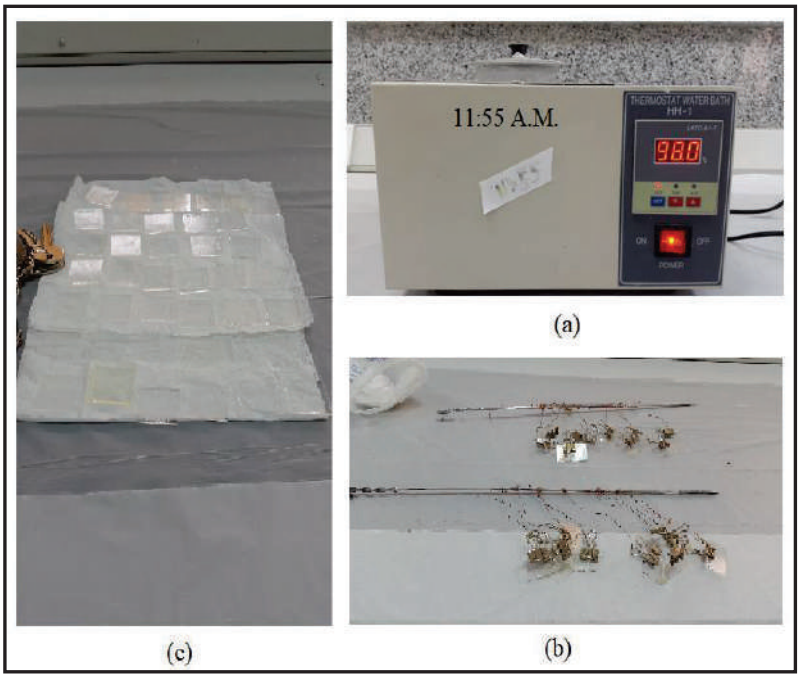

Figure (3.22) Chemical prepared steps of tracks.

3.4.3.3 Optical Microscope

Counting the engraved tracks on a detector is the only need. The widths and forms of etch pit "tracks" vary, of course: vertically incident Alpha particles generate circular etch pits. The bulk of etch pits is elliptical, as a result of Alpha particles colliding with the detector surface at lesser dip angles. Then any minor etch pits are continuously ignored, and any scratches are readily overlooked[122]. A microscopic treatment is used in this work to quantify radon concentrations in ornamental materials using the TASLIMAGE technology.

The TASLIMAGE dosimeter system as shown in figure (3.23) is a full laboratory system that includes a "TASLIMAGE microscope", "an etch tank", "a drying cabinet", "trays", and a PC that runs the analysis software [122].

Our neutron dosimetry system is a complete system for measuring fast neutrons, comprising the TASLIMAGE microscope based analysis system, etch tank, drying cabinet, trays and a PC running the analysis software. From the moment detectors are returned for analysis, they can be mounted in a tray which can be used for keeping them in place during the etching and afterwards be placed on the TASLIMAGE system for subsequent analysis .

The TASLIMAGE analysis system is a fully automated microscope based track analysis system, based on ultra-fast 3-axis motorized control and high quality Nikon optics. It can be used as a fully automatic readout system for dosimetry services with a throughput of 30-60 seconds per detector or detectors can be scanned individually. The scan data is automatically converted into a dose measurement and the measured dose and the track density are displayed in a database, indicating any issues which might have resulted in a poor result [123].

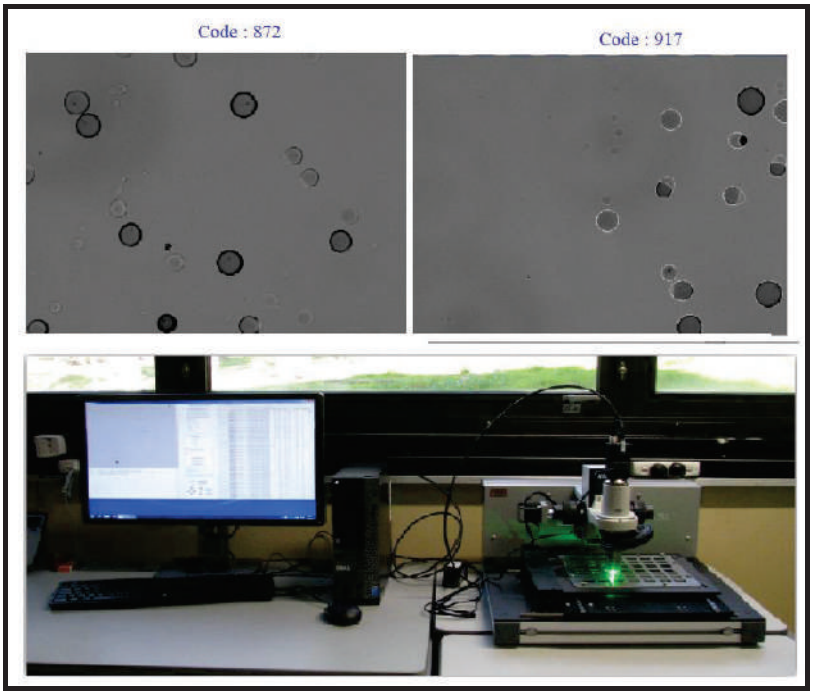

Figure (3.23) TASLEIMAGE system.

The main characteristics of TASLIMAGE are [123]:

1. A highly sophisticated image analysis system supplied with 64-bit Dell computer & Windows 10 (upgrade to Windows 11 pending).

2. Fully automated high specification system with high throughput and unparalleled accuracy and low background. The system can read both our own proprietary format of detectors, and also the "Auto-scan" style of detectors, including automatic ID reading.

3. Nikon optics with x20 objective. Other lens sizes are available. Highly stable, long-life LED light source.

4. GO-5000-USB Camera providing10 bit images (1024 grey levels) and 2560 x 2048 pixels. Standard magnification is 0.5 mm per pixel and corresponding image frame 1.278 x 1.024 mm.

5. Sophisticated autofocus, including live tracking of the plastic surface. Download presentation showing the autofocus and live tracking.

6. Ultrafast scanning speed, typically 100 mm^2 s^{-1} on exposed plastics.

7. All necessary software and work instructions.

8. Optional stainless steel mounting frames for plastic etching and analysis, standard size or customer specified.

9. The scan data are translated to dosage automatically, and the findings are instantly shown in the TASLIMAGE software's record-keeping database. Data can also be exported using tools like Excel [124].

3.5 Calculations of gamma and alpha emitters

In this point, the theoretical equations that work in the calculation of concentration and risk factors of radioactivity and radon are discussed, which include both gamma and alpha emitters.

3.5.1 Gamma Emitters

3.5.1.2 *Specific Activity (A)*

The following equation (3 − 10) is accustomed to compute the specific activity of ^{238}U, ^{232}Th, and ^{40}K (A_U, A_{Th}, and A_k) radionuclides[125][126].

$$A\left(\frac{Bq}{Kg}\right) = \frac{C}{I\gamma\,\varepsilon\,M\,t} \pm \frac{\sqrt{C}}{I\gamma\,\varepsilon\,M\,t} \dots\dots\dots (3-10)$$

Where, C is net area (under photo peak), I_γ is the probability of gamma-ray emitted, ε is the detector efficiency, M and t are the mass samples, and the time measured, respectively. But to calculate the specific activity of ^{235}U [125][126] .

$$A_{^{235}U} = \frac{A_{^{238}U}}{21.7} \dots\dots\dots (3-11)$$

3.5.1.3 External Hazard Index (H_{ex})

Using the following equation (3− 12), the external hazard index is calculated [127].

$$H_{ex} = \frac{A_u}{370} + \frac{A_{Th}}{259} + \frac{A_k}{4810} \dots\dots\dots (3-12)$$

3.5.1.4 Internal Hazard Index (H_{in})

The following equation (3-13) is used to determine the internal hazard index[127].

$$H_{in} = \frac{A_u}{185} + \frac{A_{Th}}{259} + \frac{A_k}{4810} \dots\dots\dots (3-13)$$

3.5.1.5 Representative Level Index (I_γ)

The following equation (3-14) is used to generate the representative level index[14].

$$I_\gamma = \frac{1}{150} A_u + \frac{1}{100} A_{Th} + \frac{1}{1500} A_k \dots\dots\dots (3-14)$$

3.5.1.6 Alpha Index

The following equation (3-15) is used to determine the alpha index[127].

$$I_\alpha = \frac{A_u}{200\ (\frac{Bq}{Kg})} \dots\dots\dots (3-15)$$

3.5.1.7 Radium Equivalent Activity (Ra_{eq})

The following equation (3-16) is used to compute radium equivalent activity[128].

$$R_{aeq}\left(\frac{Bq}{Kg}\right) = A_u + 1.43\ A_{Th} + 0.077\ A_k \dots\dots\dots (3-16)$$

3.5.1.8 Exposure Rate (X)

The following equation (3-17) is used to compute the exposure rate[127][128].

$$X\left(\frac{\mu R}{h}\right) = 1.90 A_u + 2.82\ A_{Th} + 0.197\ A_k \dots\dots\dots (3-17)$$

3.5.1.9 Absorbed Dose Rate in Air (D_r)

The following equation (3-18) is used to get the D_r a distance of 1 meter [129].

$$D_r\left(\frac{nGy}{h}\right) = 0.462A_u + 0.604A_{Th} + 0.0417\,A_k \dots\dots\dots (3-18)$$

3.5.1.10 Annual Gonadal Equivalent Dose (AGED)

Equation (3-19) can be used to compute the annual gonadal equivalent dose [130].

$$AGED\left(\frac{mSv}{y}\right) = 3.09A_u + 4.18A_{Th} + 0.314\,A_k \dots\dots\dots (3-19)$$

3.5.1.11 Annual Effective Dose Equivalent (AEDE)

Equation (3-20) can be used to compute the AEDE outdoor[131].

$$AEDE_{out} = D_r\left(\frac{nGy}{h}\right) \times 8760\ (h) \times 0.2 \times 0.7 \times \frac{Sv}{Gy} \times 10^{-3} \dots\dots\dots (3-20)$$

3.5.1.12 Excess Lifetime Cancer Risk (ELCR)

The ELCR for the public due to natural radioactivity is estimated using equation (3-21), based on DL " Duration of Life" that equal 70 years, as well as RF " Risk Factor" that equal 0.05 Sv/y), as following[131].

$$ELCR = AEDE \times DL \times RF \dots\dots\dots (3-21)$$

3.5.2 Alpha Emitters

The formula (3-22) is used to compute the radon concentration in the tube's airspace (C)[132].

$$C\left(\frac{Bq}{m^3}\right) = \frac{\rho}{Kt} \dots\dots\dots (3-22)$$

ρ is the number of tracks per cm^2 in the (CR-39) detector, t is the exposure period (90) day, and K is the calibration factor of CR-39 plastic path detector's, where figure (3.24) shows the value of slope as a calibration factor (K) for dosimeters exposed is (0.28±0.043) $Track.cm^{-2}$ /$Bq.m^{-3}$.day. Other people's calibration factors for CR-39 detectors. Table (3.4) shows the results of previous research.

The radon concentration in the sample are used to compute as in equation (3-23)[132].

$$C_{Rn}\left(\frac{Bq}{m^3}\right) = C\ \frac{\lambda ht}{L} \dots\dots\dots (3-23)$$

Where, C_{Rn} is the ^{222}Rn concentration in the sample (in Bq/m^3), h is the sample thickness (3cm), and L is the distance between the detector to sample, which equal (9 cm).

The annual effective dose (AED) attributable to radon concentrations in samples is determined using the formulas found in equation (3-24)[132].

$$AED\left(\frac{mSv}{y}\right) = C \times F \times H \times T \times D \dots\dots\dots (3-24)$$

Where H is the occupancy factor (0.8), F is the equilibrium factor (0.4), T is the year in hours (8760 h/y), and D is the dose conversion factor [$9x10^{-6}$ (mSv) / ($Bq.h.m^{-3}$). The radium content in the sample is to be computed by equation (3-25)[133].

$$C_{Ra}\left(\frac{Bq}{Kq}\right) = \left(\frac{\rho}{K\,.\,T_{eff}}\right)\left(\frac{hA}{M}\right) \dots\dots\dots (3-25)$$

C_{Ra} is the radium activity of samples, M is the sample mass, A is the cross-sectional area of the cylindrical container, and t_{eff} is the actual exposure time, which could be calculated using the formula below[134].

$$T_{eff} = [\,T - \lambda_{Rn}^{-1}\left(1 - e^{-\lambda_{Rn}T}\right) \dots\dots\dots (3-26)$$

For the emission of ^{222}Rn Radon gas, the mass exhalation rate (E_M) of the samples is estimated[135].

$$E_M = \frac{CV\lambda}{MT_{eff}} \dots\dots\dots (3-27)$$

For the emission of Radon gas, the surface exhalation rate (E_A) of the samples is estimated using the formula[136].

$$E_A = \frac{CV\lambda}{A\,T_{eff}} \dots\dots\dots (3-28)$$

The uranium activity (C_U) of the samples is found using formula[137].

$$C_U(ppm) = \frac{W_U}{W_S} \dots\dots\dots (3-29)$$

The weight of uranium in samples is W_U, while the weight of the sample is W_S .

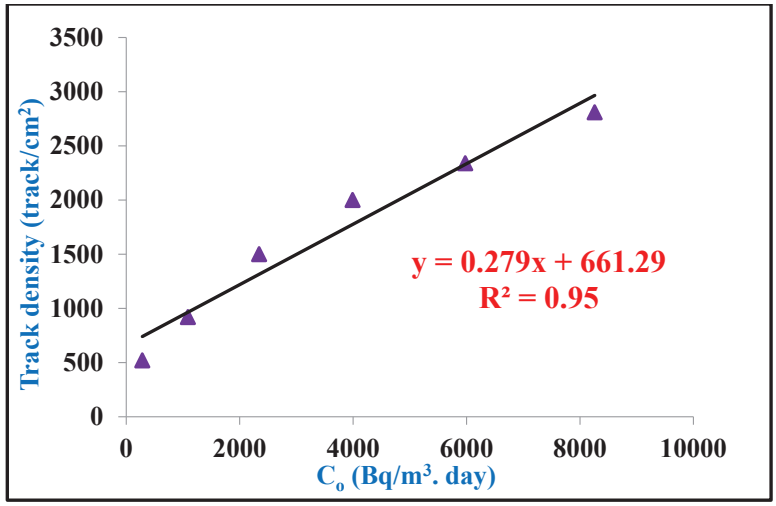

Figure (3.25): Curve of calibration factor for CR-39 in the present study.

Table (3.4) Comparison of K in this study.

No.	K (Track.cm^{-2} /Bq.m^{-3}.day)	Reference
1	0.2	[138]
2	0.18	[139]
3	0.2217	[140]
4	0.2279	[141]
6	0.212	[142]
7	0.2758	[143]
8	**0.28**	**This study**

4.1 Introduction

This chapter shows the results of the natural radioactivity due to long-lived gamma emitters (^{238}U,^{232}Th, and ^{40}K) and alpha emitters (^{222}Rn, ^{226}Ra, and ^{238}U) in one-hundred samples of soil samples (40 samples from Kufa city and 60 samples from Najaf city) using more than one technique: Dosimeter, Gamma spectroscopy with NaI(Tl) detector, solid-state nuclear track detectors (CR-39) and RAD-7. As well as, the results of radiological based on Gamma emitters and Alpha emitters are shown and drawn with GIS (ArcGIS 10.7.1). Next, discussions, conclusions and recommendations are shown.

4.2 Results of Dosimeter Detector

Background radiation in soil samples for all one-hundred samples is determined by using a portable Radiation Alert Inspector dosimeter (S.E. International Inc., USA), named Geiger Mueller (G.M.).

4.2.1 Results of Kufa City

The present study focuses on Dose rate (D), Annual Average Effective Dose (AAED), and Excess Lifetime Cancer Risk (ELCR) due to the natural background in soil samples at different sites in Kufa city at Najaf governorate. The average values of D, AAED, and ELCR are 0.127±0.005 μSv/h, 1.12±0.04 mSv/y and (3.90±0.15) $\times 10^{-3}$, respectively. The highest values of D and AAED are 0.203±0.020 μSv/hr, and 1.78 mSv/y in Alshorta district which are lower than the average of worldwide limits of 0.247 μSv/hr and 2.4 mSv/y, respectively.

From Table (4.1), the values of dose rates are ranged from 0.047±0.005 μSv/h to 0.203±0.020 μSv/hr, with an average value of 0.127±0.005 μSv/h. Results of AAED ranged (0.41 mSv/y–1.78 mSv/y), an average value of 1.12±0.04mSv/y, while ELCR ranged (1.44×10^{-3} –6.22×10^{-3}), an average value (3.90±0.15) × 10^{-3}. The highest dose rate value is found in sample K22 from Alshorta districts, while the lowest is in sample K39 from Alsadar – Third 1 districts.

Table (4.1) Results of Dose rate, AAED, and ELCR in soil samples of Kufa city.

Sample code	*Dose rate (μSv/h)*		*AAED (mSv/y)*	*ELCR×10^{-3}*
	Average	*±S.E.*		
K1	0.083	0.008	0.73	2.54
K2	0.137	0.014	1.20	4.20
K3	0.113	0.011	0.99	3.46
K4	0.131	0.013	1.15	4.02
K5	0.095	0.010	0.83	2.91
K6	0.131	0.013	1.15	4.02
K7	0.089	0.009	0.78	2.73
K8	0.119	0.012	1.04	3.65
K9	0.107	0.011	0.94	3.28
K10	0.155	0.016	1.36	4.75
K11	0.137	0.014	1.20	4.20
K12	0.191	0.019	1.67	5.86
K13	0.113	0.011	0.99	3.46
K14	0.143	0.014	1.25	4.38
K15	0.167	0.017	1.46	5.12
K16	0.143	0.014	1.25	4.38
K17	0.185	0.019	1.62	5.67
K18	0.155	0.016	1.36	4.75
K19	0.079	0.008	0.69	2.42
K20	0.131	0.013	1.15	4.02
K21	0.125	0.013	1.10	3.83
K22	0.203	0.020	1.78	6.22
K23	0.107	0.011	0.94	3.28
K24	0.131	0.013	1.15	4.02
K25	0.137	0.014	1.20	4.20

Next

K26	0.107	0.011	0.94	3.28
K27	0.089	0.009	0.78	2.73
K28	0.125	0.013	1.10	3.83
K29	0.161	0.016	1.41	4.94
K30	0.101	0.010	0.88	3.10
K31	0.179	0.018	1.57	5.49
K32	0.143	0.014	1.25	4.38
K33	0.125	0.013	1.10	3.83
K34	0.131	0.013	1.15	4.02
K35	0.119	0.012	1.04	3.65
K36	0.149	0.015	1.31	4.57
K37	0.101	0.010	0.88	3.10
K38	0.113	0.011	0.99	3.46
K39	0.047	0.005	0.41	1.44
K40	0.095	0.010	0.83	2.91
Average± S.E.	***0.127±0.005***		***1.12±0.04***	***3.90±0.15***

4.2.2 Results of Najaf City

The dose rate to the background radiation of soil samples collected from all Najaf city at Najaf governorate, Iraq. Also, annual average effective dose (AAED) and excess lifetime cancer risk (ELCR) are determined as well as all results are drawn by the GIS (ArcGIS 10.7.1) technique. The results show that the average values with stander error for dose rate (μSv/h), AAED (mSv/y), and ELCR$\times 10^{-3}$ are 0.121±0.004, 1.06±0.03, and 3.73±0.12, respectively.

From Table (4.2), it is found the values of dose rates are ranged from 0.077μSv/h to 0.191μSv/hr, with an average value of 0.121±0.004 μSv/h. Also, it is found that the results of AAED are ranged from 0.67 mSv/y to 1.67 mSv/y, with an average value of 1.06±0.03 mSv/y, while ELCR in soil samples of the present study are ranged from 2.36×10^{-3} to 5.86×10^{-3} with an average value $(3.73\pm 0.12)\times 10^{-3}$. The highest dose rate value is found in sample N6 from Al Milad district, while the lowest is in sample N13 from AlMakrama-1 communities.

Table (4.2) Results of Dose rate, AAED, and ELCR in soil samples of Najaf city.

Sample code	*Dose Rate (μSv/h)*		*AAED (mSv/y)*	*ELCR×10^{-3}*
	Average	*±S.E.*		
N1	0.083	0.0083	0.73	2.54
N2	0.119	0.0119	1.04	3.65
N3	0.131	0.0131	1.15	4.02
N4	0.167	0.0167	1.46	5.12
N5	0.126	0.0126	1.10	3.83
N6	0.191	0.0191	1.67	5.86
N7	0.095	0.0095	0.83	2.91
N8	0.107	0.0107	0.94	3.28
N9	0.155	0.0155	1.36	4.75
N10	0.101	0.0101	0.88	3.10
N11	0.095	0.0095	0.83	2.91
N12	0.113	0.0113	0.99	3.46
N13	0.077	0.0077	0.67	2.36
N14	0.149	0.0149	1.31	4.57
N15	0.125	0.0125	1.10	3.83
N16	0.161	0.0161	1.41	4.94
N17	0.114	0.0114	0.99	3.46
N18	0.137	0.0137	1.20	4.20
N19	0.101	0.0101	0.88	3.10
N20	0.119	0.0119	1.04	3.65
N21	0.079	0.0079	0.67	2.36
N22	0.083	0.0083	0.73	2.54
N23	0.107	0.0107	0.94	3.28
N24	0.138	0.0138	1.20	4.20
N25	0.089	0.0089	0.78	2.73
N26	0.118	0.0118	1.04	3.65
N27	0.083	0.0083	0.73	2.54
N28	0.136	0.0136	1.20	4.20

Next

N29	0.089	0.0089	0.78	2.73
N30	0.112	0.0112	0.99	3.46
N31	0.155	0.0155	1.36	4.75
N32	0.089	0.0089	0.78	2.73
N33	0.131	0.0131	1.15	4.02
N34	0.107	0.0107	0.94	3.28
N35	0.149	0.0149	1.31	4.57
N36	0.125	0.0125	1.10	3.83
N37	0.161	0.0161	1.41	4.94
N38	0.168	0.0168	1.46	5.12
N39	0.095	0.0095	0.83	2.91
N40	0.179	0.0179	1.57	5.49
N41	0.095	0.0095	0.83	2.91
N42	0.078	0.0078	0.67	2.36
N43	0.089	0.0089	0.78	2.73
N44	0.125	0.0125	1.10	3.83
N45	0.209	0.0209	1.83	6.41
N46	0.135	0.0135	1.20	4.20
N47	0.071	0.0071	0.62	2.18
N48	0.161	0.0161	1.41	4.94
N49	0.143	0.0143	1.25	4.38
N50	0.113	0.0113	0.99	3.46
N51	0.149	0.0149	1.31	4.57
N52	0.125	0.0125	1.10	3.83
N53	0.107	0.0107	0.94	3.28
N54	0.125	0.0125	1.10	3.83
N55	0.107	0.0107	0.94	3.28
N56	0.113	0.0113	0.99	3.46
N57	0.167	0.0167	1.46	5.12
N58	0.119	0.0119	1.04	3.65
N59	0.101	0.0101	0.88	3.10
N60	0.113	0.0113	0.99	3.46

Next

Average± S.E.	*0.121±0.004*	*1.06±0.03*	*3.73±0.12*
Global limit[144]	*0.274*	*2.4*	--------

4.3 Results of Gamma spectroscopy using NaI(Tl)

Natural background radiation in soil samples for all one-hundred samples is determined by using Gamma spectroscopy, named NaI(Tl).

4.3.1 Results of Kufa city with NaI(Tl) detector

The specific activity of natural radionuclides (^{238}U, ^{232}Th,^{40}K, and ^{235}U) in the Kufa city' soil is shown in Table (4.3). While Table (4.4) and Table (4.5) show the radiological parameters R_{aeq}, H_{ex}, H_{in}, $I_{\gamma r}$, I_{α} and Exposure, D_r, AGED, $AEDE_{outdoor}$, ELCR, respectively.

The specific activity of uranium-238 in the studied area is ranged from 0.4± 0.1 Bq/kg to 17.9±0.9 Bq/kg, with an average value of 6.2±0.74 and from 0.2±0.1 Bq/kg to 24.1±0.6 Bq/kg with an average value of 6.41±0.82 Bq/kg for thorium-232, from 103.5±2.0 Bq/kg to 708.0±5.9 Bq/kg with an average value of 278.10±19.43 Bq/kg for potassium-40. In contrast, the specific activity of uranium-235 is ranged from 0.018±0.01 Bq/kg to 0.825±0.08 Bq/kg with an average value of 0.28±0.03 Bq/kg. The highest value of the specific activity of ^{238}U, ^{232}Th, and ^{235}U is seen in the K19 sample (Aljamea district), while ^{40}K is in K17sample (Alsehilia 2 district). The lowest value of the specific activity of ^{238}U, ^{232}Th, ^{40}K, and ^{235}U is found in samples K10, K26, K31, and K10, respectively.

Table (4.3) The specific activity for natural radioactivity in soil for Kufa city.

Sample code	*Specific Activity (Bq/kg)*							
	^{238}U		*^{232}Th*		*^{40}K*		*^{235}U*	
	Average	**±S.D.**	**Average**	**±S.D.**	**Average**	**±S.D.**	**Average**	**±S.D.**
K1	5.3	0.5	1.3	0.1	109.9	2.2	0.244	0.04
K2	4.9	0.5	1.2	0.1	142.4	2.5	0.226	0.04

Next

K3	2.3	0.3	0.7	0.1	145.4	2.5	0.106	0.03
K4	2.9	0.3	2.2	0.2	176.4	2.7	0.134	0.03
K5	2.8	0.3	1.4	0.2	150.0	2.6	0.129	0.03
K6	5.4	0.5	6.2	0.3	130.7	2.5	0.249	0.04
K7	1	0.2	6.9	0.4	303.0	4.0	0.046	0.02
K8	1.1	0.2	1.5	0.1	184.3	2.7	0.051	0.02
K9	9.1	0.6	1	0.1	226.5	3.3	0.419	0.06
K10	0.4	0.1	2.2	0.2	210.1	3.0	0.018	0.01
K11	0.9	0.2	3.1	0.2	167.2	2.8	0.041	0.02
K12	6.9	0.5	15.3	0.5	336.8	4.0	0.318	0.05
K13	6.6	0.6	6.7	0.3	339.3	4.1	0.304	0.05
K14	3.3	0.3	1.6	0.1	109.0	2.1	0.152	0.03
K15	4.5	0.5	13.6	0.5	443.3	4.7	0.207	0.04
K16	2.1	0.3	6.4	0.3	537.0	5.1	0.097	0.03
K17	7.6	0.6	13.2	0.5	708.0	5.9	0.350	0.05
K18	14.1	0.8	12.5	0.4	113.8	2.3	0.650	0.07
K19	17.9	0.9	24.1	0.6	389.8	4.4	0.825	0.08
K20	11.4	0.7	9.1	0.4	303.1	3.7	0.525	0.06
K21	1.2	0.2	1.4	0.1	229.3	3.1	0.055	0.02
K22	13.1	0.8	8.5	0.4	316.7	3.9	0.604	0.07
K23	8.4	0.6	10	0.4	317.9	3.8	0.387	0.05
K24	10.2	0.7	11.3	0.4	307.8	3.8	0.470	0.06
K25	5.8	0.5	15.4	0.5	396.5	4.5	0.267	0.05

K26	0.91	0.2	0.2	0.1	181.6	2.9	0.041	0.02
K27	14.2	0.8	8.5	0.4	279.0	3.6	0.654	0.07
K28	2.4	0.3	6.6	0.3	395.3	3.9	0.111	0.03
K29	14.1	0.8	9.1	0.4	320.6	3.9	0.650	0.07
K30	8.4	0.6	2.9	0.2	333.1	4.0	0.387	0.05
K31	1.7	0.2	1.5	0.1	103.5	2.0	0.078	0.02
K32	13.2	0.7	6.8	0.3	300.8	3.7	0.608	0.07
K33	3.5	0.4	8.4	0.4	292.2	3.7	0.161	0.04
K34	1.4	0.2	8.1	0.4	425.9	4.6	0.065	0.02
K35	3.2	0.4	5.7	0.3	283.9	3.7	0.147	0.03
K36	2.4	0.3	5.8	0.3	312.5	3.3	0.111	0.03
K37	6.4	0.5	2.2	0.2	241.1	3.0	0.295	0.05
K38	6.5	0.6	3.9	0.3	299.3	3.9	0.300	0.05
K39	5	0.5	0.6	0.1	238.8	3.4	0.230	0.04
K40	15.5	0.9	9.6	0.4	322.3	4.2	0.714	0.07
Average± S.D.	6.2±0.74		6.41±0.82		278.10±19.43		0.28±0.03	

Next

Table (4.4) The radiological parameters (Ra_{eq}, H_{ex}, H_{in}, $I_{\gamma r}$, and I_{α}) for nature radioactivity in soil for Kufa city.

Sample code	Ra_{eq} (Bq/kg)	H_{ex}	H_{in}	$I_{\gamma r}$	I_{α}
K1	15.6	0.042	0.057	0.122	0.027
K2	17.6	0.047	0.061	0.140	0.025
K3	14.5	0.039	0.045	0.119	0.012

Next

K4	19.6	0.053	0.061	0.159	0.015
K5	16.4	0.044	0.052	0.133	0.014
K6	24.3	0.066	0.080	0.185	0.027
K7	34.2	0.092	0.095	0.278	0.005
K8	17.4	0.047	0.050	0.145	0.006
K9	28.0	0.076	0.100	0.222	0.046
K10	19.7	0.053	0.054	0.165	0.002
K11	18.2	0.049	0.052	0.148	0.005
K12	54.7	0.148	0.166	0.424	0.035
K13	42.3	0.114	0.132	0.337	0.033
K14	14.0	0.038	0.047	0.111	0.017
K15	58.1	0.157	0.169	0.462	0.023
K16	52.6	0.142	0.148	0.436	0.011
K17	81.0	0.219	0.239	0.655	0.038
K18	40.7	0.110	0.148	0.295	0.071
K19	82.4	0.222	0.271	0.620	0.090
K20	47.8	0.129	0.160	0.369	0.057
K21	20.9	0.056	0.060	0.175	0.006
K22	49.6	0.134	0.169	0.383	0.066
K23	47.2	0.127	0.150	0.368	0.042
K24	50.1	0.135	0.163	0.386	0.051
K25	58.4	0.158	0.173	0.457	0.029
K26	15.2	0.041	0.043	0.129	0.005

Next

K27	47.8	0.129	0.168	0.366	0.071
K28	42.3	0.114	0.121	0.346	0.012
K29	51.8	0.140	0.178	0.399	0.071
K30	38.2	0.103	0.126	0.307	0.042
K31	11.8	0.032	0.036	0.095	0.009
K32	46.1	0.124	0.160	0.357	0.066
K33	38.0	0.103	0.112	0.302	0.018
K34	45.8	0.124	0.127	0.374	0.007
K35	33.2	0.090	0.098	0.268	0.016
K36	34.8	0.094	0.100	0.282	0.012
K37	28.1	0.076	0.093	0.225	0.032
K38	35.1	0.095	0.112	0.282	0.033
K39	24.2	0.065	0.079	0.199	0.025
K40	54.0	0.146	0.188	0.414	0.078
Average ± S.E.	36.79±2.78	0.099±0.007	0.116±0.008	0.290±0.021	0.031±0.003

Table (4.5) The radiological parameters (X, D_r, AGED, $AEDE_{outdoor}$, and ELCR) for nature radioactivity in soil for Kufa city.

Sample code	*X(μR/h)*	*D_r (nGy/h)*	*AGED (mSv/y)*	*$AEDE_{outdoor}$ (mSv/y)*	*ELCR×10^{-3}*
K1	35.4	7.8	56.3	0.010	0.034
K2	40.7	8.9	64.9	0.011	0.038
K3	35.0	7.5	55.7	0.009	0.032
K4	46.5	10.0	73.5	0.012	0.043
K5	38.8	8.4	61.6	0.010	0.036

Next

K6	53.5	11.7	83.6	0.014	0.050
K7	81.0	17.3	127.1	0.021	0.074
K8	42.6	9.1	67.5	0.011	0.039
K9	64.7	14.3	103.4	0.017	0.061
K10	48.4	10.3	76.4	0.013	0.044
K11	43.4	9.3	68.2	0.011	0.040
K12	122.6	26.5	191.0	0.032	0.114
K13	98.3	21.2	154.9	0.026	0.091
K14	32.3	7.0	51.1	0.009	0.030
K15	134.2	28.8	209.9	0.035	0.124
K16	127.8	27.2	201.9	0.033	0.117
K17	191.1	41.0	301.0	0.050	0.176
K18	84.5	18.8	131.6	0.023	0.081
K19	178.8	39.1	278.4	0.048	0.168
K20	107.0	23.4	168.4	0.029	0.100
K21	51.4	11.0	81.6	0.013	0.047
K22	111.2	24.4	175.5	0.030	0.105
K23	106.8	23.2	167.6	0.028	0.099
K24	111.9	24.4	175.4	0.030	0.105
K25	132.6	28.5	206.8	0.035	0.122
K26	38.0	8.1	60.6	0.010	0.035
K27	105.9	23.3	167.0	0.029	0.100
K28	101.0	21.6	159.1	0.026	0.093

K29	115.6	25.4	182.3	0.031	0.109
K30	89.8	19.5	142.7	0.024	0.084
K31	27.8	6.0	44.0	0.007	0.026
K32	103.5	22.7	163.7	0.028	0.098
K33	87.9	18.9	137.7	0.023	0.081
K34	109.4	23.3	171.9	0.029	0.100
K35	78.1	16.8	122.9	0.021	0.072
K36	82.5	17.6	129.8	0.022	0.076
K37	65.9	14.3	104.7	0.018	0.062
K38	82.3	17.8	130.4	0.022	0.077
K39	58.2	12.6	92.9	0.015	0.054
K40	120.0	26.4	189.2	0.032	0.113
Average ± S.E.	***84.66±6.21***	***18.33±1.34***	***133.301±9.70***	***0.022±0.001***	***0.078±0.005***

The results of Ra_{eq} are ranged from 11.8 Bq/kg to 82.4 Bq/kg, with an average value of 36.79±2.78 Bq/kg. Also, the minimum and the maximum values of H_{ex}, H_{in}, $I_{\gamma r}$, and I_{α} in the same sample K31 and K19, as shown in Table (4.4). H_{ex} and H_{in} values ranged from 0.032 to 0.222, with an average of 0.099±0.007, and 0.036 to 0.271, with an average of 0.116±0.008, respectively. In addition, results of other parameters $I_{\gamma r}$ and I_{α} ranged 0.095 - 0.655, with an average of 0.290±0.021, and 0.009 - 0.09, with an average of 0.031±0.003, respectively.

The minimum and maximum values of all radiological parameters shown in Table (4.4) are in samples K31 (Kenda 2) and samples K19 (Aljamea), except the value of $I_{\gamma r}$ the most is in samples K17 (Alsehilia 2). The results of radiological parameters (Ra_{aeq}, H_{ex}, H_{in}, $I_{\gamma r}$, and I_{α}) in Table (4.4) for all soil samples under study are less than 370 Bq/kg for R_{aeq} and less than unity for the values of H_{ex}, H_{in}, $I_{\gamma r}$, and I_{α} .

Results of another radiological parameter shown in Table (4.5), X ranged from 27.8 μR/h to 191.1 μR/h, with an average value 84.66±6.21μR/h, the values of D_r ranged from 6.0 nGy/h to 41.0 nGy/h, with an average value of 18.33±1.34 nGy/h.

At the same time, results of AGED, $AEDE_{outdoor}$, and $ELCR\times10^{-3}$ are 44.0-301.0 mSv/y with an average value 133.301±9.70, 0.007-0.050 mSv/y with an average value of 0.022±0.001mSv/y, and 0.026-0.176 with an average value of 0.078±0.005, respectively. The minimum value of all radiological parameters shown in Table (4.5) which are (X, D_r, AGED, $AEDE_{outdoor}$, and ELCR) is in samples K31 (Kenda 2). In comparison, the maximum value is found in samples K17 (Alsehilia 2).

4.3.2 Results of Najaf City with NaI(Tl) Detector

The specific activity of natural radionuclides (^{238}U, ^{232}Th, ^{40}K, and ^{235}U) in the Najaf city soil is shown in Table (4.6). While Table (4.7) and Table (4.8) show the results of radiological parameters (Ra_{eq}, H_{ex}, H_{in}, I_γ, and I_α) and (X, D_r, AGED, $AEDE_{outdoor}$, and ELCR), respectively. The specific activity of uranium-238 in the studied area is ranged from 1.9± 0.3 Bq/kg to 46.5±1.7 Bq/kg, with an average value of 18.01±1.24, from 0.8±0.2 Bq/kg to 32.6±1.5 Bq/kg with an average of 13.4±0.91 Bq/kg for thorium-232, from 109.4±2.3 Bq/kg to 422.9±5.3 Bq/kg with an average value of 256.9±12.23 Bq/kg for potassium-40. In contrast, the specific activity of uranium-235 ranges from 0.09±0.3 Bq/kg to 2.14±1.66 Bq/kg with an average value of 0.83± 0.08 Bq/kg. The highest value of the specific activity of ^{238}U and ^{235}U is seen in the N17 sample Aljameea (Alresalah-1), while ^{40}K is in the N53 sample (Alkudos-1), and ^{232}Th is in sample N30 (Alkarama). The lowest value of the specific activity of ^{238}U, ^{40}K, and ^{235}U is found in sample N16, while ^{232}Th is seen in sample N24.

Table (4.6) The specific activity for natural radioactivity in soil for Najaf city.

Sample code	*Specific Activity (Bq/kg)*							
	^{238}U		^{232}Th		^{40}K		^{235}U	
	Average	**±S.D.**	**Average**	**±S.D.**	**Average**	**±S.D.**	**Average**	**±S.D.**
N1	8.8	0.7	6.0	0.6	192.2	3.3	0.4	0.06
N2	3.8	0.5	3.3	0.4	147.1	2.9	0.2	0.04
N3	23.5	1.0	18.2	0.9	210.5	3.0	1.1	0.09
N4	4.2	0.5	3.1	0.4	159.2	2.8	0.2	0.04
N5	11.3	0.7	14.8	0.8	374.7	4.1	0.5	0.06

N6	10.9	0.8	24.5	1.1	249.5	3.6	0.5	0.06
N7	19.4	1.0	27.0	1.2	274.7	3.9	0.9	0.08
N8	25.8	1.2	22.3	1.1	276.1	3.9	1.2	0.10
N9	8.0	0.6	7.4	0.6	140.5	2.6	0.4	0.05
N10	29.3	1.2	14.9	0.9	324.7	4.1	1.4	0.10
N11	11.7	0.8	24.7	1.1	371.1	4.2	0.5	0.06
N12	27.0	1.0	13.1	0.7	258.8	3.2	1.2	0.10
N13	10.1	0.7	12.0	0.8	285.9	3.8	0.5	0.06
N14	25.9	1.0	9.8	0.6	149.5	2.5	1.2	0.10
N15	13.6	0.9	6.4	0.6	134.1	2.8	0.6	0.07
N16	1.9	0.3	5.6	0.5	109.4	2.3	0.1	0.03
N17	46.5	1.7	17.9	1.0	351.3	4.6	2.1	0.13
N18	17.4	1.0	19.4	1.0	368.8	4.4	0.8	0.08
N19	21.4	0.9	9.2	0.6	130.7	2.3	1.0	0.09
N20	23.9	1.1	4.1	0.4	160.0	2.8	1.1	0.09
N21	21.3	1.0	4.4	0.5	153.6	2.7	1.0	0.09
N22	12.3	0.9	19.7	1.1	218.1	3.6	0.6	0.07
N23	17.7	0.9	11.7	0.8	355.5	4.2	0.8	0.08
N24	26.9	1.3	0.8	0.2	158.8	3.2	1.2	0.10
N25	14.2	0.8	12.8	0.8	224.2	3.3	0.7	0.07
N26	30.5	1.2	21.7	1.0	334.1	4.0	1.4	0.10
N27	14.1	0.7	14.2	0.7	193.2	2.7	0.7	0.07
N28	14.6	0.9	26.6	1.2	298.4	3.9	0.7	0.07
N29	5.5	0.5	16.1	0.9	230.0	3.3	0.3	0.04
N30	29.8	1.4	32.6	1.5	422.9	5.3	1.4	0.10
N31	28.4	1.2	22.0	1.1	373.4	4.4	1.3	0.10
N32	21.1	1.0	7.7	0.6	293.0	3.7	1.0	0.09
N33	19.5	1.0	15.4	0.9	250.4	3.7	0.9	0.08
N34	19.0	1.0	15.0	0.9	350.9	4.4	0.9	0.08
N35	4.9	0.5	3.3	0.4	111.0	2.2	0.2	0.04
N36	13.7	0.8	5.0	0.5	316.2	3.9	0.6	0.07
N37	10.1	0.7	13.8	0.8	349.8	4.2	0.5	0.06
N38	16.2	0.8	8.0	0.6	230.4	3.1	0.7	0.08
N39	5.7	0.6	20.8	1.1	330.1	4.2	0.3	0.05
N40	13.4	0.7	7.2	0.5	240.4	3.2	0.6	0.07
N41	20.8	0.9	10.7	0.7	128.7	2.3	1.0	0.09
N42	16.5	1.0	10.6	0.8	129.7	2.8	0.8	0.08
N43	3.2	0.4	13.0	0.9	281.5	4.2	0.1	0.03
N44	20.0	1.0	16.7	1.0	283.1	3.9	0.9	0.08
N45	19.3	0.9	17.8	0.9	369.7	4.1	0.9	0.08
N46	22.7	1.1	13.8	0.9	241.3	3.6	1.0	0.09
N47	24.5	1.0	23.4	1.0	262.8	3.3	1.1	0.09
N48	9.0	0.6	13.9	0.8	194.9	2.9	0.4	0.06
N49	2.6	0.4	14.7	0.8	282.4	3.7	0.1	0.03
N50	40.3	1.5	21.5	1.1	223.2	3.6	1.9	0.12

N51	28.2	1.3	11.0	0.8	350.8	4.4	1.3	0.10
N52	24.4	1.1	9.6	0.7	373.0	4.5	1.1	0.09
N53	25.8	1.3	11.8	0.9	533.8	6.0	1.2	0.10
N54	6.2	0.5	1.1	0.2	243.7	3.2	0.3	0.05
N55	13.4	0.8	5.6	0.5	155.5	2.9	0.6	0.07
N56	18.9	0.9	18.9	0.9	149.8	2.6	0.9	0.08
N57	37.5	1.5	14.2	0.9	436.5	5.0	1.7	0.12
N58	33.4	1.5	3.0	0.5	202.9	3.8	1.5	0.11
N59	9.8	0.6	13.6	0.7	125.3	2.1	0.5	0.06
N60	21.0	1.0	14.7	0.8	339.9	4.0	1.0	0.09
Average±S.D.	***18.01±1.24***		***13.36±0.91***		***256.86±12.23***		***0.83±0.44***	

Table (4.7) The radiological parameters (Ra_{eq}, H_{ex}, H_{in}, I_{γ}, and I_{α}) for nature radioactivity in soil for Najaf city.

Sample code	*Ra_{eq} (Bq/kg)*	*H_{ex}*	*H_{in}*	*I_{γ}*	*I_{α}*
N1	32.3	0.09	0.11	0.25	0.04
N2	19.9	0.05	0.06	0.16	0.02
N3	65.8	0.18	0.24	0.48	0.12
N4	20.9	0.06	0.07	0.17	0.02
N5	61.3	0.17	0.20	0.47	0.06
N6	65.1	0.18	0.21	0.48	0.05
N7	79.2	0.21	0.27	0.58	0.10
N8	79.0	0.21	0.28	0.58	0.13
N9	29.3	0.08	0.10	0.22	0.04
N10	75.7	0.20	0.28	0.56	0.15
N11	75.5	0.20	0.24	0.57	0.06
N12	65.7	0.18	0.25	0.48	0.14
N13	49.2	0.13	0.16	0.38	0.05
N14	51.5	0.14	0.21	0.37	0.13
N15	33.0	0.09	0.13	0.24	0.07
N16	18.3	0.05	0.05	0.14	0.01
N17	99.2	0.27	0.39	0.72	0.23
N18	73.5	0.20	0.25	0.56	0.09
N19	44.6	0.12	0.18	0.32	0.11
N20	42.0	0.11	0.18	0.31	0.12
N21	39.5	0.11	0.16	0.29	0.11
N22	57.3	0.15	0.19	0.42	0.06
N23	61.8	0.17	0.21	0.47	0.09
N24	40.3	0.11	0.18	0.29	0.13
N25	49.8	0.13	0.17	0.37	0.07
N26	87.2	0.24	0.32	0.64	0.15
N27	49.3	0.13	0.17	0.36	0.07
N28	75.7	0.20	0.24	0.56	0.07

Next

N29	46.3	0.12	0.14	0.35	0.03
N30	109.1	0.29	0.38	0.81	0.15
N31	88.7	0.24	0.32	0.66	0.14
N32	54.7	0.15	0.20	0.41	0.11
N33	60.8	0.16	0.22	0.45	0.10
N34	67.5	0.18	0.23	0.51	0.10
N35	18.1	0.05	0.06	0.14	0.02
N36	45.2	0.12	0.16	0.35	0.07
N37	56.8	0.15	0.18	0.44	0.05
N38	45.4	0.12	0.17	0.34	0.08
N39	60.9	0.164	0.180	0.466	0.029
N40	42.3	0.114	0.151	0.322	0.067
N41	46.0	0.124	0.181	0.332	0.104
N42	41.6	0.112	0.157	0.302	0.082
N43	43.5	0.118	0.126	0.339	0.016
N44	65.7	0.177	0.232	0.489	0.100
N45	73.2	0.198	0.250	0.553	0.096
N46	61.1	0.165	0.226	0.451	0.113
N47	78.2	0.211	0.278	0.573	0.122
N48	43.9	0.119	0.143	0.329	0.045
N49	45.3	0.122	0.130	0.352	0.013
N50	88.1	0.24	0.35	0.63	0.20
N51	71.0	0.19	0.27	0.53	0.14
N52	66.8	0.18	0.25	0.51	0.12
N53	83.8	0.23	0.30	0.65	0.13
N54	26.5	0.07	0.09	0.21	0.03
N55	33.4	0.09	0.13	0.25	0.07
N56	57.5	0.16	0.21	0.42	0.09
N57	91.4	0.25	0.35	0.68	0.19
N58	53.3	0.14	0.23	0.39	0.17
N59	39.0	0.11	0.13	0.29	0.05
N60	68.2	0.18	0.24	0.51	0.10
Average± S.E.	***56.9±2.65***	***0.15±0.007***	***0.20±0.009***	***0.43±0.019***	***0.09±0.006***

Table (4.8) The radiological parameters (X, D_r, AGED, $AEDE_{outdoor}$, and ELCR) for nature radioactivity in soil for Najaf city.

Sample code	*X (μR/h)*	*D_r (nGy/h)*	*AGED (mSv/y)*	*$AEDE_{outdoor}$ (mSv/y)*	*ELCR×10^{-3}*
N1	71.7	15.7	112.9	0.019	0.07
N2	45.6	9.9	71.8	0.012	0.04
N3	137.5	30.7	215.0	0.038	0.13
N4	48.2	10.5	76.1	0.013	0.04

N5	137.1	29.8	214.5	0.037	0.13
N6	138.9	30.2	214.4	0.037	0.13
N7	167.1	36.7	259.0	0.045	0.16
N8	166.4	36.9	259.8	0.045	0.16
N9	63.6	14.0	99.6	0.017	0.06
N10	161.7	36.1	254.9	0.044	0.15
N11	164.8	35.8	255.6	0.044	0.15
N12	139.3	31.2	219.5	0.038	0.13
N13	109.3	23.8	171.0	0.029	0.10
N14	106.4	24.1	168.1	0.030	0.10
N15	70.2	15.7	110.7	0.019	0.07
N16	40.9	8.8	63.5	0.011	0.04
N17	208.1	47.0	328.9	0.058	0.20
N18	160.3	35.1	250.4	0.043	0.15
N19	92.4	20.9	145.7	0.026	0.09
N20	88.3	20.2	141.0	0.025	0.09
N21	83.2	18.9	132.5	0.023	0.08
N22	122.0	26.7	189.0	0.033	0.11
N23	136.6	30.0	215.1	0.037	0.13
N24	84.7	19.5	136.3	0.024	0.08
N25	107.2	23.6	167.8	0.029	0.10
N26	184.8	41.1	289.7	0.050	0.18
N27	104.9	23.1	163.6	0.028	0.10
N28	161.6	35.3	250.2	0.043	0.15
N29	101.2	21.9	156.6	0.027	0.09
N30	232.0	51.1	361.4	0.063	0.22
N31	189.6	42.0	297.1	0.052	0.18
N32	119.5	26.6	189.4	0.033	0.11
N33	129.9	28.8	203.4	0.035	0.12
N34	147.5	32.5	231.6	0.040	0.14
N35	40.4	8.9	63.7	0.011	0.04
N36	102.4	22.5	162.6	0.028	0.10
N37	127.1	27.6	198.9	0.034	0.12
N38	98.7	21.9	155.8	0.027	0.09
N39	134.6	29.0	208.3	0.036	0.12
N40	93.3	20.6	147.3	0.025	0.09
N41	95.1	21.4	149.5	0.026	0.09
N42	86.6	19.4	135.7	0.024	0.08
N43	98.3	21.1	152.8	0.026	0.09
N44	140.9	31.2	220.6	0.038	0.13
N45	159.6	35.1	250.0	0.043	0.15
N46	129.7	28.9	203.8	0.035	0.12
N47	164.4	36.4	256.2	0.045	0.16
N48	94.7	20.7	147.1	0.025	0.09
N49	102.0	21.8	158.1	0.027	0.09

N50	181.0	40.9	284.2	0.050	0.18
N51	153.8	34.3	243.3	0.042	0.15
N52	146.8	32.6	232.5	0.040	0.14
N53	187.5	41.3	296.7	0.051	0.18
N54	62.8	13.7	100.1	0.017	0.06
N55	71.9	16.1	113.6	0.020	0.07
N56	118.8	26.4	184.6	0.032	0.11
N57	197.3	44.1	312.3	0.054	0.19
N58	111.8	25.7	179.3	0.031	0.11
N59	81.8	18.0	126.7	0.022	0.08
N60	148.2	32.7	232.9	0.040	0.14
Average± S.E.	***122.5±5.59***	***27.1±1.24***	***192.2±8.74***	***0.033±0.001***	***0.12±0.005***

The results of R_{aeq} range from 18.14 Bq/kg to 109.06 Bq/kg, with an average value of 56.9±2.65 Bq/kg. Also, the minimum and the maximum values of H_{ex}, H_{in}, I_{γ}, and I_{α} as shown in Table (4.7). H_{ex} and H_{in} values range from 0.05 to 0.29, with an average of 0.15±0.007, and 0.05 to 0.39, with an average of 0.20±0.009, respectively. In addition, results of other parameters I_{γ} and I_{α} range 0.14 - 0.81, with an average of 0.43±0.019, and 0.01 - 0.23, with an average of 0.09±0.006, respectively. The minimum and maximum values of all radiological parameters are shown in Table (4.7).

Results of another radiological parameter shown in Table (4.8), X ranged from 40.43 μR/h to 232.01 μR/h, with an average value 122.5±5.59 μR/h, the importance of D_r changes from 8.8 nGy/h to 51.13 nGy/h, with an average value of 27.1±1.24 nGy/h. At the same time, results of AGED, $AEDE_{outdoor}$, and $ELCR\times10^{-3}$ are 63.51-361.71 mSv/y with an average value 192.2±8.74, 0.01-0.06 mSv/y with an average value of 0.30.033±0.001 mSv/y, and 0.04- 0.22 with an average value of 0.12±0.005, respectively.

The minimum value of all radiological parameters shown in Table (4.8) (X, D_r, AGED, $AEDE_{outdoor}$, and ELCR). For AGED, $AEDE_{outdoor}$, and D_r are in sample N16 (Alaskari-2), also for $ELCR\times10^{-3}$ are in samples N2, N4, N16, and N35. In comparison, the maximum values of all radiological parameters are clear in sample N30 (Alkarama).

4.4 Results of CR-39 Detector

Radon (^{222}Rn) gas concentrations and also uranium and radium (^{238}U and ^{226}Ra) are measured for all one-hundred samples in the soil taken from Kufa and Najaf cities, Iraq. The

study is achieved by using Solid State Nuclear Track Detector (SSNTD), commercially known as CR-39, and purchased from TASTRAK Analysis System.

4.4.1 Results of Kufa City with CR-39 Detector

Table (4.9) shows the results of radon-222 gas concentration in air space (C), the radon-222 concentration in the samples (C_{Rn}), the specific activity of radium-226 (C_{Ra}), and uranium concentrations (C_U). Table (4.9) also shows the ranges of C and C_{Rn} values with its average value. The maximum value of C and C_{Rn} are found in sample K19, while the minimum is in sample K34. Also, Table (4.9) shows the range values of C_{Ra} and C_U and their average values. The maximum value of each C_{Ra} and C_U are observed in sample K22. While the minimum value of each C_{Ra} and C_U are observed in sample K34.

Table (4.10) shows the results of radiological risk such as annual effective dose (AED), radon exhalation rate per unit mass (E_M), and per unit surface (E_S), and Excess Lifetime Cancer Risk (ELCR), which are calculated in all soil samples. Table (4.10) shows the range and the average value of the results of the AED. Also shown in the Table (4.10) the range value of E_M (mBq/kg.h) and E_S (mBq/m^2.h) and their average values. Also the range value of ELCR due to radon gas in air space of the container, as shown in Table (4.10). It is noted that the range with an average value of the results AED is 0.019 - 0.603 mSv/y, 0.359±0.02 mSv/y. The range value of each E_M (mBq/kg.h) and E_S (mBq/m^2.h) with an average value that shown in Table (4.10) are 0.01-0.33, 0.18±0.08 and 0.71-22.72, 14±1 respectively. The range value of ELCR due to radon gas in air space of container as shown in Table(4.10) are 0.002×10^{-3}-0.09×10^{-3}, with an average $(0.048\pm0.008)\times10^{-3}$.

Table (4.9) Results of alpha emitters in soil samples of Kufa city.

Sample code	*C (Bq/m^3)*	*C_{Rn}(Bq/m^3)*	*C_{Ra}(Bq/kg)*	*C_U(ppm)*
k1	18.04	1177.80	0.034	0.056
k2	16.96	1107.84	0.030	0.051
k3	2.14	113.28	0.004	0.006
k4	14.14	923.20	0.022	0.037
k5	11.10	724.95	0.020	0.034
k6	18.39	1201.13	0.039	0.066
k7	3.57	233.23	0.007	0.013
k8	1.85	120.50	0.004	0.006

k9	19.64	1099.51	0.039	0.066
k10	0.92	60.25	0.002	0.003
k11	1.55	101.07	0.003	0.005
k12	16.79	887.38	0.028	0.046
k13	19.76	1290.53	0.050	0.084
k14	14.40	761.51	0.029	0.048
k15	14.35	936.80	0.031	0.052
k16	11.61	757.99	0.023	0.038
k17	17.95	1171.97	0.044	0.074
k18	21.40	1397.43	0.052	0.087
k19	23.90	1560.69	0.046	0.077
k20	19.32	1261.38	0.039	0.065
k21	1.82	118.56	0.003	0.005
k22	23.57	1539.31	0.053	0.090
k23	19.05	1243.89	0.036	0.060
k24	20.48	1337.18	0.046	0.076
k25	16.37	1068.96	0.040	0.068
k26	1.93	126.33	0.004	0.007
k27	21.58	1409.09	0.045	0.076
k28	15.89	1037.87	0.026	0.043
k29	22.71	1482.95	0.040	0.067
k30	18.51	1208.90	0.030	0.050
k31	2.83	184.64	0.005	0.008
k32	21.49	1403.26	0.053	0.088
k33	12.68	827.96	0.025	0.042
k34	0.74	48.59	0.001	0.002
k35	13.72	725.32	0.023	0.039
k36	16.76	1094.23	0.028	0.046
k37	19.14	1249.72	0.030	0.050
k38	14.94	789.83	0.034	0.057
k39	15.00	792.98	0.033	0.055
k40	23.10	1220.93	0.044	0.075
Minimum	***0.74***	***48.59***	***0.001***	***0.002***
Maximum	***23.90***	***1560.69***	***0.053***	***0.09***
Average± S.E.	***14±1***	***895±74***	***0.028±0.008***	***0.048±0.008***

Table (4.10) Results of AED, E_M, E_S, and ELCR in soil samples of Kufa city.

Sample code	*AED (mSv/y)*	*E_M (mBq/kg.h)*	*E_S (mBq/m^2.h)*	*ELCR X10^{-3}*
k1	0.455	0.21	17.15	1.59
k2	0.428	0.19	16.13	1.50
k3	0.054	0.02	2.04	0.19
k4	0.357	0.14	13.44	1.25
k5	0.280	0.13	10.55	0.98
k6	0.464	0.25	17.49	1.62

k7	0.090	0.05	3.40	0.32
k8	0.047	0.02	1.75	0.16
k9	0.496	0.24	18.67	1.73
k10	0.0239	0.015	0.88	0.08
k11	0.039	0.02	1.47	0.14
k12	0.423	0.18	15.96	1.48
k13	0.499	0.31	18.79	1.74
k14	0.363	0.19	13.69	1.27
k15	0.362	0.19	13.64	1.27
k16	0.293	0.14	11.03	1.02
k17	0.453	0.28	17.06	1.58
k18	0.540	0.32	20.34	1.89
k19	0.603	0.29	22.72	2.11
k20	0.487	0.24	18.36	1.71
k21	0.046	0.02	1.73	0.16
k22	0.595	0.33	22.41	2.08
k23	0.481	0.22	18.11	1.68
k24	0.517	0.28	19.47	1.81
k25	0.413	0.25	15.56	1.45
k26	0.049	0.02	1.84	0.17
k27	0.544	0.28	20.51	1.91
k28	0.401	0.16	15.11	1.40
k29	0.573	0.25	21.59	2.01
k30	0.467	0.18	17.60	1.63
k31	0.071	0.03	2.69	0.25
k32	0.542	0.33	20.43	1.90
k33	0.320	0.16	12.05	1.12
k34	0.019	0.01	0.71	0.07
k35	0.346	0.15	13.04	1.21
k36	0.423	0.17	15.93	1.48
k37	0.483	0.18	18.19	1.69
k38	0.377	0.22	14.20	1.32
k39	0.378	0.21	14.26	1.32
k40	0.583	0.29	21.96	2.04
Minimum	***0.019***	***0.01***	***0.71***	***0.07***
Maximum	***0.603***	***0.33***	***22.72***	***2.11***
Average± S.E.	***0.36±0.08***	***0.18±0.08***	***14±1***	***1±0.1***

4.4.2 Results of Najaf City with CR-39 Detector

Table (4.11) shows the results of radon-222 gas concentration in air space (C), the radon-222 concentration in the samples (C_{Rn}), specific activity of radium-226 (C_{Ra}), and uranium concentrations (C_U).Table (4.11) also shows the ranges of C and C_{Rn} values with its

average value. The maximum value of C and C_{Rn} are found in sample N17 and N50, while the minimum value of C and C_{Rn} is in sample N2. Also, Table (4.11) shows the range values of C_{Ra} and C_U and their average values. The maximum value of each C_{Ra} and C_U are observed in sample N17, While the minimum value of each C_{Ra} and C_U are observed in the same sample N2.

Table (4.12) shows the results of radiological risk such as annual effective dose (AED), radon exhalation rate per unit mass (E_M), and per unit surface (E_S), and Excess Lifetime Cancer Risk (ELCR), which are calculated in all soil samples. It is noted that the range of minimum and maximum values with an average value of the results AED is 0.02-3.664 mSv/y, 0.406±0.079 mSv/y. The range value of minimum and maximum of each E_M (mBq/kg.h) and E_S (mBq/m^2.h) with an average value that shown in Table (4.12) are 0.011-1.666, 0.767-140.326 and 0.19±0.037,15.56±3.059, respectively. The range value of ELCR due to radon gas in air space of container as shown in Table(4.12) are (0.07×10^{-3}- 12.825×10^{-3}), with an average $(1.422\pm0.279)\times10^{-3}$.

Table (4.11) Results of alpha emitters in soil samples of Najaf city.

No.	*C (Bq/m^3)*	*C_{Rn} (Bq/m^3)*	*C_{Ra} (Bq/kg)*	*C_U (ppm)*
N1	10.32	409.08	0.020	0.024
N2	0.79	31.47	0.002	0.002
N3	19.44	952.35	0.043	0.053
N4	7.94	314.67	0.014	0.018
N5	9.92	393.34	0.017	0.021
N6	9.13	361.87	0.014	0.018
N7	12.30	487.74	0.021	0.026
N8	19.05	755.22	0.032	0.039
N9	1.19	47.20	0.002	0.002
N10	10.71	424.81	0.018	0.022
N11	4.37	173.07	0.007	0.009
N12	17.86	708.02	0.025	0.031

Next

N13	9.13	361.87	0.022	0.027
N14	11.90	472.01	0.021	0.025
N15	3.97	157.34	0.008	0.009
N16	3.57	141.60	0.008	0.010
N17	145.24	5758.52	0.253	0.313
N18	9.13	361.87	0.018	0.022
N19	13.49	534.94	0.023	0.028
N20	10.32	409.08	0.021	0.025
N21	13.89	550.68	0.026	0.032
N22	13.89	550.68	0.026	0.032
N23	7.14	283.21	0.011	0.014
N24	16.27	645.08	0.031	0.038
N25	7.14	283.21	0.012	0.015
N26	30.56	1211.49	0.050	0.062
N27	4.76	233.23	0.008	0.010
N28	9.52	466.46	0.019	0.024
N29	2.38	116.61	0.004	0.005
N30	36.11	1431.76	0.069	0.085
N31	20.63	1010.66	0.038	0.047
N32	13.89	550.68	0.023	0.029
N33	19.44	770.95	0.032	0.040
N34	17.46	855.17	0.036	0.044
N35	5.56	220.27	0.009	0.011
N36	3.97	157.34	0.008	0.010
N37	10.71	424.81	0.017	0.021
N38	6.35	310.97	0.015	0.018
N39	3.97	194.36	0.007	0.009
N40	8.33	330.41	0.015	0.018

N41	16.27	645.08	0.028	0.035
N42	2.78	110.14	0.005	0.006
N43	3.97	157.34	0.008	0.010
N44	4.76	188.80	0.008	0.010
N45	5.56	272.10	0.011	0.013
N46	14.29	699.69	0.024	0.030
N47	7.14	283.21	0.011	0.014
N48	4.76	188.80	0.008	0.010
N49	1.98	97.18	0.004	0.005
N50	126.19	6180.56	0.249	0.308
N51	5.56	220.27	0.012	0.015
N52	7.94	314.67	0.013	0.017
N53	23.41	928.29	0.045	0.055
N54	5.56	220.27	0.009	0.011
N55	17.86	708.02	0.027	0.034
N56	14.68	582.15	0.028	0.035
N57	65.87	3226.33	0.123	0.152
N58	34.13	1353.10	0.073	0.090
N59	6.35	251.74	0.010	0.012
N60	15.48	613.61	0.021	0.026
Minimum	***0.79***	***31.47***	***0.002***	***0.002***
Maximum	***145.24***	***6180.56***	***0.253***	***0.313***
Average± S.E.	***16.10±3.166***	***684.92±140.5***	***0.029±0.0058***	***0.036±0.0072***

Table (4.12) Results of AED, E_M, E_S, and ELCR in soil samples of Najaf city.

No.	*AED (mSv/y)*	*E_M(mB_q/kg.h)*	*E_S(mB_q/m^2.h)*	*ELCR ×10^{-3}*
N1	0.260	0.129	9.969	0.911
N2	0.020	0.011	0.767	0.070

N3	0.491	0.266	18.787	1.717
N4	0.200	0.093	7.668	0.701
N5	0.250	0.114	9.585	0.876
N6	0.230	0.095	8.818	0.806
N7	0.310	0.139	11.886	1.086
N8	0.481	0.210	18.403	1.682
N9	0.030	0.012	1.150	0.105
N10	0.270	0.119	10.352	0.946
N11	0.110	0.047	4.217	0.385
N12	0.451	0.164	17.253	1.577
N13	0.230	0.145	8.818	0.806
N14	0.300	0.135	11.502	1.051
N15	0.100	0.049	3.834	0.350
N16	0.090	0.053	3.451	0.315
N17	3.664	1.666	140.326	12.825
N18	0.230	0.116	8.818	0.806
N19	0.340	0.150	13.036	1.191
N20	0.260	0.135	9.969	0.911
N21	0.350	0.170	13.419	1.226
N22	0.350	0.170	13.419	1.226
N23	0.180	0.074	6.901	0.631
N24	0.410	0.204	15.720	1.437
N25	0.180	0.082	6.901	0.631
N26	0.771	0.332	29.522	2.698
N27	0.120	0.049	4.601	0.420
N28	0.240	0.120	9.202	0.841
N29	0.060	0.024	2.300	0.210
N30	0.911	0.455	34.890	3.189
N31	0.521	0.237	19.937	1.822
N32	0.350	0.155	13.419	1.226
N33	0.491	0.210	18.787	1.717
N34	0.441	0.224	16.870	1.542
N35	0.140	0.059	5.368	0.491
N36	0.100	0.053	3.834	0.350
N37	0.270	0.109	10.352	0.946
N38	0.160	0.091	6.134	0.561
N39	0.100	0.045	3.834	0.350
N40	0.210	0.098	8.052	0.736
N41	0.410	0.188	15.720	1.437
N42	0.070	0.030	2.684	0.245
N43	0.100	0.052	3.834	0.350

N44	0.120	0.053	4.601	0.420
N45	0.140	0.066	5.368	0.491
N46	0.360	0.152	13.803	1.261
N47	0.180	0.073	6.901	0.631
N48	0.120	0.055	4.601	0.420
N49	0.050	0.028	1.917	0.175
N50	3.184	1.548	121.923	11.143
N51	0.140	0.082	5.368	0.491
N52	0.200	0.088	7.668	0.701
N53	0.591	0.294	22.621	2.067
N54	0.140	0.058	5.368	0.491
N55	0.451	0.179	17.253	1.577
N56	0.370	0.185	14.186	1.296
N57	1.662	0.767	63.645	5.817
N58	0.861	0.480	32.973	3.013
N59	0.160	0.066	6.134	0.561
N60	0.390	0.140	14.953	1.367
Minimum	***0.02***	***0.011***	***0.767***	***0.07***
Maximum	***3.664***	***1.666***	***140.326***	***12.825***
Average± S.E.	***0.406±0.079***	***0.19±0.037***	***15.56±3.059***	***1.422±0.279***

4.5 Results of RAD-7 Detector

In this study, radon concentrations are measured by using RAD-7 detector in some selected samples soil of Kufa and Najaf cities.

4.5.1 Results of Kufa City with RAD-7 Detector

Table (4.13) represents the values of radon concentration in 20 soil samples in Kufa city. From Table (4.13), it can be seen that radon concentrations varied from 2.4±0.30 Bq/m^3 in location (K3 sample) to 33.1±4.14 Bq/m^3 in location (K24 sample) with an average value 18.15±1.91 Bq/m^3.

Table (4.13) ^{222}Rn concentration measured by RAD-7 detector in soil – gas samples for Kufa city.

Sample Code	***^{222}Rn concentration (Bq/m^3)***
K3	2.4±0.30
K6	16.55±2.07
K8	2.6±0.33

K12	24.9±3.11
K14	24±3.00
K16	16.55±2.07
K23	24.5±3.06
K24	33.1±4.14
K26	6.62±0.83
K27	24.9±3.11
K28	9±1.13
K29	26±3.25
K31	11.58±1.45
K32	25±3.13
K33	18±2.25
K35	19±2.38
K36	26.48±3.31
K37	25.5±3.19
K38	18.2±2.28
K39	8.275±1.03
Average± S.E	***18.15±1.91***
Minimum	***2.4***
Maximum	***33.1***

4.5.2 Results of Najaf City with RAD-7 Detector

Table (4.14) represents the values of radon concentration in 30 soil samples in Kufa city. From Table (4.14), it can be seen that radon concentrations varied from 2.4±0.63 Bq/m^3 in locations (N60 and N40 samples) to 99±4.06 Bq/m^3 in location (N50 sample) with an average value 20.33±3.49 Bq/m^3.

Table (4.14) ^{222}Rn concentration measured by RAD-7 detector in soil – gas samples for Najaf city.

Sample Code	***^{222}Rn concentration (Bq/m^3)***
N2	8.27±1.17
N5	16±1.63
N7	16.5±1.66
N9	8.275±1.17
N11	11.03±1.36
N14	9±1.22
N16	8.275±1.17
N18	8±1.15
N19	16.55±1.66

N21	16±1.63
N23	11.03±1.36
N25	15±1.58
N26	25±2.04
N29	7±1.08
N32	14±1.53
N34	17±1.68
N36	24±2.00
N38	15.55±1.61
N40	2.4±0.63
N42	18±1.73
N44	41±2.61
N46	24.8±2.03
N48	16.55±1.66
N50	99±4.06
N52	25±2.04
N53	30.5±2.25
N55	9±1.22
N57	66±3.32
N59	29±2.20
N60	2.4±0.63
Average± S.E	***20.33±3.49***
Minimum	***2.4***
Maximum	***99***

4.6 Discussions

The discussion of results for all detectors is divided into two parts: Kufa city and Najaf city as shown below, where contour maps by GIS had been used to draw the radiological hazards for all areas under study.

4.6.1 Discussion of Dosimeter Detector

4.6.1.1 Discussion of Kufa City

Background radiation, measured in soil samples by using a portable dosimeter, has different values in each study area. For Kufa city this difference can be related to a difference in the geographical nature of each region, such as soil type (Clay or sand). Comparison between background according to dose rate in μSv/h, AAED in mSv/y and ELCR for all the

samples as shown in Figures (4.1), (4.2) and (4.3) for Kufa city. In all present study samples, the dose rate and AAED are compared with the global standard values, as shown in Figures (4.1) and (4.2), respectively. From figure (4.1), the dose rate values in all present study samples are lower than the global limit that recommended value of 0.274 μSv/h[144]. Also, from Figure (4.2), all values of AAED are lower than the global limit that recommended value 2.4 mSv/y according to UNSCEAR 2008 report[144]. Also, the value of the results of ELCR is little; therefore, the risk of cancer is negligible.

4.6.1.2 Discussion of Najaf City

From Figure (4.4)states that the importance of dose rate in all samples of the present study is lower than the global limit that recommended value 0.274 μSv/y[145][146]. Also, from Figure (4.2), all matters of AAED are lower than the worldwide limit that recommended value 2.4 mSv/y according to UNSCEAR 2008 report [144]. Also, the value of the results of ELCR is little; therefore, it may be decided that the risk of cancer is negligible.

The comparison between the background, according to dose rate in μSv/h, AAED in mSv/y, and ELCR for all the samples, are shown in Figures (4.4), (4.5), and (4.6) which it is drawn by GIS technology, where different colors are used to distinguish between high, medium and low quantities.

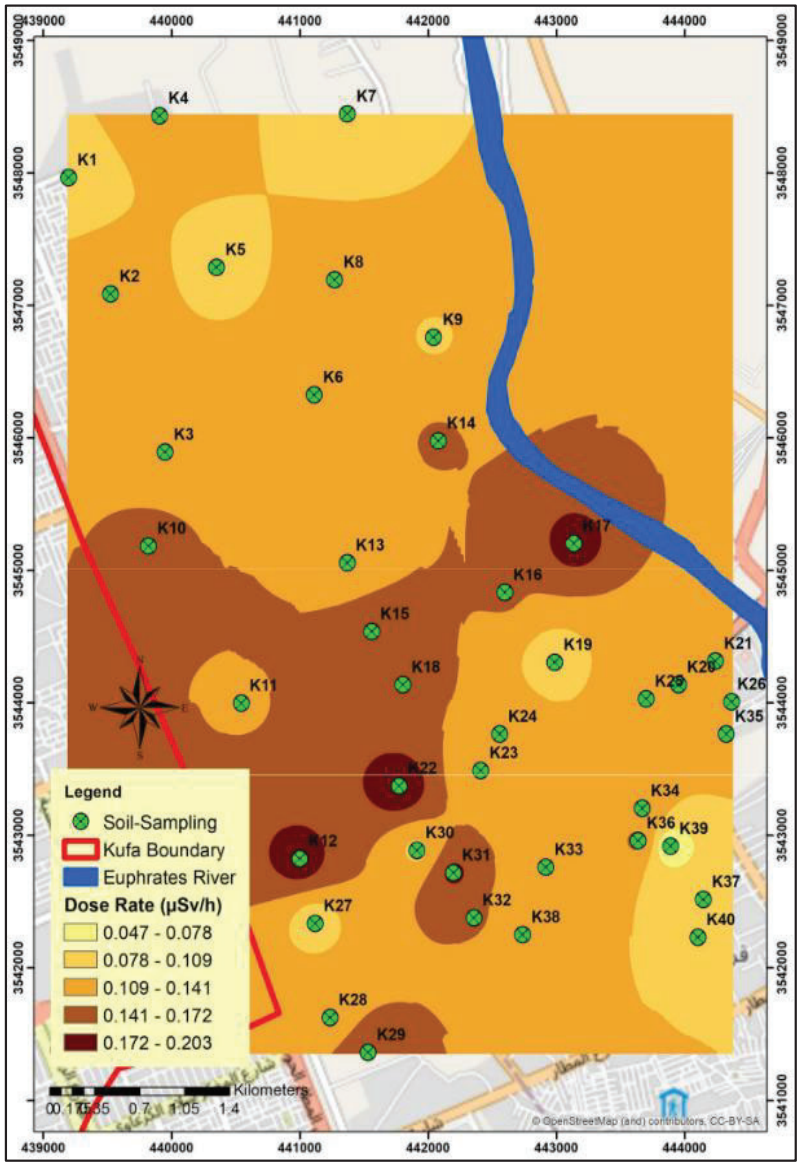

Figure (4.1) The choropleth maps of the values of dose rate for Kufa city

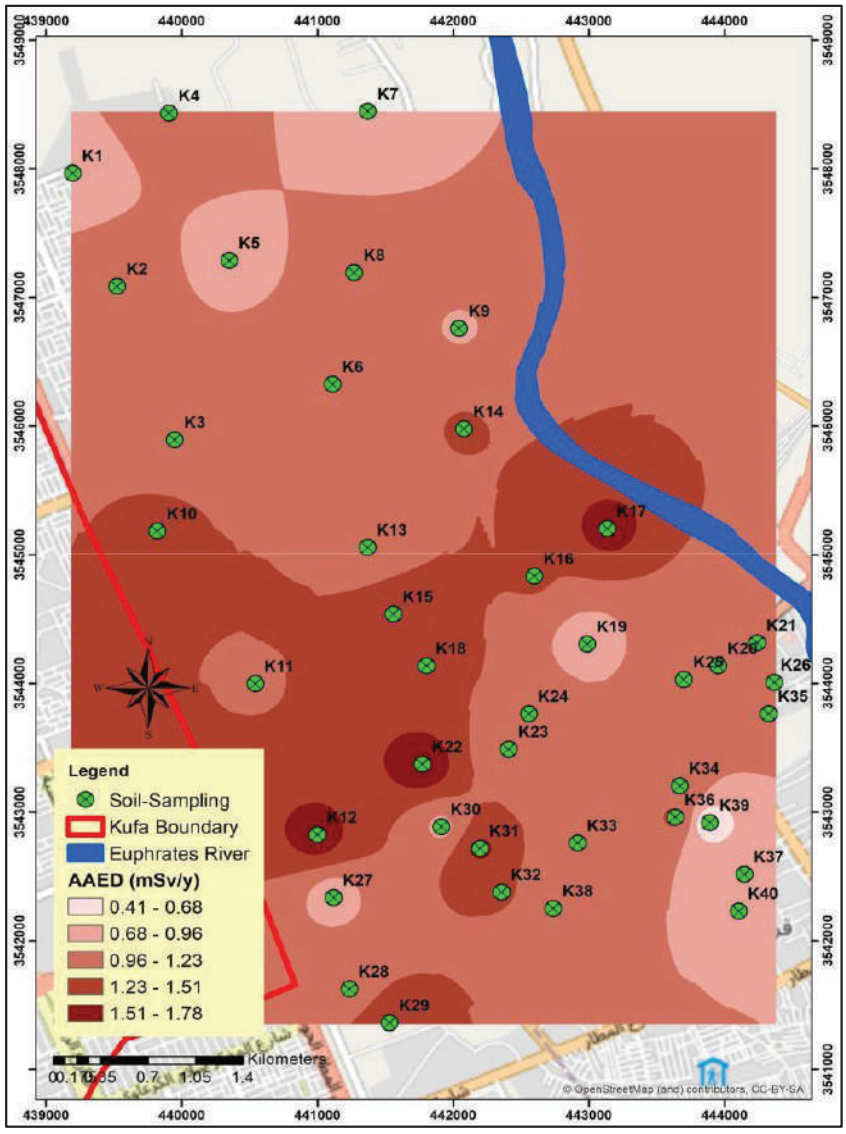

Figure (4.2) The choropleth maps of the values of AAED for Kufa city.

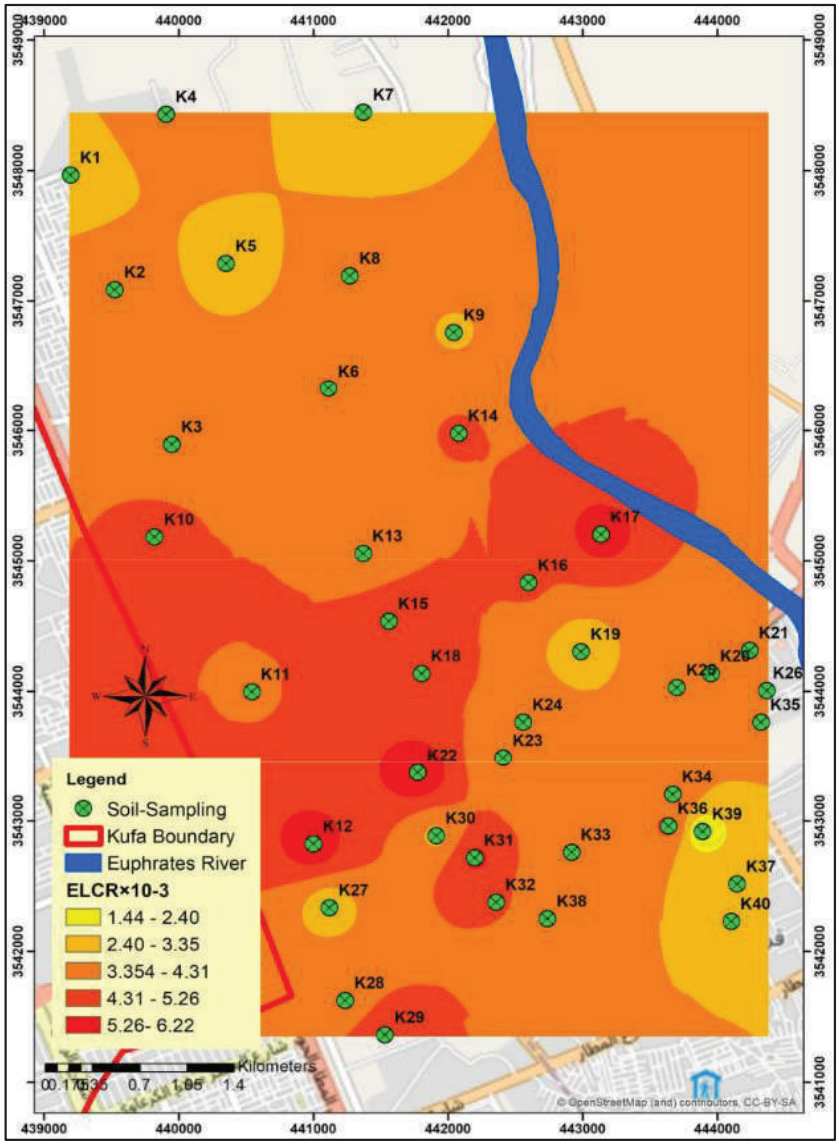

Figure (4.3) The choropleth maps of the values of ELCR for Kufa city.

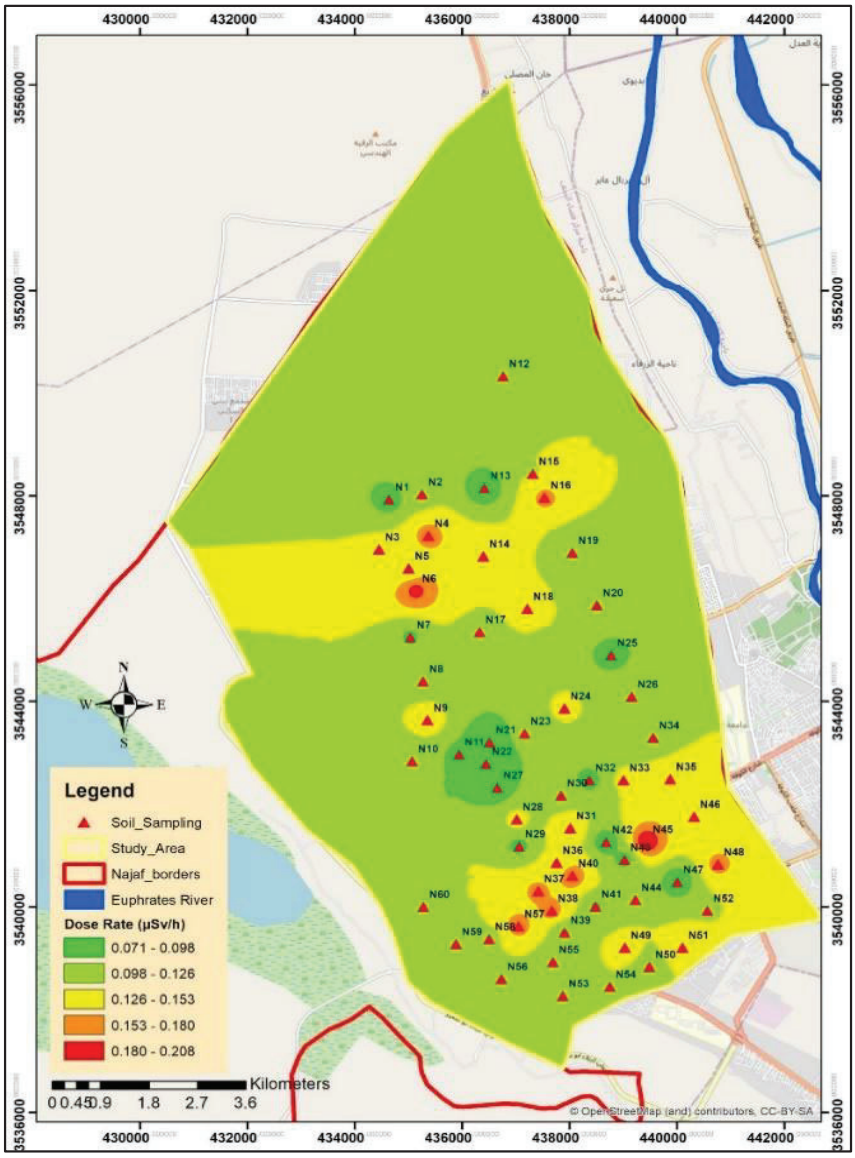

Figure (4.4) The choropleth maps of the values of dose rate for Najaf city.

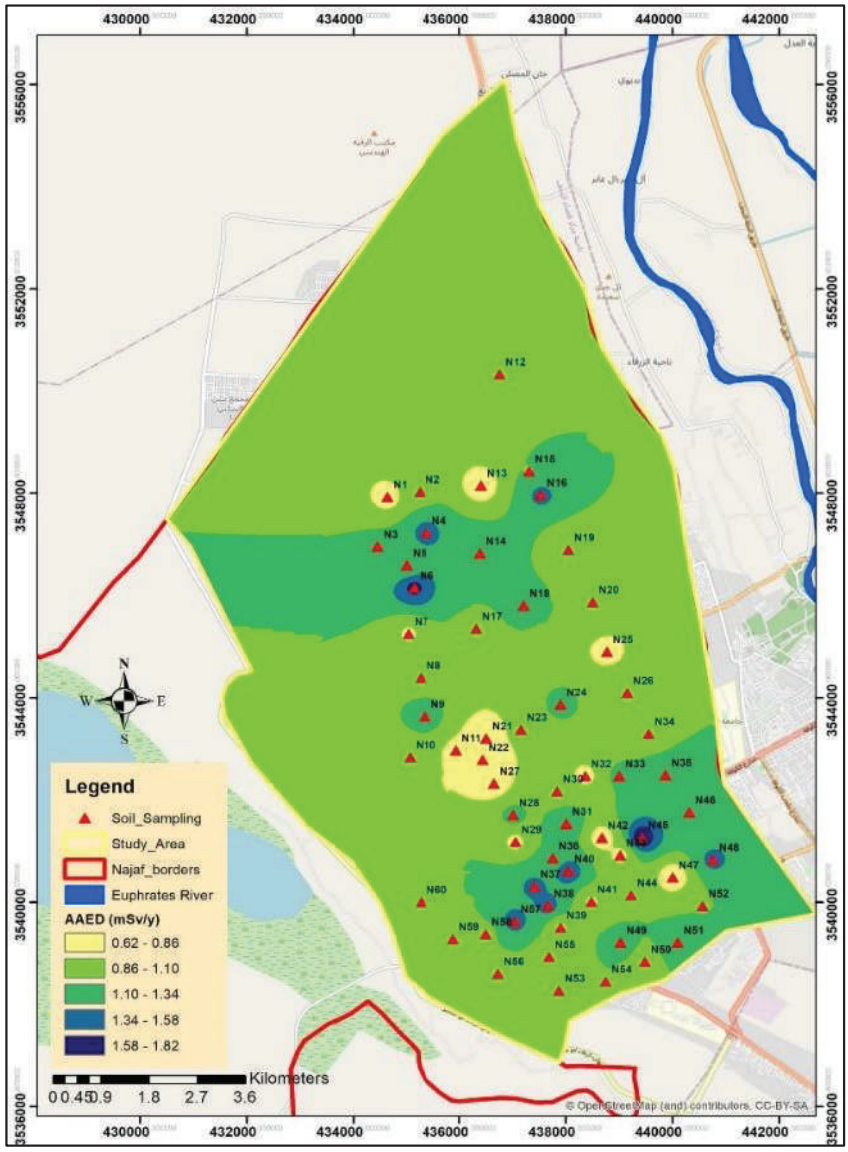

Figure (4.5) The choropleth maps of the values of AAED for Najaf city.

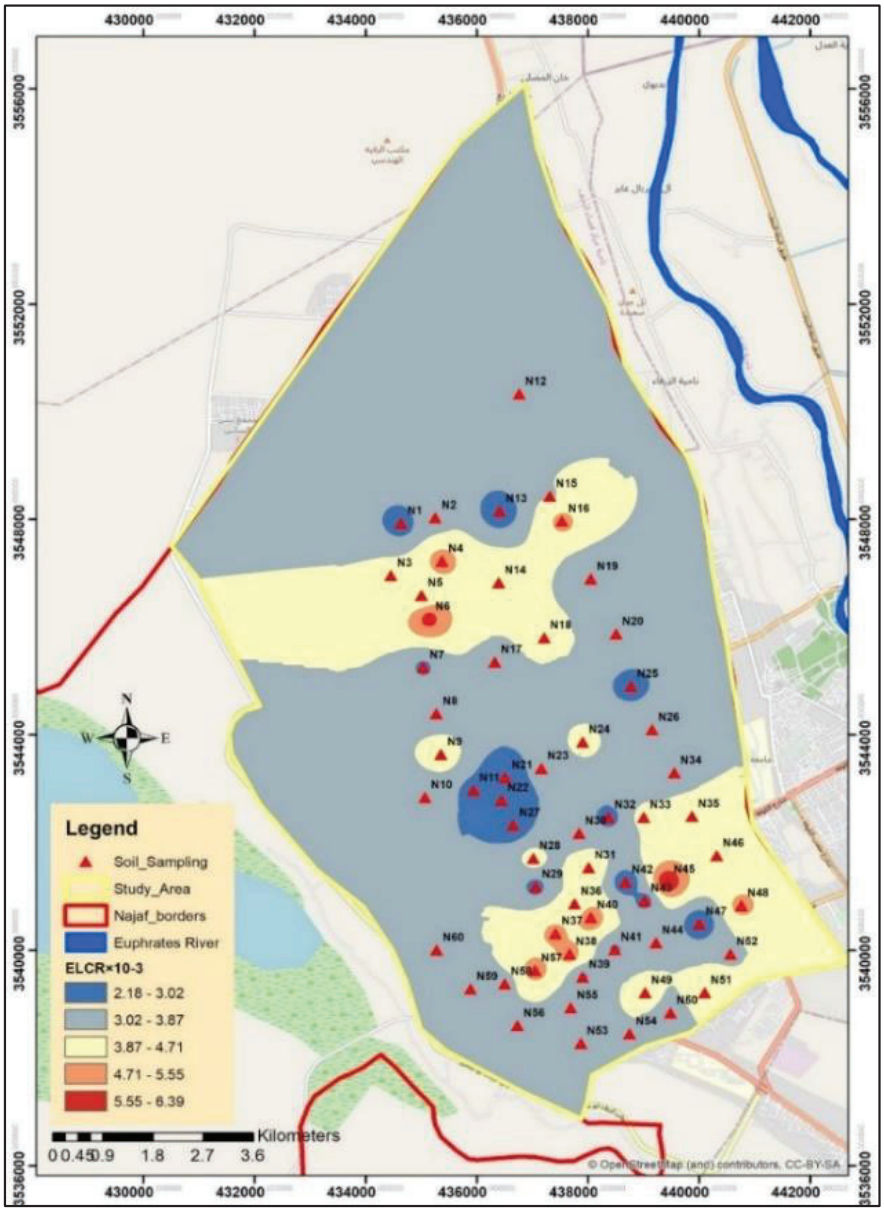

Figure (4.6) The choropleth maps of the values of ELCR for Najaf city.

4.6.3 Discussion of NaI(Tl) Detector

4.6.3.1 Discussion of Kufa City

The average values of the specific activity of ^{238}U, ^{232}Th, and ^{40}K according to recommendations by UNSCEAR 2008 are 33 Bq/kg, 45 Bq/kg, and 420 Bq/kg, respectively [16]. Therefore, the specific activity of ^{238}U and ^{232}Th shown in table (4-3) in all location sites is within UNSCEAR 2008, while samples K15, K16, and K17 have a particular activity of ^{40}K larger than the world average activity that is recommended by UNSCEAR 2008. Distribution of a map (color contour map) of the specific activities in a unit of Bq/kg for radioisotopes ^{238}U, ^{232}Th, ^{40}K, and ^{235}U in all soil samples of the present study shown in Figures (4.7),(4.8),(4.9) and (4.10) below which is drawn by geographic information system (GIS) technology.

Also, The results of radiological parameters (Ra_{eq}, H_{ex}, H_{in}, $I_{\gamma r}$, and I_{α}) in Table (4.4) for all soil samples under study are less than 370 Bq/kg for R_{aeq} [16] and less than unity for the values of H_{ex}, H_{in}, $I_{\gamma r}$, and I_{α} [147].

Parameters Ra_{eq} and H_{ex} due to radioisotopes ^{238}U, ^{232}Th, and ^{40}K in all soil samples of the present study shown by the color contour map as in Figures (4.11) and (4.12). At the same time, Results of another radiological parameter (X, D_r, AGED, $AEDE_{outdoor}$, and ELCR) for nature radioactivity in soil for Kufa city shown in Table (4.5), The results of D_r in-unit nGy/h for all of the soil samples studied are less than the average world value equal to 55 nGy/h.

Also, it noted that the results of AGED in-unit mSv/y are lower than the global average value that equal 55 [147], except sample K17, which is higher than the limit permissible.

$AEDE_{outdoor}$ in all soil samples in the present study is less than the world average of 0.07mSv/y. The results of ELCR in all location samples are lower when compared with the world average permissible limit of 0.29×10^{-3}[147] as shown in figure (4.13) in the map in bold color, the highest value is in the area of sample K17 and K19 in the map of dark color.

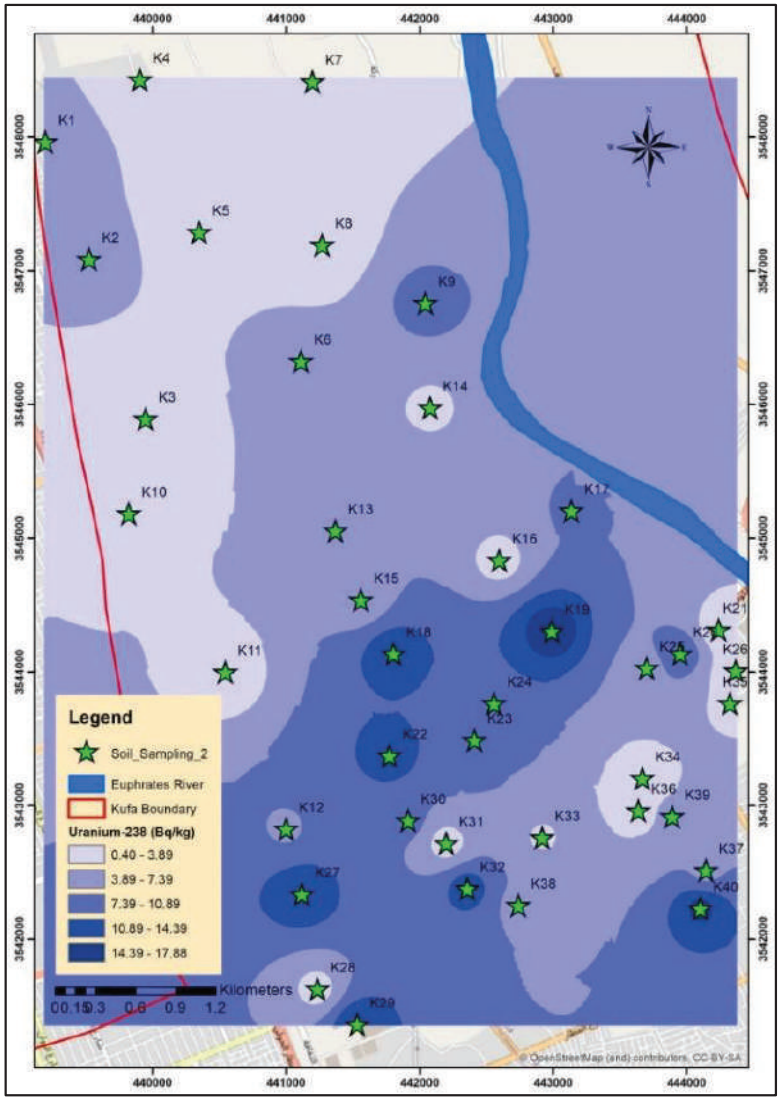

Figure (4.7) Distribution of ^{238}U in the soil of Kufa city.

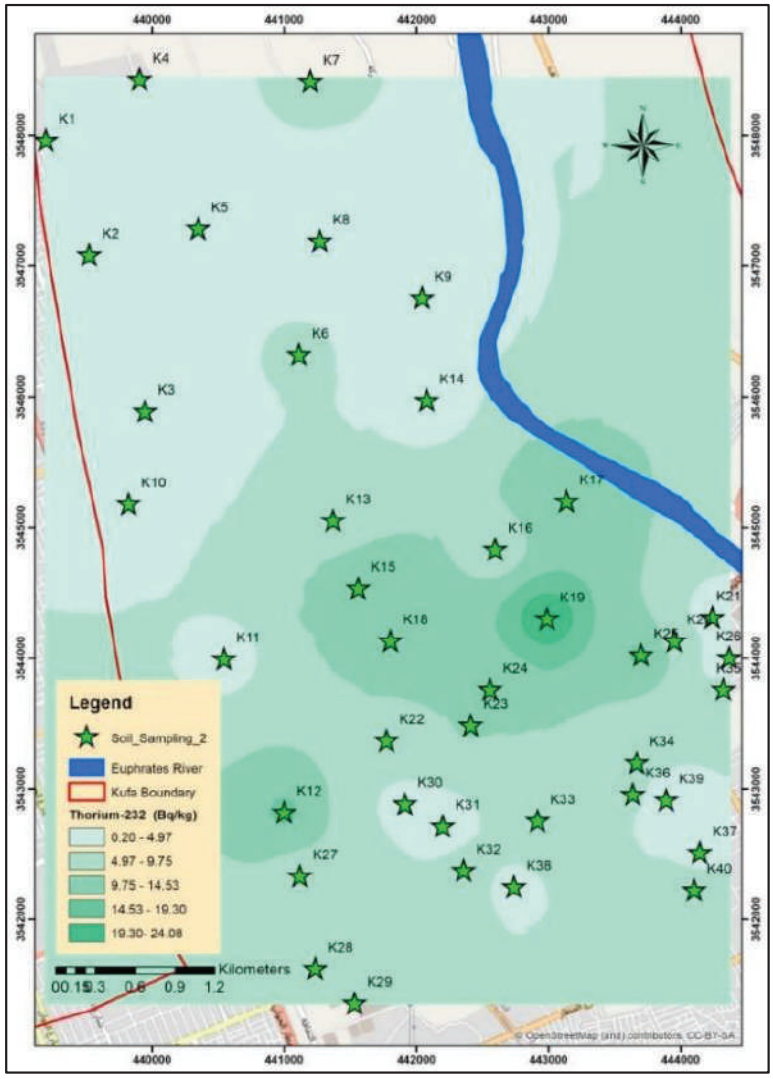

Figure (4.8) Distribution of ^{232}Th in the soil of of Kufa city.

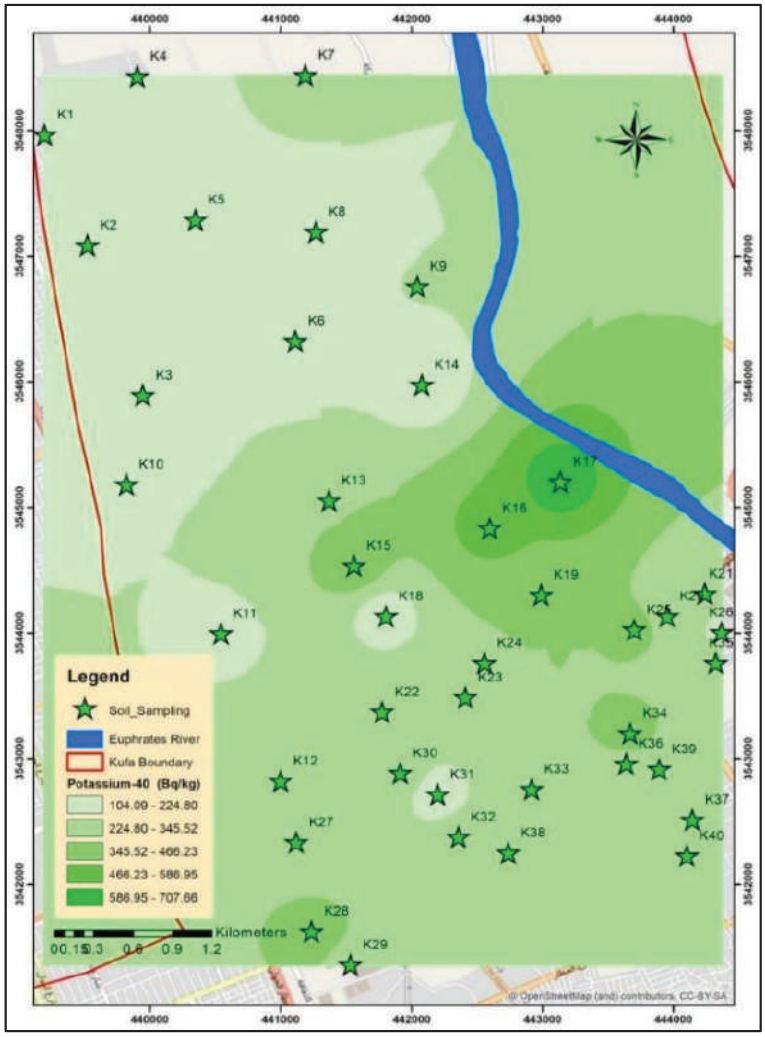

Figure (4.9) Distribution of ^{40}K in the soil of of Kufa city.

.

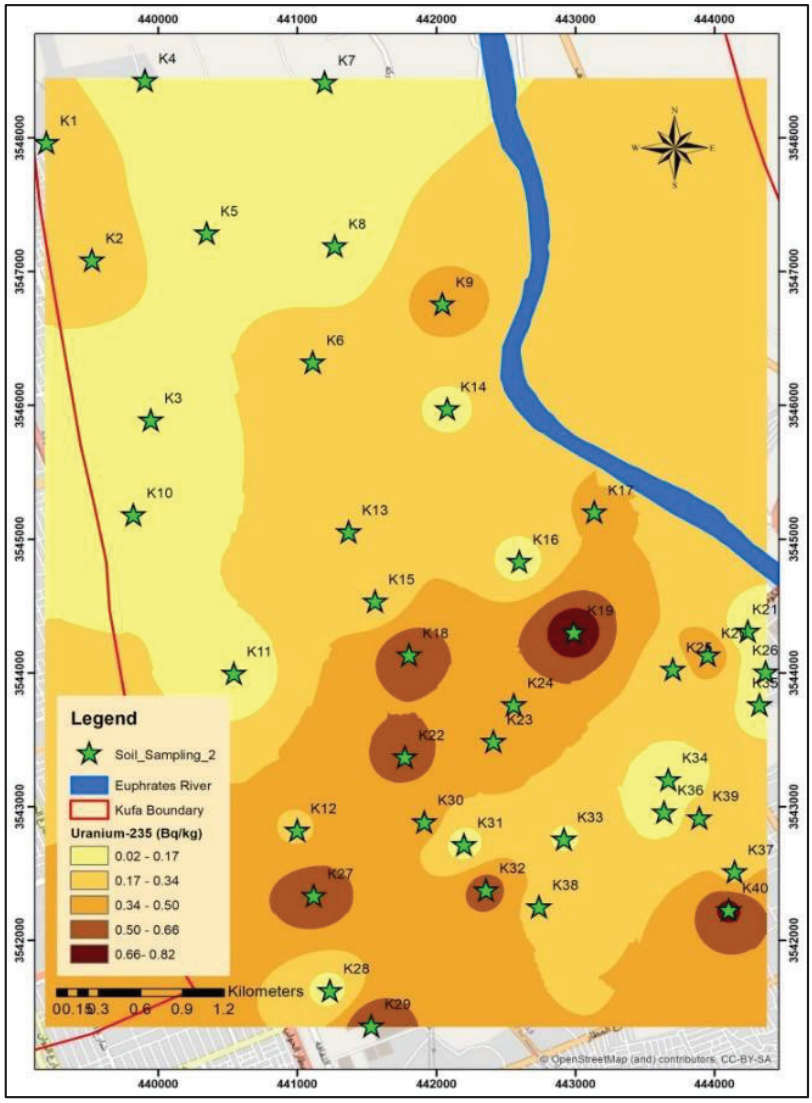

Figure (4.10) Distribution of ^{235}U in the soil of of Kufa city

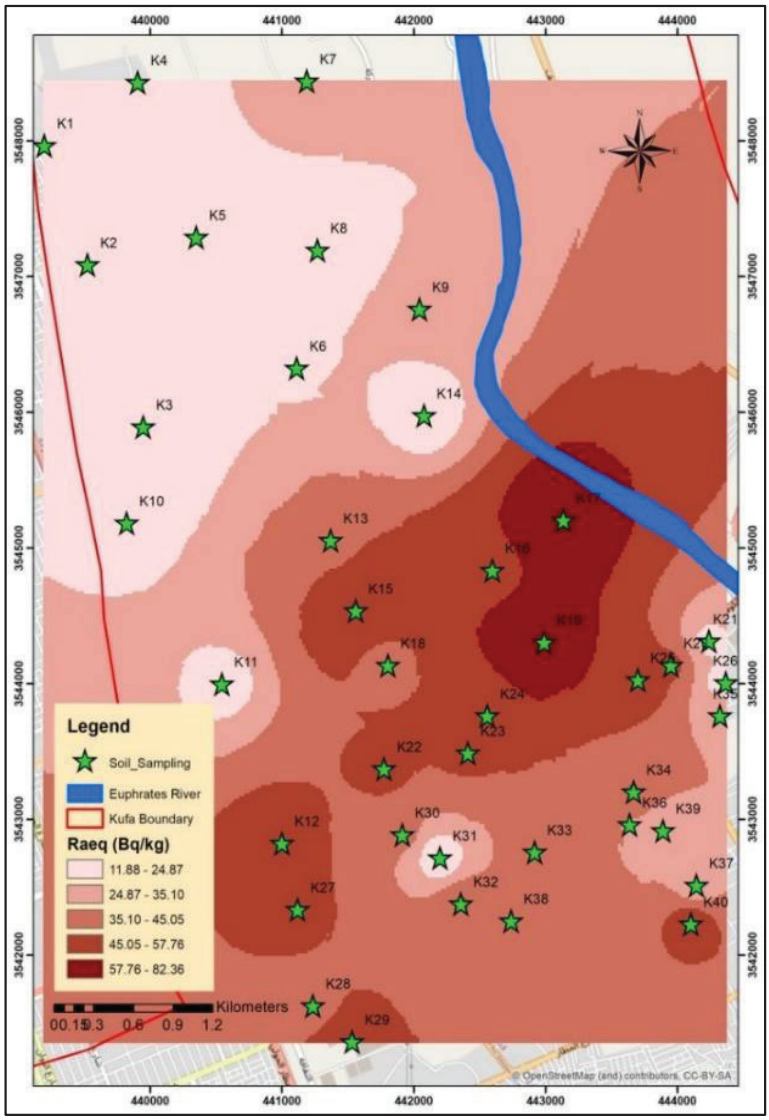

Figure (4.11) Distribution of R_{aeq} in the soil of of Kufa city.

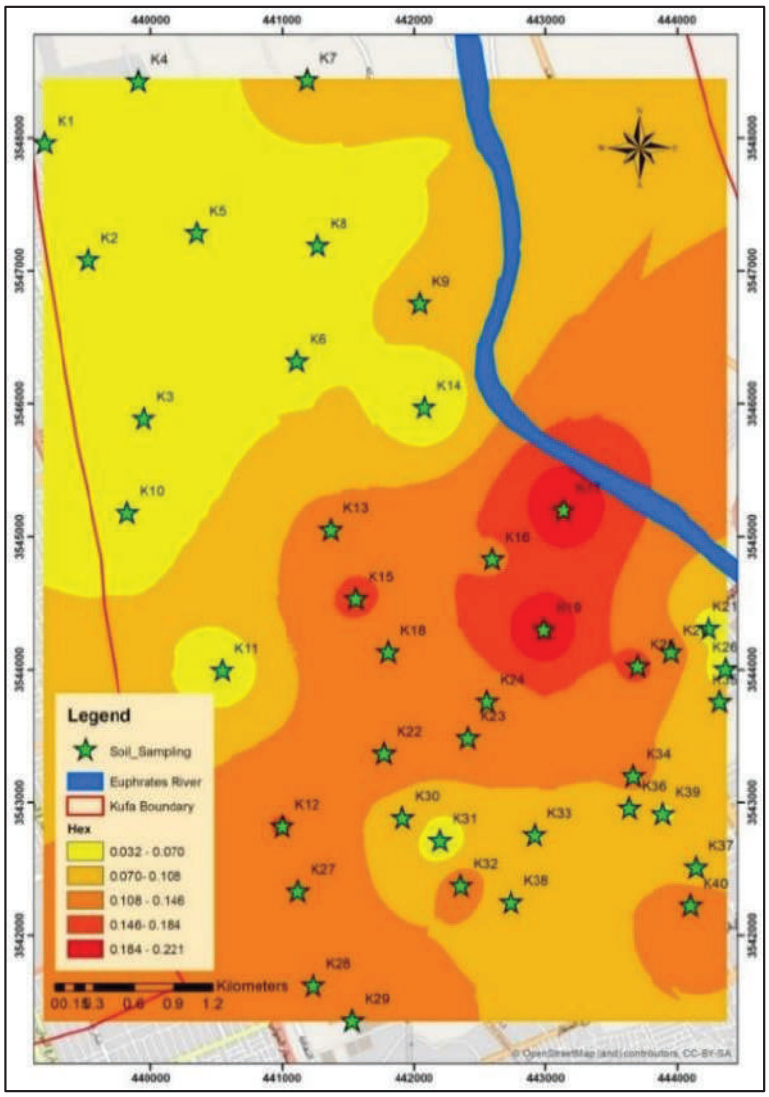

Figure (4.12) Distribution of H_{ex} in the soil of of Kufa city.

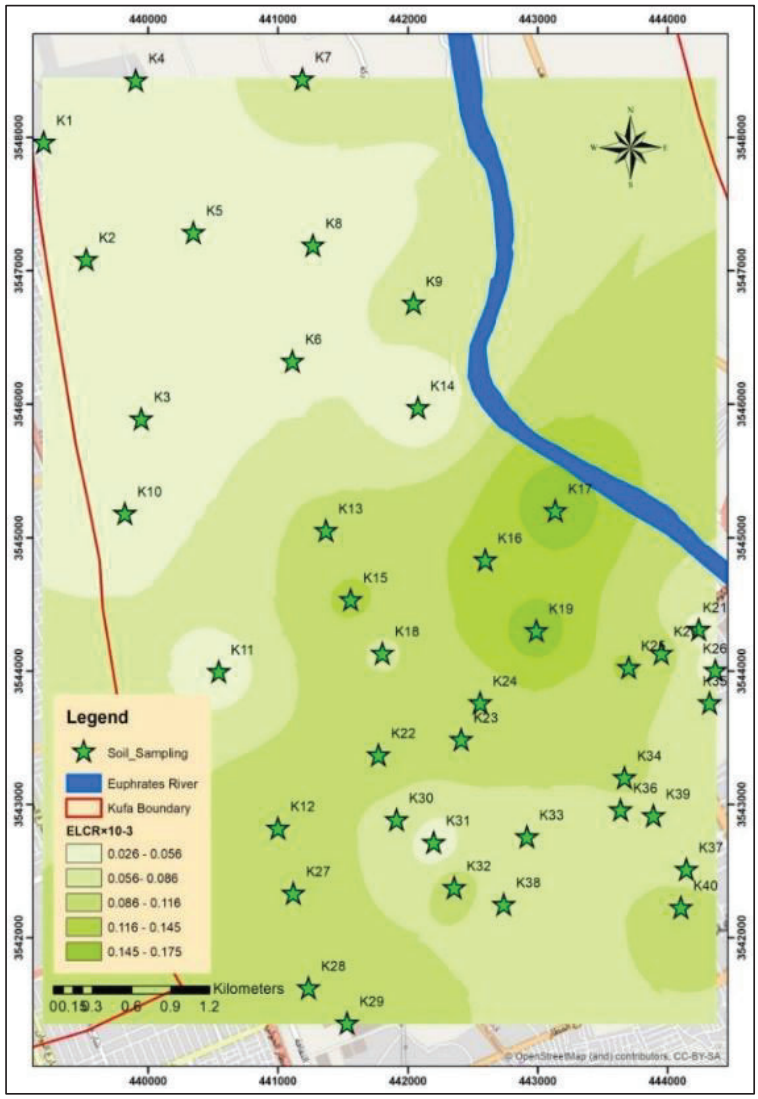

Figure (4.13) Distribution of ELCR in the soil of of Kufa city.

4.6.3.2 Discussion of Najaf City

The average values of the specific activity of ^{238}U, ^{232}Th, and ^{40}K according to recommendations by UNSCEAR 2008 are 33 Bq/kg, 45 Bq/kg, and 420 Bq/kg, respectively[144]. Therefore, the specific activity of ^{238}U and ^{232}Th shown in table (4.6) in all location sites is within UNSCEAR 2008 except N17, N50, N57, and N58 for ^{238}U, while samples N30, N53, and N57 have a particular activity of ^{40}K larger than the world average activity that is recommended by UNSCEAR 2008. Distribution of a map (color contour map) of the specific activities in a unit of Bq/kg for radioisotopes ^{238}U, ^{232}Th, ^{40}K, and ^{235}U in all soil samples of the present study showed in Figures (4.14), (4.15), (4.16), and (4.17), respectively, which is drawn by geographic information system (GIS) technology. The results of radiological parameters (Ra_{eq}, H_{ex}, H_{in}, I_{γ}, and I_{α}) in Table (4.7) for all soil samples under study are less than 370 Bq/kg for R_{aeq} [148] and less than unity for the values of H_{ex}, H_{in}, I_{γ}, and I_{α} [147].

The parameters Ra_{eq} and H_{ex} due to radioisotopes ^{238}U, ^{232}Th, and ^{40}K in all soil samples of the present study are shown by the color contour map as in Figures (4.18) and (4.19), drawn by geographic information system (GIS) technology. The results of ELCR shown in the map (bold color) of Figure (4.20), the highest value is in the area of sample N17 and N30 in the map of dark color.

The results of D_r in-unit nGy/h in Table (4.8) for all of the soil samples studied are less than the average world value equal to 55 nGy/h [144]. Also, it noted that all the results of AGED in-unit mSv/y are lower than the global average value equal 300 [144][149]except for sample N30. $AEDE_{outdoor}$ in all soil samples in the present study is less than the world average of 0.07mSv/y [149] .The results of ELCR in all location samples are lower when compared with the world average permissible limit of 0.29×10^{-3} [144], which shown in the map (bold color) of Figure (4.20), the highest value is in the area of sample N17 and N30 in the map of dark color.

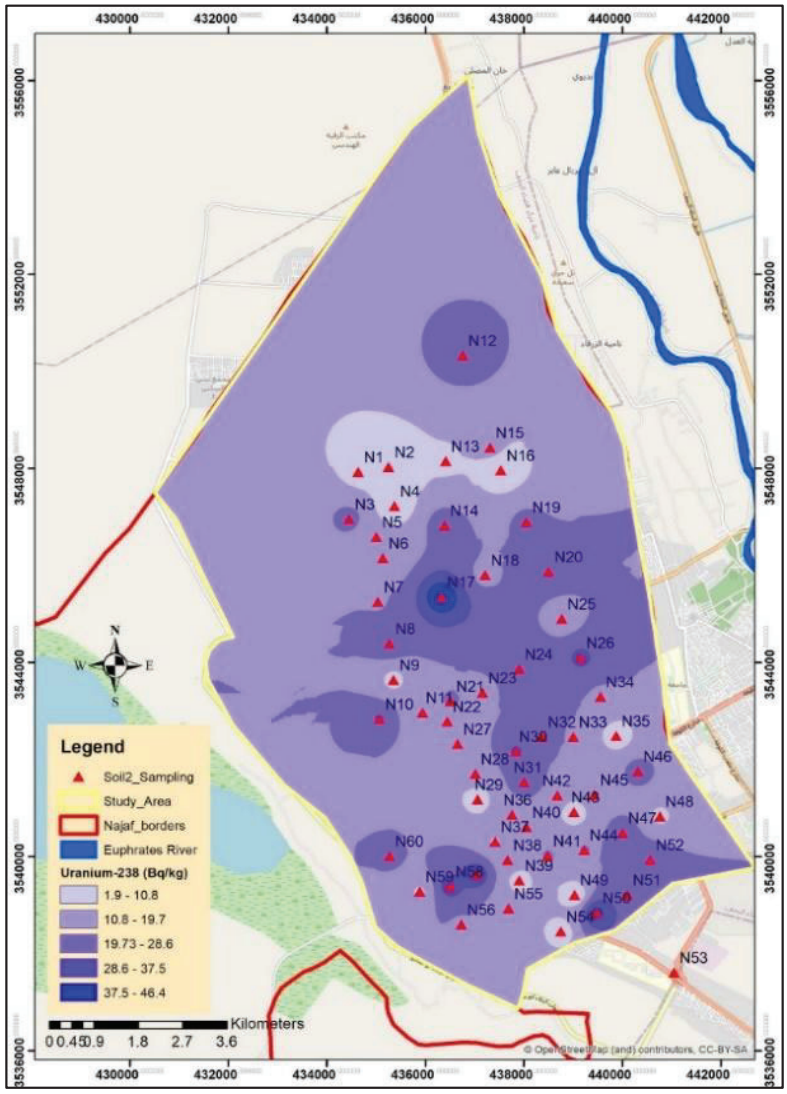

Figure (4.14) Distribution of ^{238}U in the soil of Najaf city.

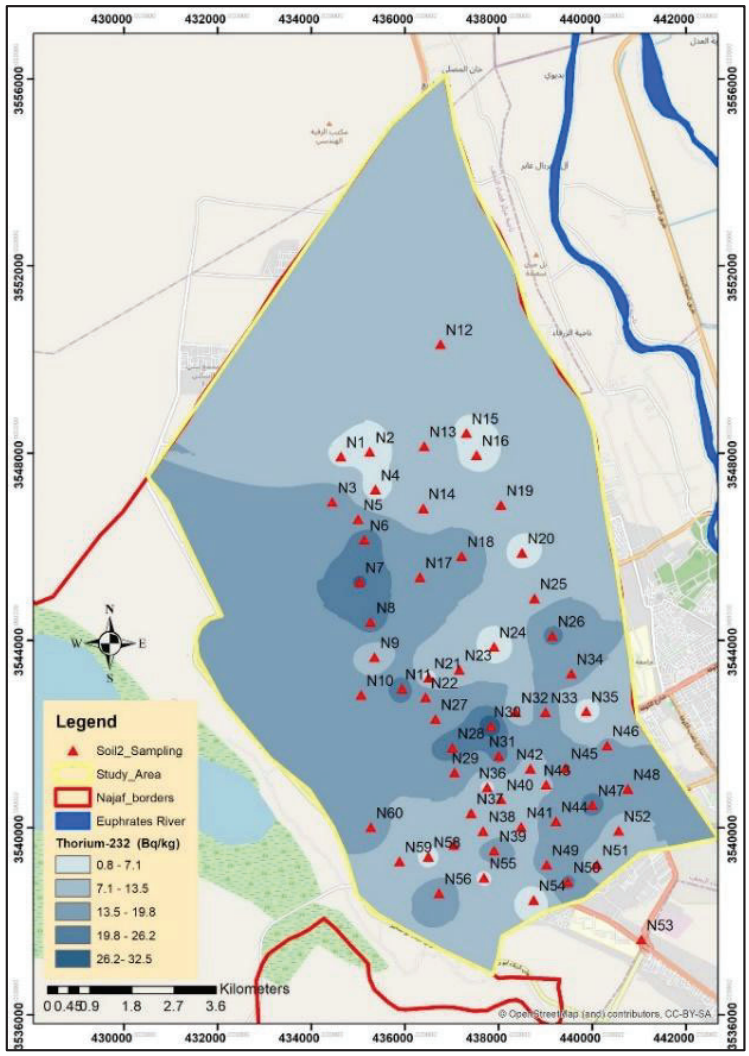

Figure (4.15) Distribution of ^{232}Th in the soil of of Najaf city.

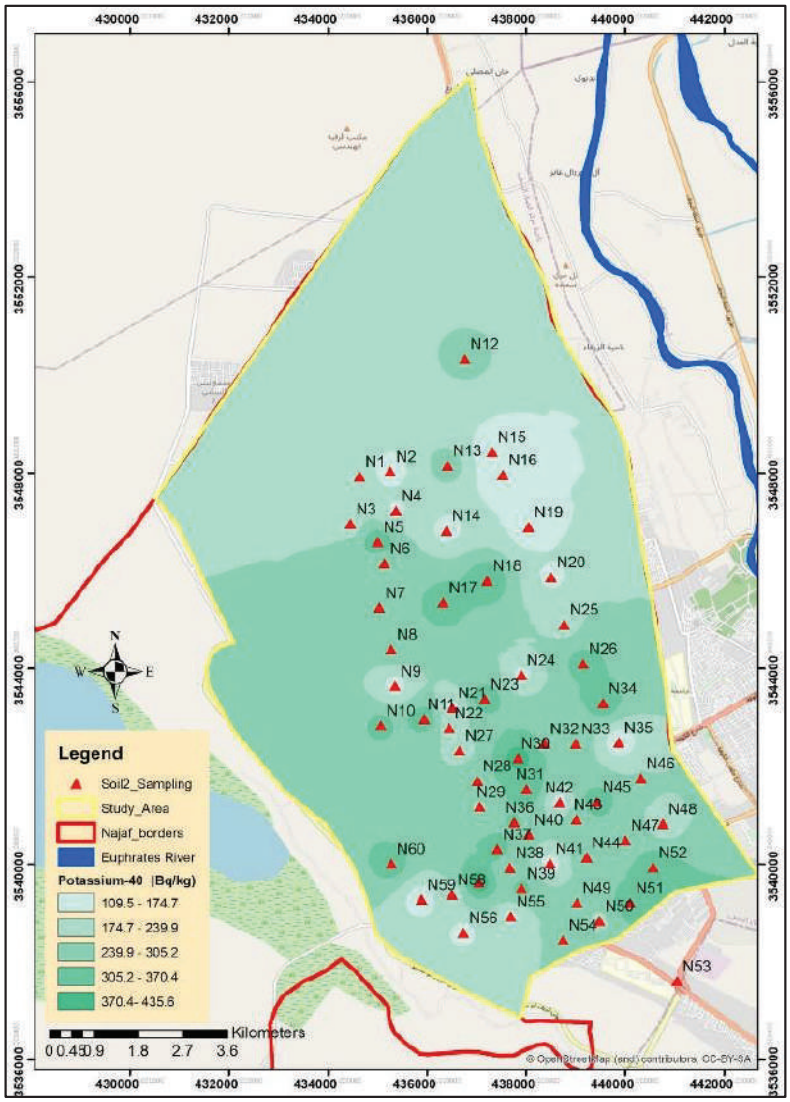

Figure (4.16) Distribution of ^{40}K in the soil of of Najaf city.

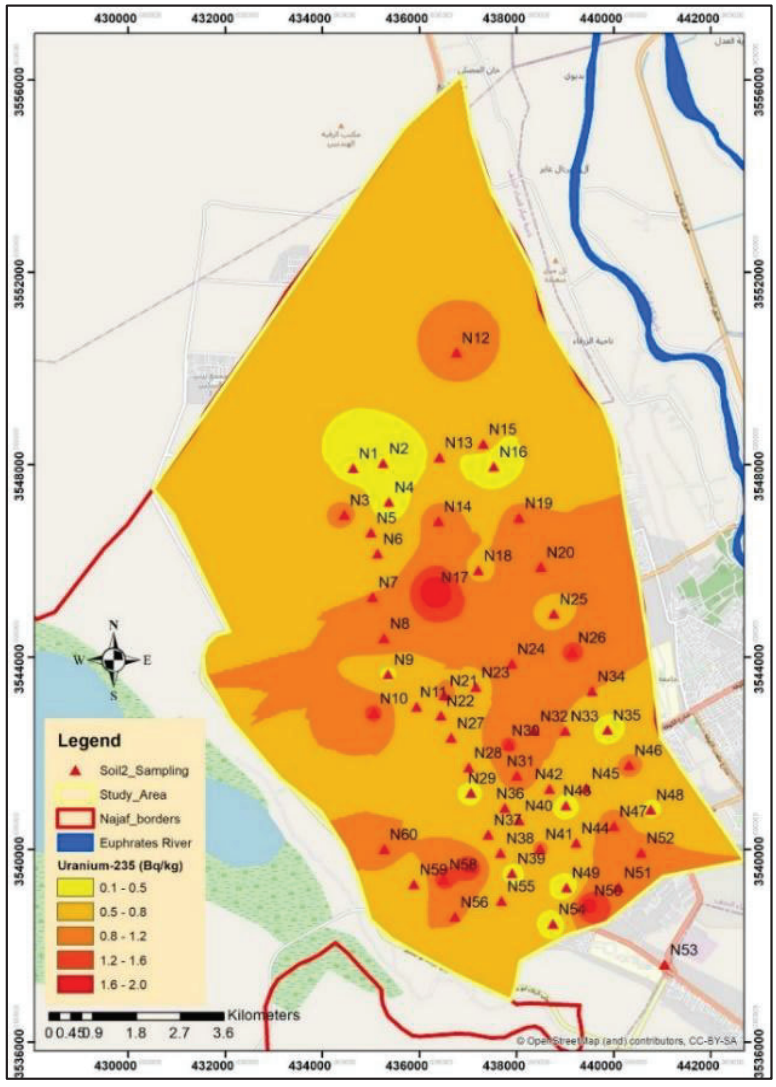

Figure (4.17) Distribution of ^{235}U in the soil of of Najaf city.

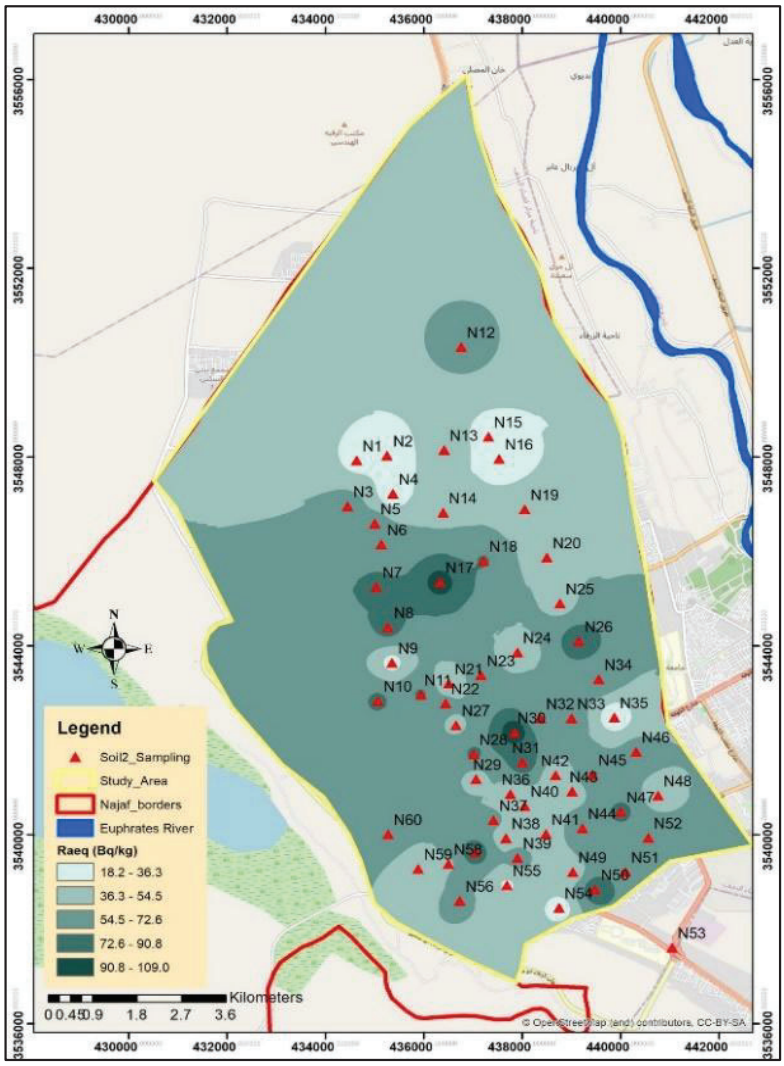

Figure (4.18) Distribution of Ra_{eq} in the soil of Najaf city.

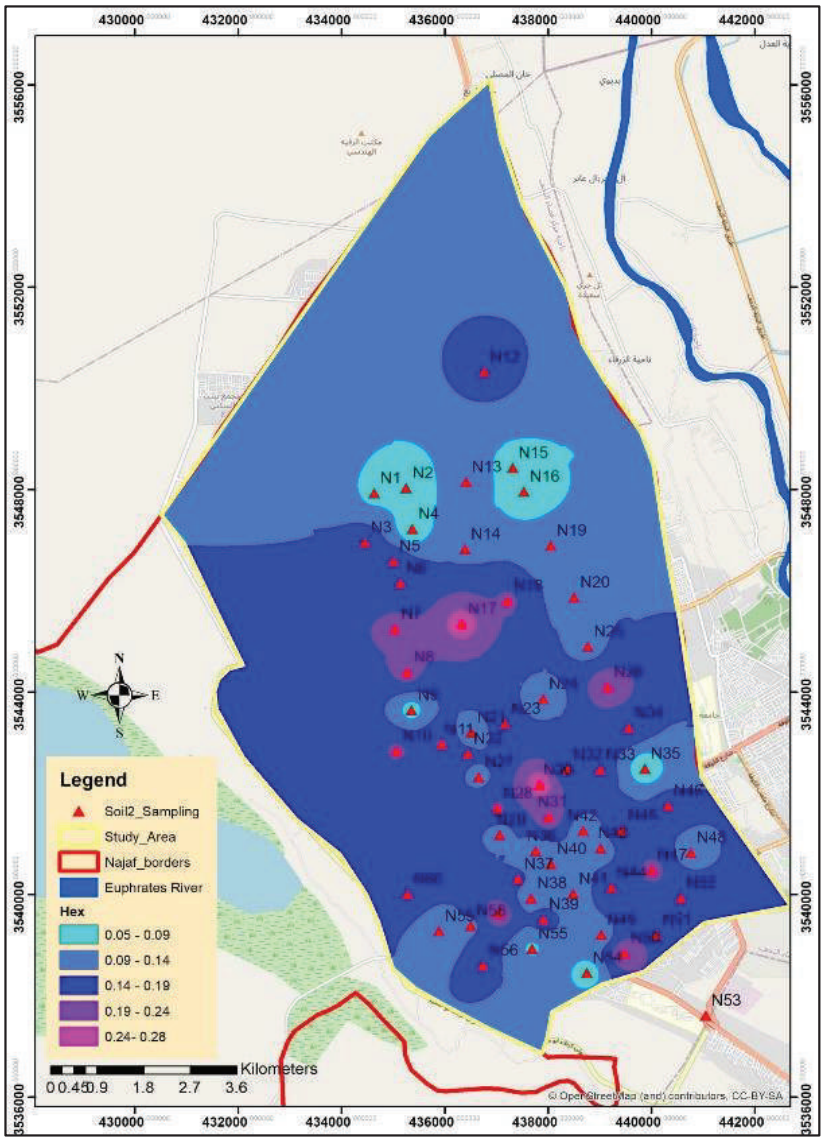

Figure (4.19) Distribution of H_{ex} in the soil of Najaf city.

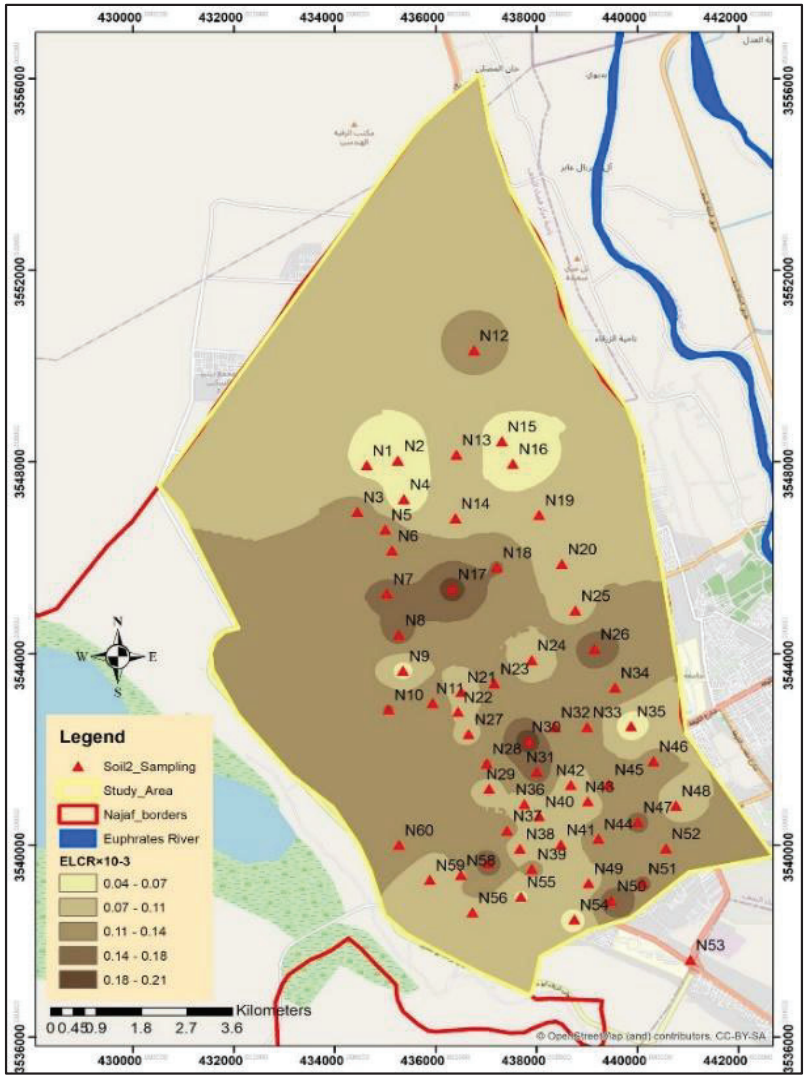

Figure (4.20) Distribution of ELCR in the soil of Najaf city.

4.6.4 Discussion of CR-39 Detector

4.6.4.1 Discussion of Kufa City

Table (4.9) shows that all minimum and maximum values of C and C_{Rn} are less than the world average of radon gas in air (100) Bq/m^3 according to WHO [150]and (7400) Bq/m^3 according to UNSCEAR 2000 [144].Also, the range values of C_{Ra} and C_U are below the global average value of 35 Bq/kg for C_{Ra} [151] and 11 (ppm) for C_U [3]. From Table(4.10) All values of AED due to radon gas are within action levels of (3–10) mSv/y according to ICRP [149] and (1.2) mSv/y by UNSCEAR1994 [152]. Also shown in the table (4.10) the range value of E_M (m.Bq/kg.h) and E_S (m.Bq/m^2.h) and their average values. It is seen that all values of E_S and E_M in the present study are smaller than the action levels of (57.6 Bq/m^2.h) [3]. Also the range value of ELCR due to radon gas in air space of the container, as shown in the Table(4.10) are 0.07×10^{-3} - 2.11×10^{-3}, with an average $(1\pm0.1)\times10^{-3}$. Thus, the value of ELCR in the present area is low and not dangerous[152].Figures (4.21)-(4.26) show the distribution of (C, C_{Rn} ,C_{Ra}, C_U , AED and ELCR) respectively .

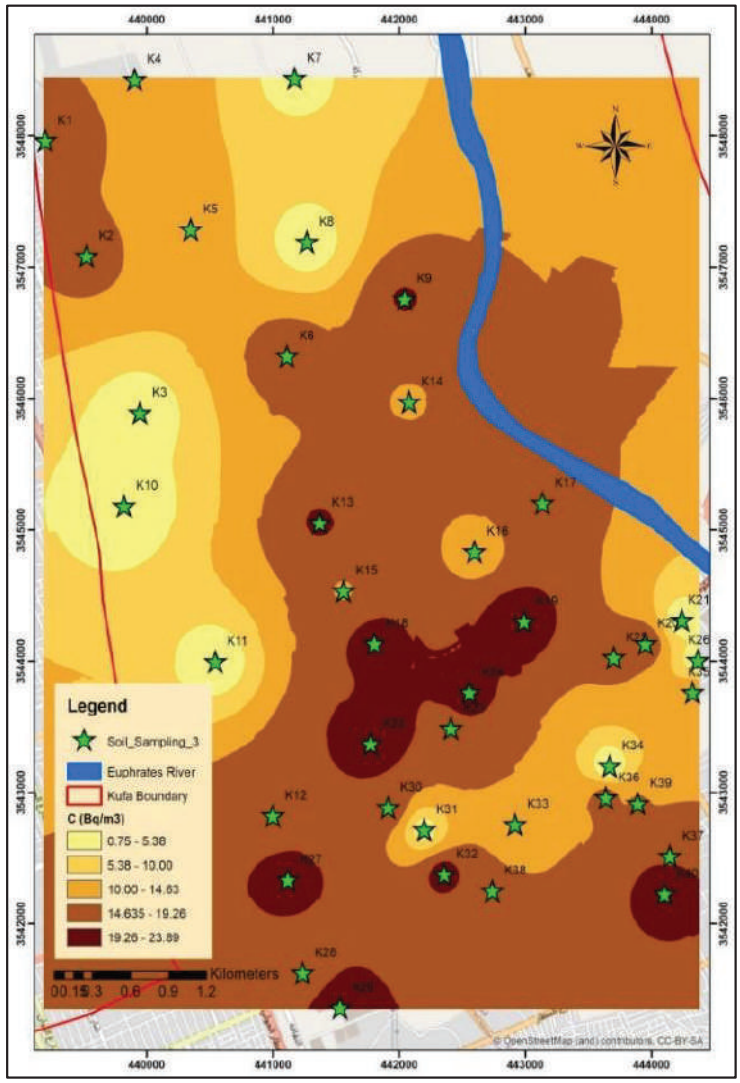

Figure (4.21) Distribution of the results of C in soil samples in Kufa city.

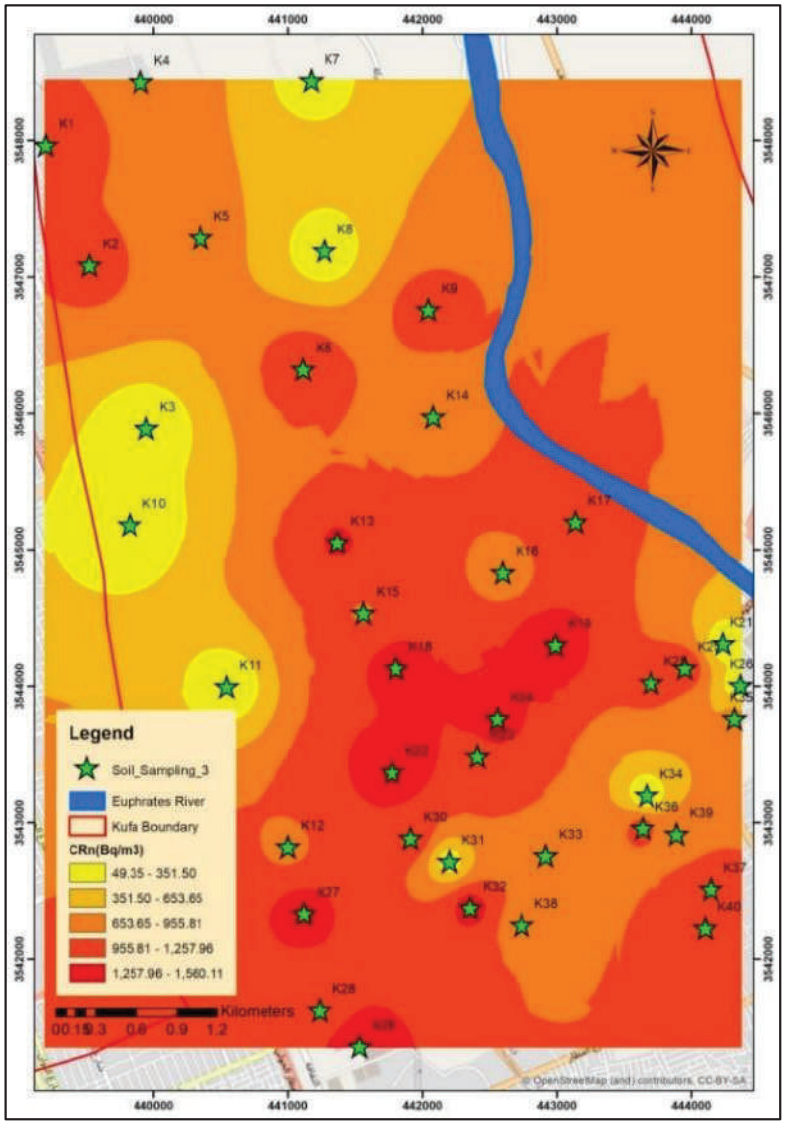

Figure (4.22) Distribution of the results of C_{Rn} in soil samples in Kufa city.

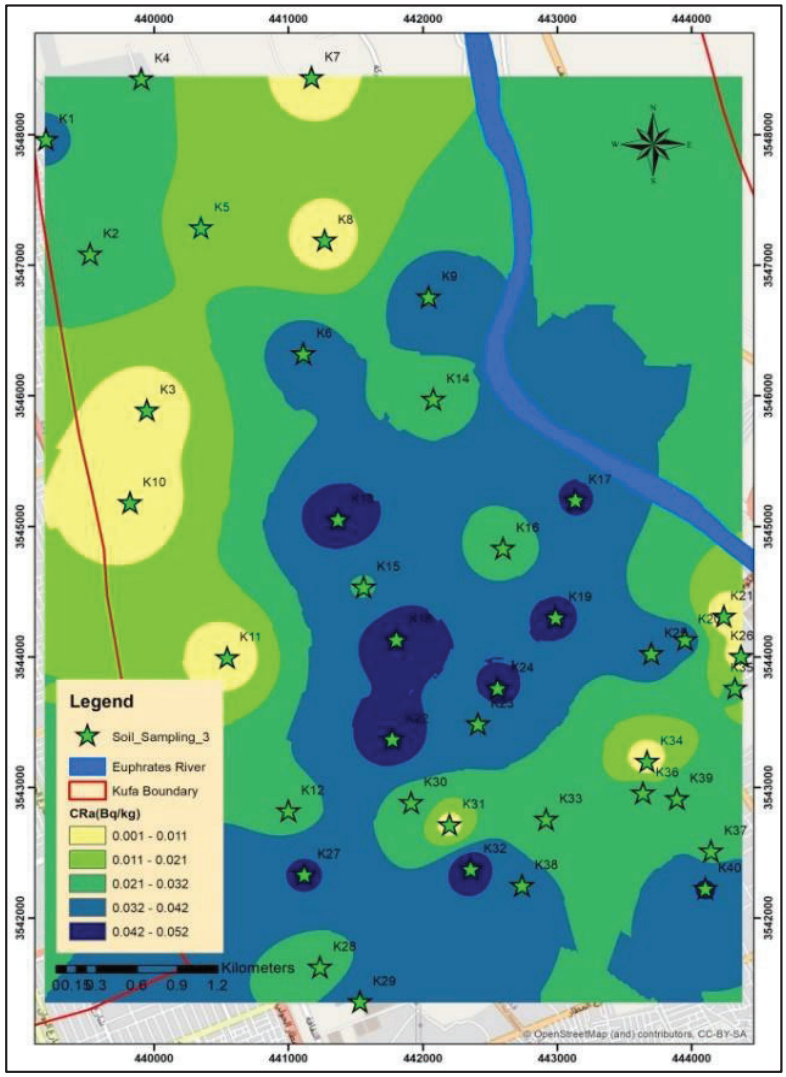

Figure (4.23) Distribution of the results of C_{Ra} in soil samples in Kufa city.

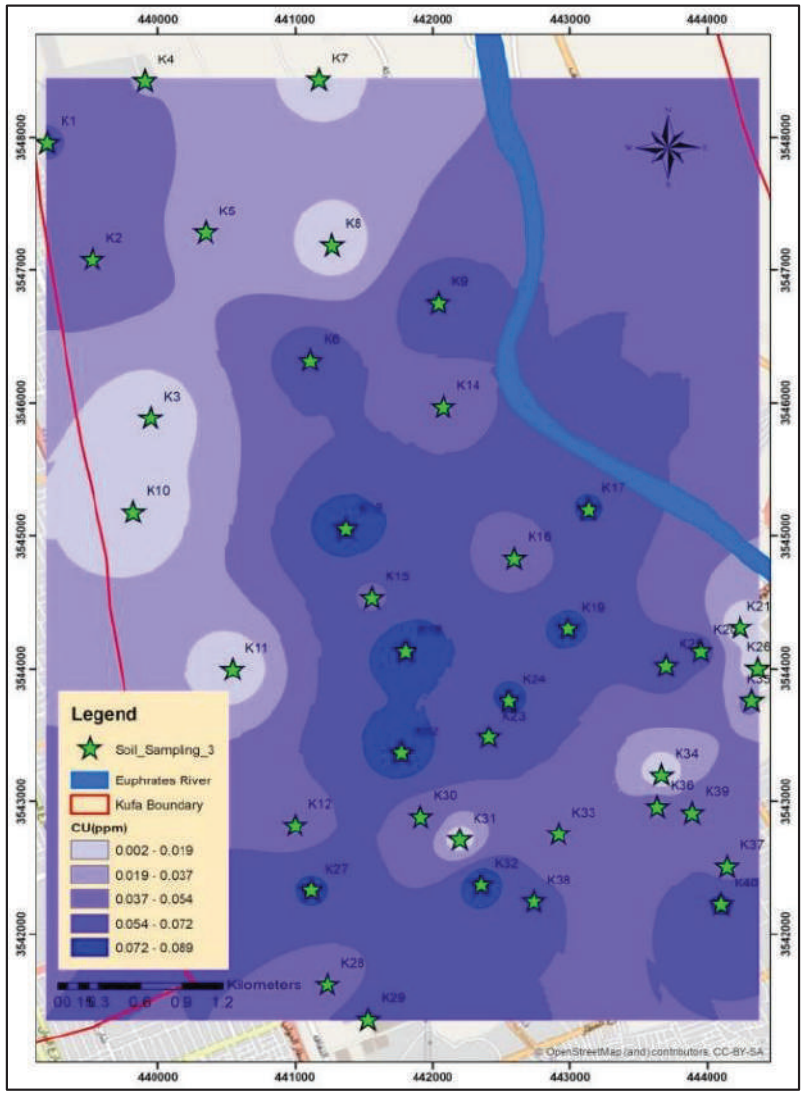

Figure (4.24) Distribution of the results of Cu in soil samples in Kufa city.

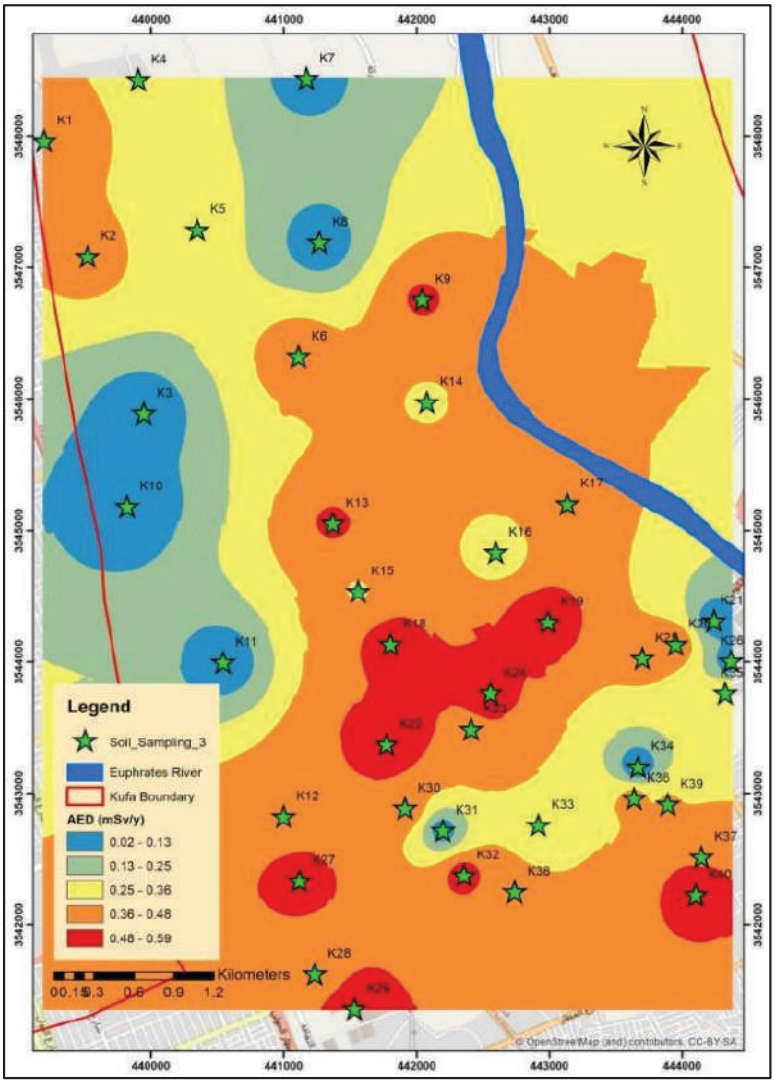

Figure (4.25) Distribution of the results of AED in soil samples of Kufa city.

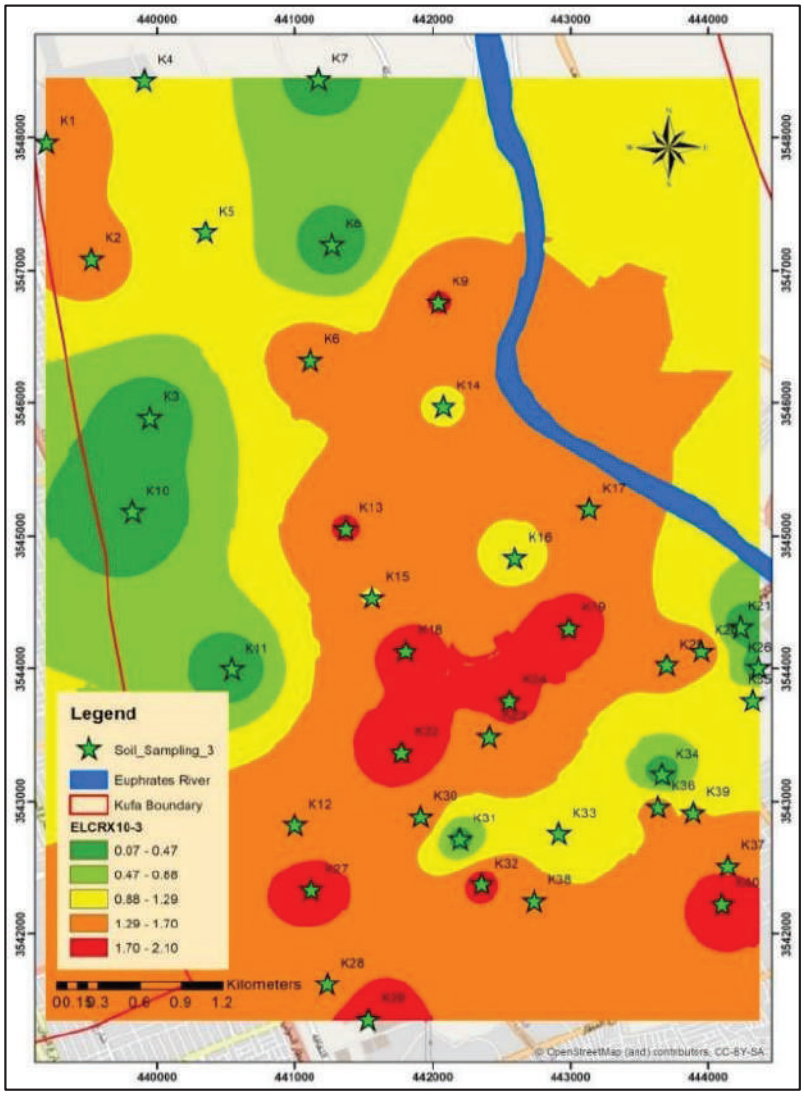

Figure (4.26) Distribution of the results of ELCR in soil samples of Kufa city.

4.6.4.2 Discussion of Najaf City

Table (4.11) shows that minimum and maximum values of C and C_{Rn} which are in sample N17 and N59 ,where the value of C in N17 is higher than the acceptable limit and N50 is less than the world average of radon gas in air (100) Bq/m^3 according to WHO [150]and (7400) Bq/m^3 according to UNSCEAR 2000 [144]. Also, the range values of C_{Ra} and C_U are below the global average value of 35 Bq/kg for C_{Ra} [151] and 11 (ppm) for C_U [3]. From Table(4.12) All values of AED due to radon gas are within action levels of (3–10) mSv/y according to ICRP [149] and (1.2) mSv/y by UNSCEAR [152]. Also shown in the table (4.12) the range value of E_M (m.Bq/kg.h) and E_S (m.Bq/m^2.h) and their average values. It is seen that all values of E_S and E_M in the present study are smaller than the action levels of (57.6 Bq.m^2.h)[3] . Also the range value of ELCR due to radon gas in air space of the container, as shown in the Table (4.12) are 0.07×10^{-3} - 12.825×10^{-3}, with an average $(1.422\pm0.279)\times10^{-3}$. Thus, the value of ELCR in the present area is low and not dangerous[152].Figures (4.27) - (4.32) show the distribution of (C, C_{Rn} ,C_{Ra}, C_U , AED and ELCR) respectively .

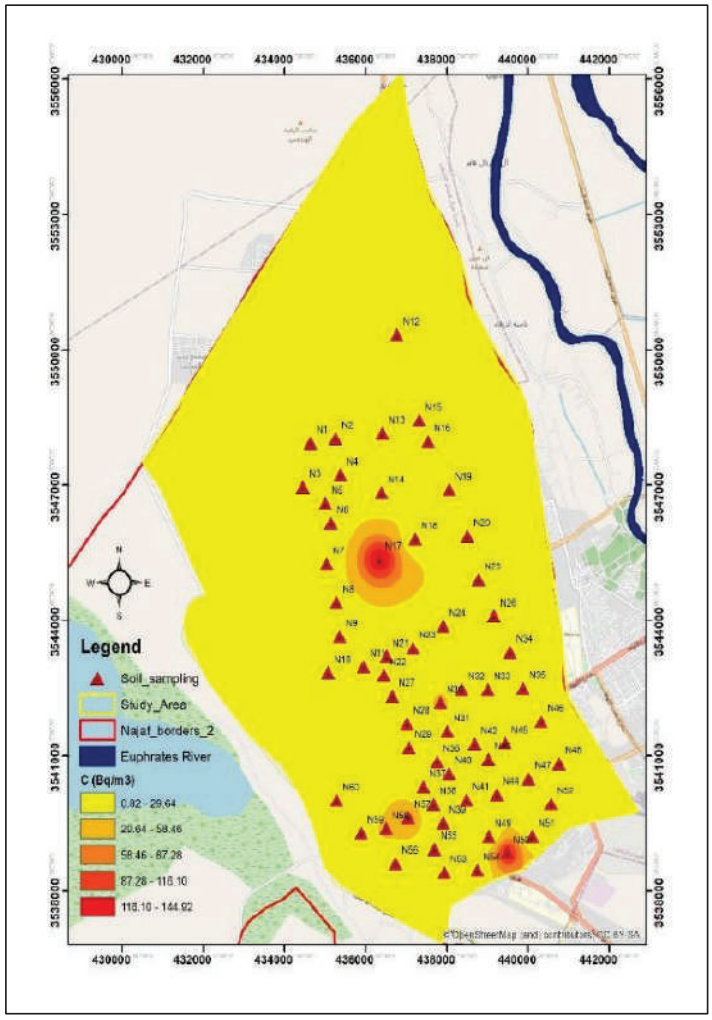

Figure (4.27) Distribution of the results of C in soil samples in Najaf city.

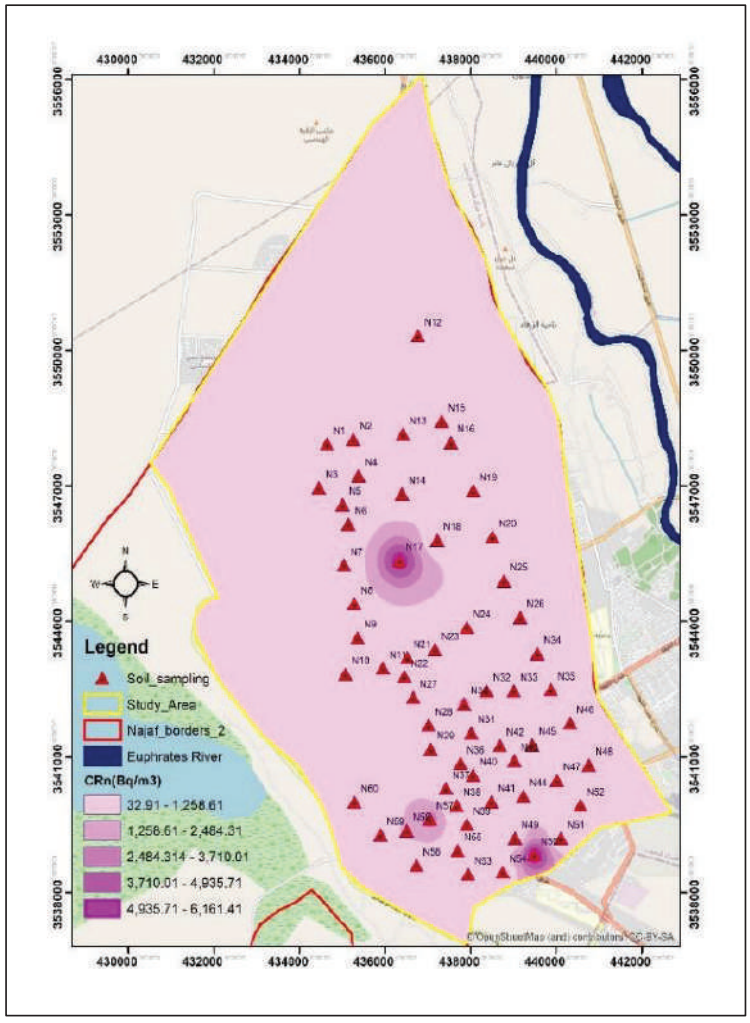

Figure (4.28) Distribution of the results of C_{Rn} in soil samples in Najaf city.

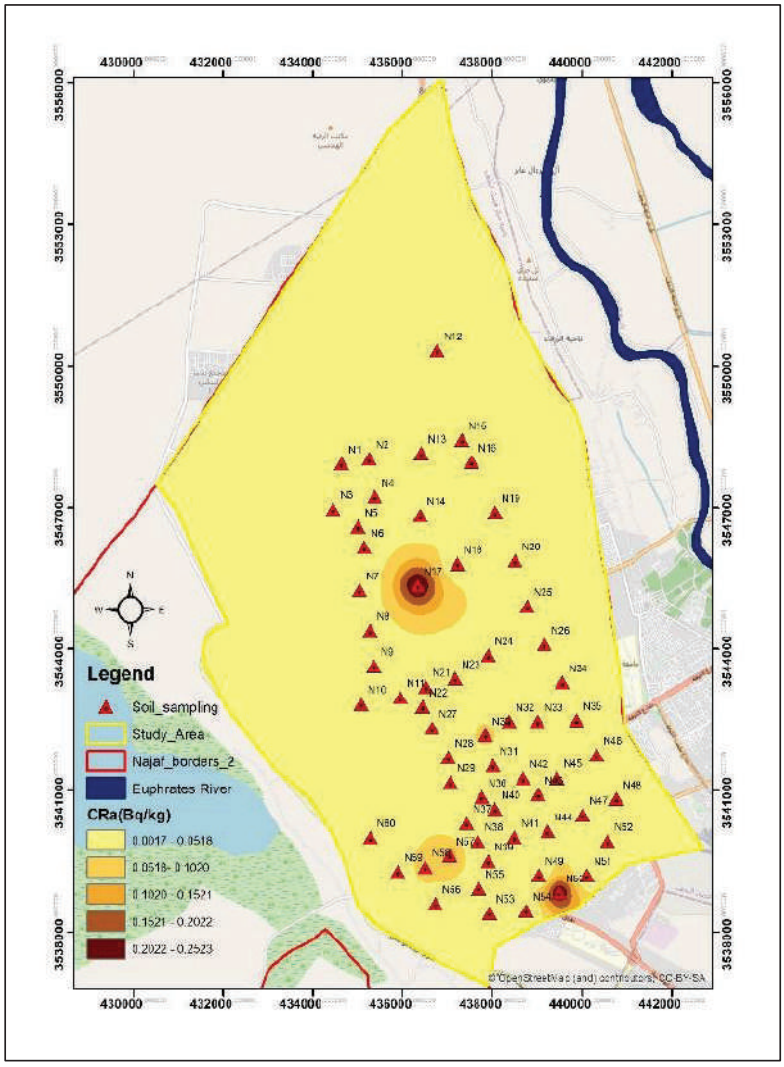

Figure (4.29) Distribution of the results of C_{Ra} in soil samples in Najaf city.

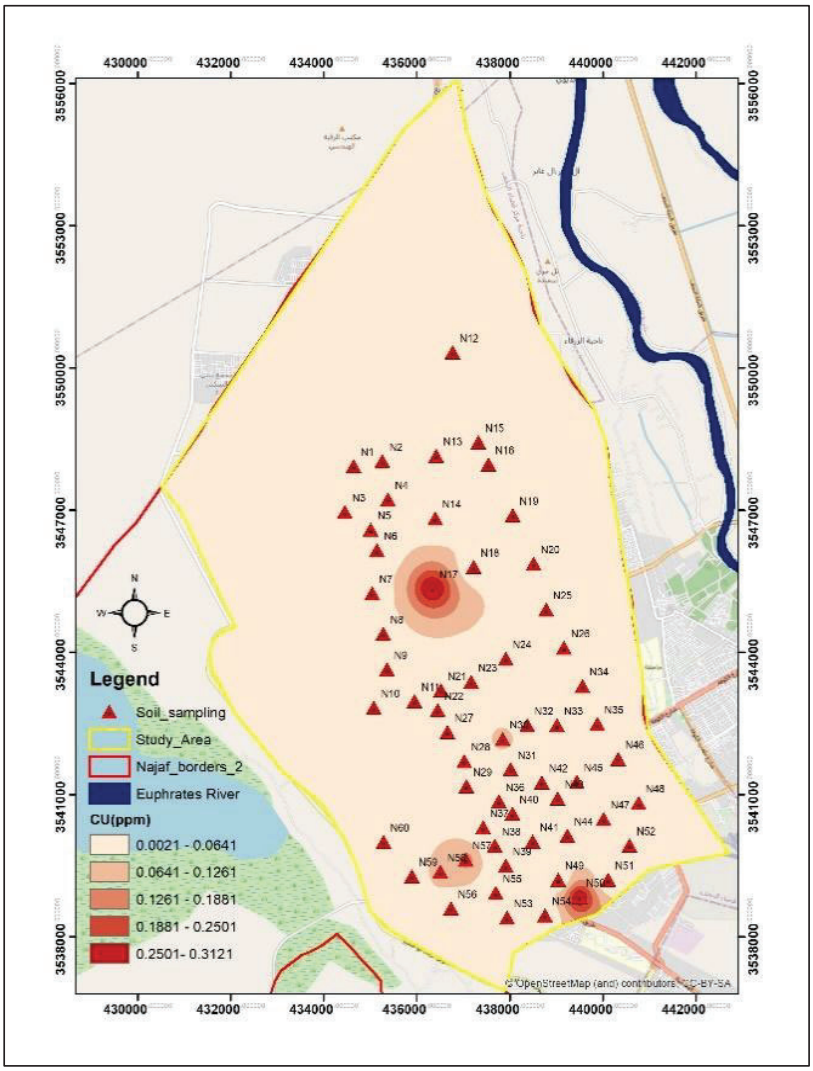

Figure (4.30) Distribution of the results of Cu in soil samples in Najaf city.

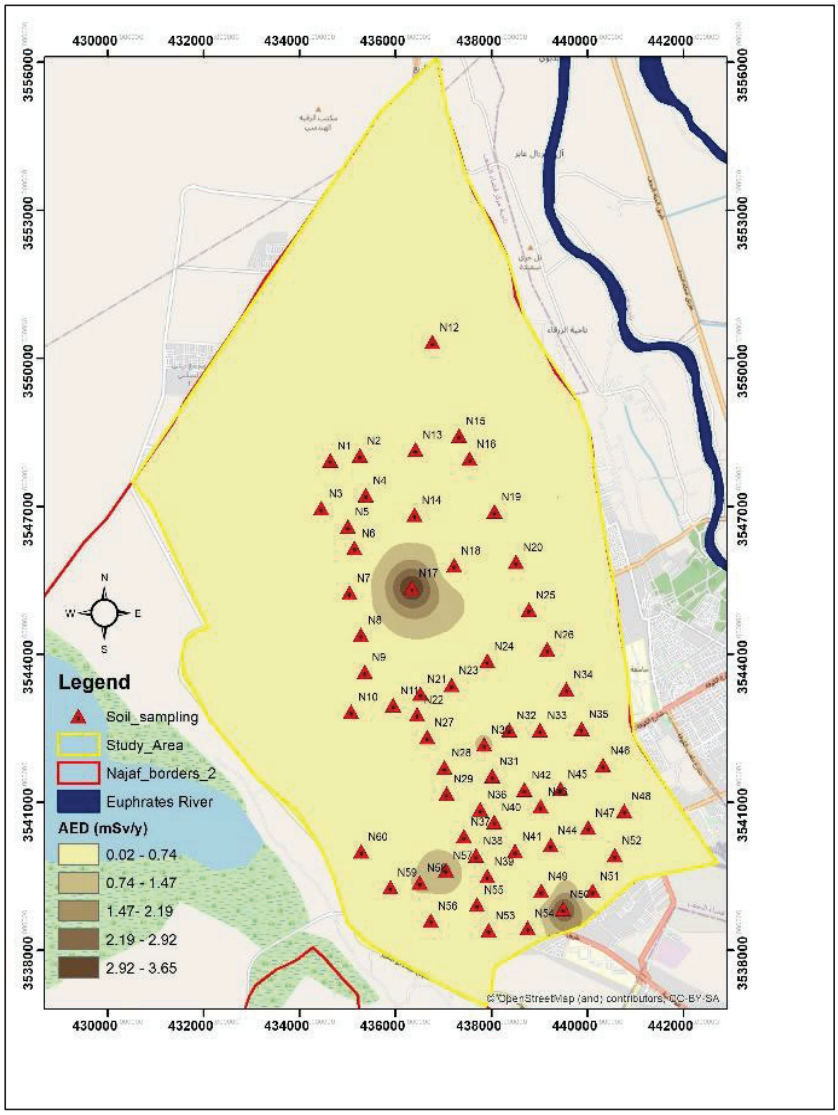

Figure (4.31) Distribution of the results of AED in soil samples in Najaf city.

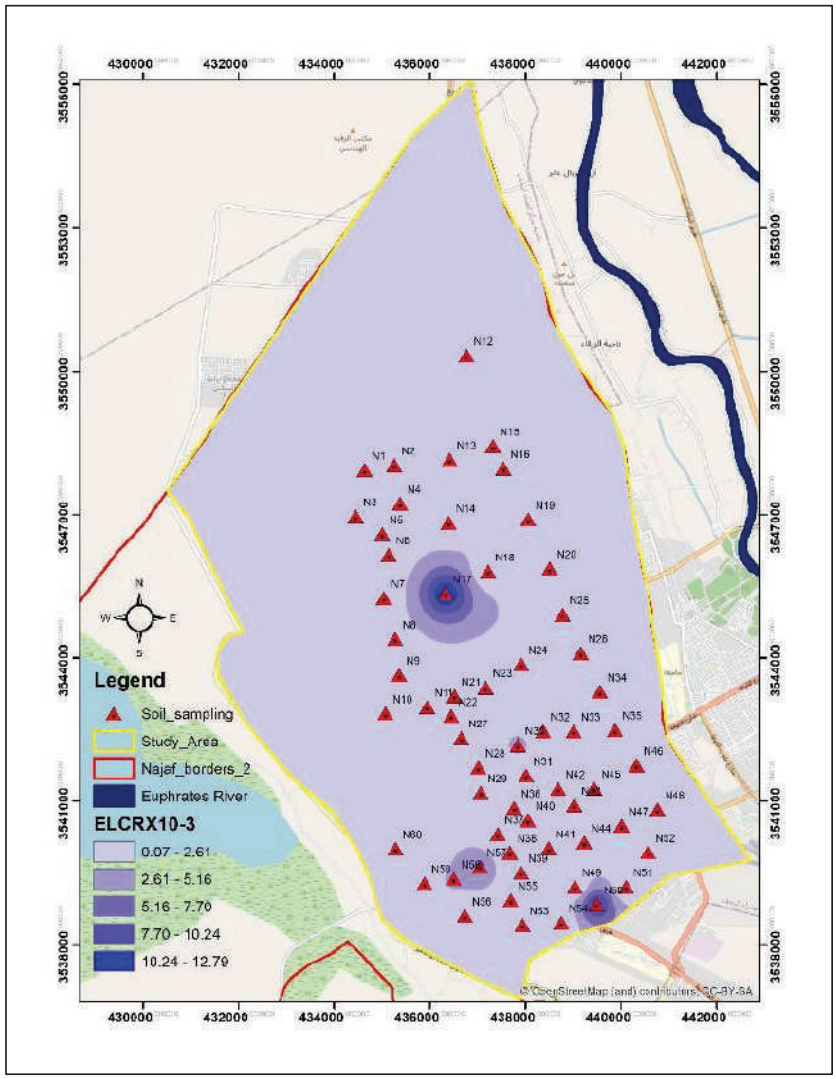

Figure (4.32) Distribution of the results of ELCR in soil samples in Najaf city.

4.6.5 Discussion of RAD-7 Detector

4.6.5.1 Discussion of Kufa and Najaf Cities

The average value of Radon Activity in Bq/m^3 is measured for 20 samples of Kufa and 30 samples of Najaf using RAD-7. All the results are listed in Table(4.13) and (4.14).The radioactive level of ^{222}Rn for soil samples for both minimum and maximum values are well below the allowed levels which is range (0.4-40) KBq/m^3 [153].

Finally, Average value of specific activity for (^{238}U,^{235}U, ^{232}Th and ^{40}K) and radiological effects inside two locations Najaf government (Kufa and Najaf), Iraq by using two major techniques are summarized in Tables (4-13) and (4-14).

4.7 Values Comparison Between Kufa and Najaf Cities

Tables (4.15),(4.16), and (4.17) summarize the results of Kufa and Najaf cities by using Dosimeter, NaI(Tl) and CR-39 respectively.

In the table (4.15), the average dose rate for the current study using a Dosimeter detector for Kufa and Najaf are found to be approximate to each other, and at the same time below the preassembly limit.

In the table (4.16), the average specific activity for the current study using NaI(TI) detector for Kufa and Najaf are found in different values. ^{238}U, ^{232}Th, and ^{235}U in Najaf city are found higher than in Kufa city, except for ^{40}K in Kufa city is found higher than in Najaf city but also the results are in saved limit.

In table (4.17), the average of alpha emitters for the current study using CR-39 detector shows that ^{222}Rn gas concentration in air space (C) for Kufa city is lower than for Najaf city. While the ^{222}Rn concentration in the samples (C_{Rn}) is high in Kufa than in Najaf. The specific activity of radium-226 (C_{Ra}) for both Kufa and Najaf are closed to each other, and uranium concentrations (C_U) in kufa is higer than in Najaf.All results in table (4-17) are in preassembly limit.

Table (4.15) The average dose rate for the current study using the **Dosimeter** detector.

No.	Location	Dose rate ***(μSv/h)***
1	Kufa	0.127±0.005
2	Najaf	0.121±0.004

Table (4.16) The average specific activity for the current study using **NaI(Tl)** detector.

No.	Location	Specific activity (Bq/kg)			
		^{238}U	^{232}Th	^{40}K	^{235}U
1	Kufa	6.2±0.74	6.41±0.82	278.10±19.43	0.28±0.03
2	Najaf	18.01±1.24	13.36±0.91	256.86±12.23	0.83±0.44

Table (4.17) The average of alpha emitters for the current study using **CR-39** detector.

No.	Location	C (Bq/m^3)	C_{Rn}(Bq/m^3)	C_{Ra}(Bq/kg)	C_U(ppm)
1	Kufa	14±1	895±74	0.028±0.008	0.048±0.008
2	Najaf	16.10±3.166	684.92±140.5	0.029±0.0058	0.036±0.0072

4.8 Correlation Relations Between Different Detectors

This will deal with the numerical values of the correlation coefficient between three techniques for all areas under study(Kufa and Najaf) : first dosimeter and NaI (Tl) detectors, second NaI (Tl) and CR-39 detectors, and third CR-39 with RAD-7 detectors, as shown in tables (4.18),(4.19) and (4.20) below.

The numerical values of the correlation coefficient for the dosimeter and NaI (Tl) detectors are shown in table (4.18). The relation between dosimeter and ^{238}U is negative correlation (-0.08), the P-Value is (0.41),so the result is not significant at $p < 0.05$. Also, the relation between dosimeter and ^{232}Th is weak(-0.03) , the P-Value is(0.79). The result is not significant at $p < 0.05$. The relation between dosimeter and ^{40}K is positive correlation and the the P-Value is (0.15). The result is not significant at p <0 .05.

Table (4.19) shows the correlation relation between NaI (Tl) for(^{238}U, ^{232}Th and ^{40}K) and CR-39 (^{222}Rn) detectors. The relation between ^{238}U and ^{222}Rn shows a positive and weak correlation (0.6), the result is significant at $p < 0.05$. The relation between ^{232}Th and ^{222}Rn is a positive and weak correlation (0.24).The result is significant at $p < 0.05$. The relation

between ^{40}K and ^{222}Rn shows a positive correlation (0.18) . The result is not significant at $p < 0.05$.

Table (4.20) the correlation relation between CR-39 and RAD-7 detectors for Kufa city and shows a positive correlation (0.82). The result is significant at $p < 0.05$. At the same time the correlation relation between CR-39 and RAD-7 detectors for Najaf city shows also a positive correlation (0.88). The result is significant at $p < 0.05$.

The study proves the presence of a high correlation factor of all the present study samples, and it is evident that the soils samples under study are original and it is also affected with goegical area and filtration.Thus, the correct sequence of the uranium-238 basket can be achieved. Also, a good association between the Uranium-238 and Radon -222 and would be considered statistically significant. But there is a weak association of all sites in the present study, between radon-222 with thorium-232 and potassium-40. This because no relation is found between radon-222 with thorium-232 series inside and potsium-40 from another side,.Also, there is a very good relation between passive and active technique.

Table (4.18) Correlation relation between dosimeter and NaI (Tl) detectors.

Radionuclides	***NaI(Tl)Detector***		
Dose Rate (μSv/h)	^{238}U	^{232}Th	^{40}K
	-0.08	-0.03	0.15
^{238}U	1.00	0.50	0.16
^{232}Th	0.50	1.00	0.40
^{40}K	0.15	0.40	1.00

Table (4.19) Correlation relation between NaI (Tl) and CR-39 detectors.

Radionuclides	^{238}U	^{232}Th	^{40}K	^{222}Rn
^{238}U	1.00	0.50	0.16	0.60
^{232}Th	0.50	1.00	0.40	0.24
^{40}K	0.16	0.40	1.00	0.18
^{222}Rn	0.60	0.24	0.18	1.00

Table (4.20) Correlation relation between CR-39 and RAD-7 detectors.

No.	Location	Technique	CR-39	RAD-7
1	Kufa	CR-39	1	0.82
		RAD-7	0.82	1
2	Najaf	CR-39	1	0.88
		RAD-7	0.88	1

4.9 Multivariate Statistical Analysis

In this work, the statistical analysis has been carried out by using the statistics software package SPSS version 26.0 for windows. Statistics are based on cases with no missing values for any dependent variable or factor used. Depending on the descriptive table and tests of normality. A box plot, frequency distribution, Q-Q plot, bivariate correlations coefficient and cluster analysis are drawn for dose rate,^{238}U, ^{232}Th,^{40}K, and ^{222}Rn to show the relations between these five variables.

4.9.1 Basic Statistics

Basic statistical variables : mean, median, Kurtosis, skewness and standard deviation of the parameters are measured and listed in table (4.21).

Kurtosis is the measure of the peak of a real valued random variables probability distribution, compared with the usual distribution, it charactertises the relative peak or flatness of a distribution. Positive kurtosis indicates relativalty a peak distribution and nagative kurtosis indicates relativalty a flat distribution. At the same time, positive and nagative swekness gaves the information about asymmetric distriution[154].In this sutdy, the kurtosis of dose rate is (-0.208) which means a flat distribution, while kurtosis of ^{238}U(1.284) , ^{232}Th(0.121), ^{40}K(2.230) and ^{222}Rn(50.342) all found a relatively peak distribution. On other hand, the swekness of dose rate (0.335), ^{238}U(1.046) , ^{232}Th(0.833), ^{40}K(0.909) and ^{222}Rn(6.338) are positive which indicate that the peak of the distribution is right of the mean value.Table (4.22) shows test of normallity, The Kolmogorov-Smimiov normal distribution test was used for large samples, and for this reason, it was determined whether the data were distributed or not. All variables are not distributed normally except for the dose rate and ^{222}Rn

with a significant level of 5%. The reason for using the normal distribution test is to find out which the correlation parameters we will use.

Table (4.21) Descriptive Analysis

			Statistic	Std. Error
Dose Rate	Mean		0.123	0.0034
	95% Confidence Interval for Mean	Lower Bound	0.116	/
		Upper Bound	0.130	/
	Median		0.122	/
	Variance		0.001	/
	Std. Deviation		0.031	/
	Minimum		0.05	/
	Maximum		0.20	/
	Range		0.16	/
	Skewness		0.335	0.266
	Kurtosis		-0.208	0.526
^{238}U	Mean		11.812	1.01033
	95% Confidence Interval for Mean	Lower Bound	9.802	/
		Upper Bound	13.822	/
	Median		10.150	/
	Variance		83.703	/
	Std. Deviation		9.148	/
	Minimum		0.40	/
	Maximum		46.50	/
	Range		46.10	/

Next

	Skewness		1.046	0.266
	Kurtosis		1.284	0.526
^{232}Th	Mean		10.006	0.826
	95% Confidence Interval for Mean	Lower Bound	8.361	/
		Upper Bound	11.650	/
	Median		8.450	/
	Variance		55.995	/
	Std. Deviation		7.482	/
	Minimum		0.20	/
	Maximum		32.60	/
	Range		32.40	/
	Skewness		0.833	0.266
	Kurtosis		0.121	0.526
^{40}K	Mean		262.020	12.015
	95% Confidence Interval for Mean	Lower Bound	238.113	/
		Upper Bound	285.927	/
	Median		266.750	/
	Variance		11838.4	/
	Std. Deviation		108.804	/
	Minimum		103.50	/
	Maximum		708.00	/
	Range		604.50	/
	Skewness		0.909	0.266
	Kurtosis		2.230	0.526

Next

^{222}Rn	Mean		14.279	1.817
	95% Confidence Interval for Mean	Lower Bound	10.663	/
		Upper Bound	17.894	/
	Median		13.805	/
	Variance		270.817	/
	Std. Deviation		16.456	/
	Minimum		0.74	/
	Maximum		145.24	/
	Range		144.50	/
	Skewness		6.338	0.266
	Kurtosis		50.342	0.526

Table (4.22) Test of Normality

Tests of Normality

	Kolmogorov-Smirnov[a]			Shapiro-Wilk		
	Statistic	df	Sig.	Statistic	df	Sig.
Dose Rate	0.066	82	0.200*	0.981	82	0.272
^{238}U	0.107	82	0.022	0.915	82	0.000
^{232}Th	0.104	82	0.028	0.930	82	0.000
^{40}K	0.082	82	0.200*	0.932	82	0.000
^{222}Rn	0.243	82	0.000	0.473	82	0.000

*. This is a lower bound of the true significance.
a. Lilliefors Significance Correction

4.9.2 Box-Whisker Plot

A type of graph that gives a visual representation of location, variability, and outliers is the box-whisker plot, or simply called the box plot. The box plot involves basically only a few values: the lowest value, the first quartile, median, the third quartile, and the largest value[155]. This shows how activity concentration are speard out for dose rate, ^{238}U, ^{232}Th, ^{40}K and ^{222}Rn .The median is near the center for dose rate, this means that the distribution of the data set is normally distributed and symmetracally. For ^{238}U and ^{232}Th the median is closer to the bottom of the box, then the data are likely to be left-skewed.On the other hand, ^{40}K and ^{222}Rn ^{232}Th the median is closer to the top of the box, then the data are likely to be right-skewed.

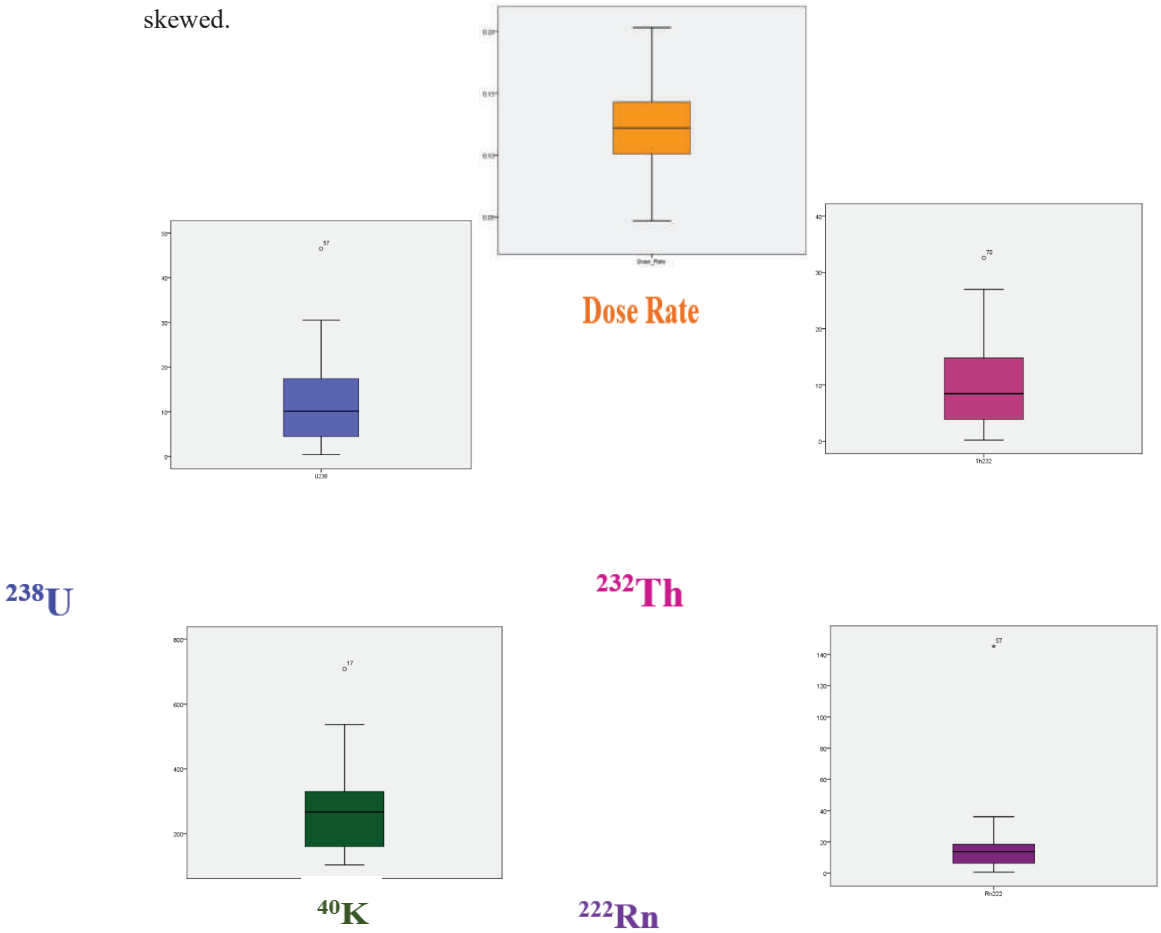

Figure (4.33) Box plot for dose rate, ^{238}U, ^{232}Th,^{40}K and ^{222}Rn of investigated soil samples

4.9.3 Correlations Coefficients

There are two types of correlation coefficients: parametric and nonparametric correlations. Parametric correlations, which are also called Pearson correlation or bivariate Pearson Correlation, produce a sample correlation coefficient that measures the strength and direction of linear relationships between pairs of continuous variables. While nonparametric correlations (spearman correlation) assumes that the variables under consideration are measured on at least an ordinal (rank order) scale, the individual observations can be ranked into two-ordered series[154] . According to this study, table (4.23) shows that the Dose rate and ^{40}K are undergo Pearson correlaion , because they have a normal distribution.At the same time, ^{238}U, ^{232}Th and ^{222}Rn are undergo spearman correlation with normal distribution.

Table (4.23) The correlation relations between dose rate, ^{238}U, ^{232}Th,^{40}K and ^{222}Rn.

Correlations		Dose Rate	^{238}U	^{232}Th	^{40}K	^{222}Rn
Dose Rate	Correlation	1	-0.193	-0.054	0.120	-0.01
	Sig. (2-tailed)	—	0.082	0.632	0.282	0.926
^{238}U	correlation	-0.193	1	0.596**	0.164	0.456**
	Sig. (2-tailed)	0.082	—	0.000	0.142	0.000
^{232}Th	correlation	-.054	0.596**	1	0.526**	0.258*
	Sig. (2-tailed)	0.632	0.000	—	0.000	0.019
^{40}K	Correlation	0.120	0.164	0.526**	1	0.331**

Next

	Sig. (2-tailed)	0.282	0.142	0.000	—	0.002
^{222}Rn	Correlation	-.010	0.456**	0.258*	0.331**	1
	Sig. (2-tailed)	0.926	0.000	0.019	0.002	—

** Correlation is significant at the 0.01 level (2-tailed).

*. Correlation is significant at the 0.05 level (2-tailed).

4.9.4 Frequency Distribution and Q-Q Plot

The frequency distribution and quantile–quantile (Q-Q) plot for dose rate, ^{238}U, ^{232}Th, ^{40}K, and ^{222}Rn are analyzed and histograms are given in figures (4.34), (4.35), (4.36), (4.37) and (4.38) respectively. The distribution of Dose rate and ^{40}K appear normal according to Pearson Correlation, while ^{238}U, ^{232}Th and ^{222}Rn ^{40}K appear normal according to Spearman Correlation. The Q-Q plot is show that all point lie approximately along the 45 – degree reference line, the distributions may be assumed to be normal.

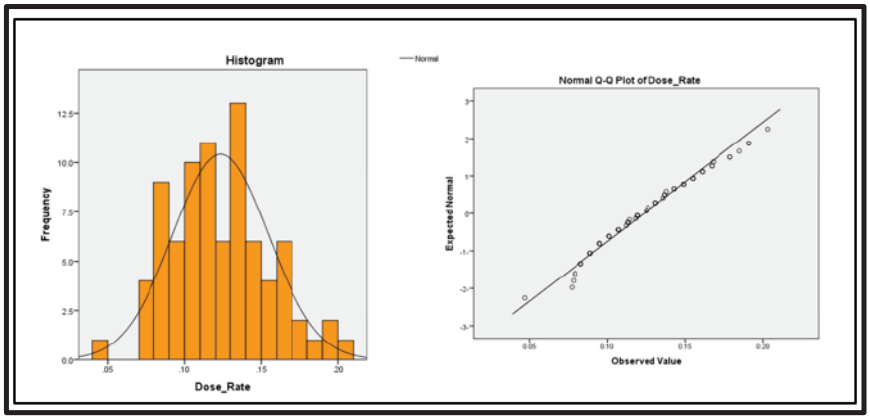

Figure (4.34) Frequency distribution and quantile–quantile (Q-Q) plot for dose rate for the investigated soil samples.

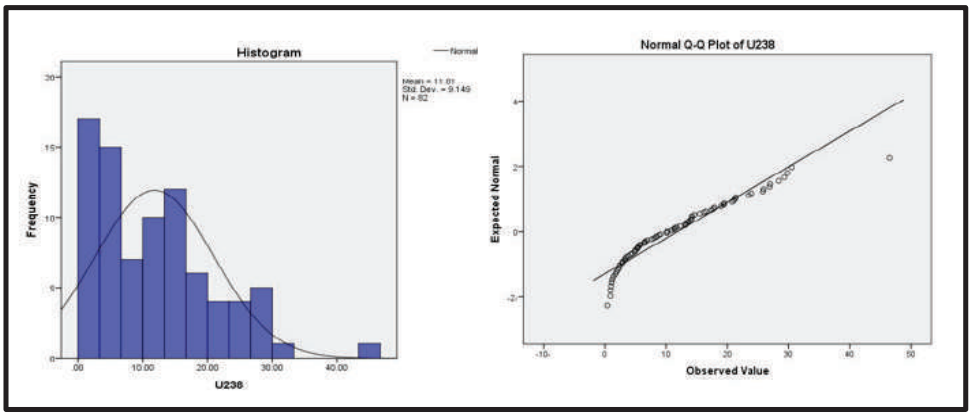

Figure (4.35) Frequency distribution and quantile-quantile (Q-Q) plot for ^{238}U for the investigated soil samples

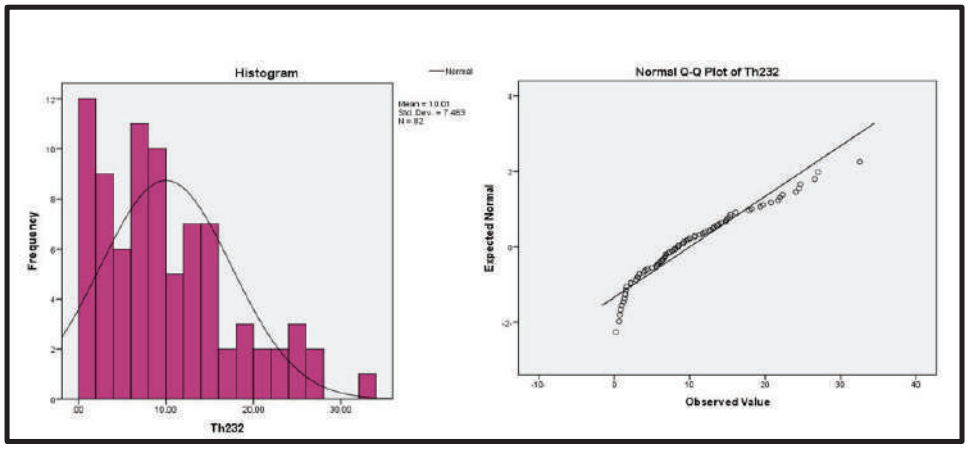

Figure (4.36) Frequency distribution and quantile-quantile (Q-Q) plot for ^{232}Th for the investigated soil samples.

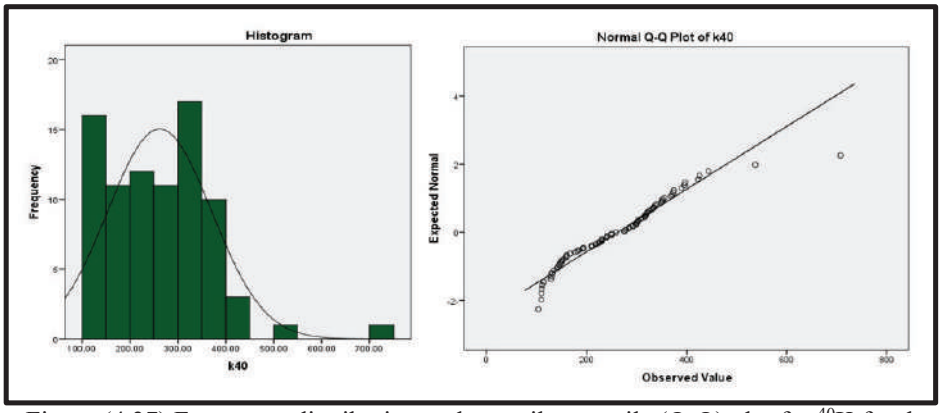

Figure (4.37) Frequency distribution and quantile-quantile (Q-Q) plot for ^{40}K for the investigated soil samples.

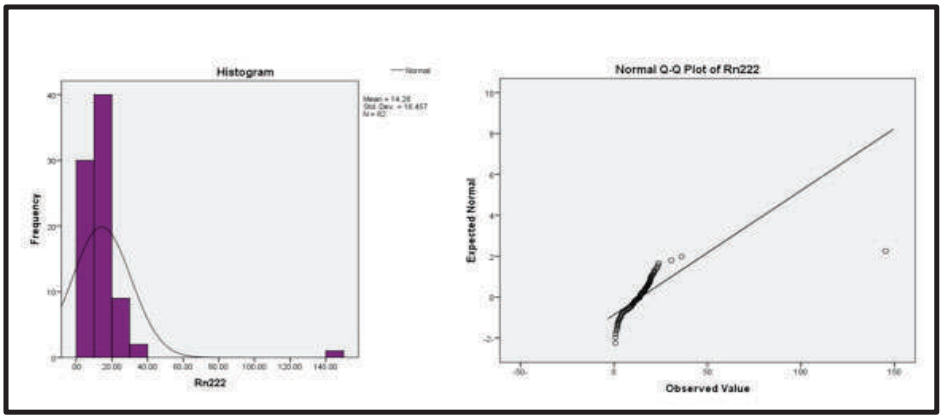

Figure (4.38) Frequency distribution and quantile-quantile (Q-Q) plot for ^{222}Rn for the investigated soil samples.

4.9.5 Cluster Analysis

Cluster analysis is used to identify and classify groups with similar features in new observation. Each observation in a cluster is most like the other group in the same cluster. The similarity is a measure of a distance between clusters relative to the greatest distance between any two variables. The zero distance means that the cluster is 100% similar in their sample measurements, while cluster areas are as disparate as the least similar region means 100% similar in size[154].

The cluster analysis is carried out to idetify similar charachteristics between dose rate and other natural radioistops in soil.In CA, figures (4.39) shows the average linkage method,number of cluster and how to perform nodes to form clusters of elements.

Agglomeration Schedule in table (4.24) shows the correlation coefficients, which means the value of the transactions on the basis of which the clusters are formed, starting from the lowest value of the transactions between ^{238}U and ^{222}Rn with 70.359 to the highest value of 165.681between Dose rate and ^{238}U. Table (4.25) shows the distribution of the elements according to the clusters formed and the specific radiation for each one.

Table (4.24) Agglomeration Schedule.

Stage	Cluster Combined		Coefficients	Stage Cluster First Appears		Next Stage
	Cluster 1	Cluster 2		Cluster 1	Cluster 2	
1	2	5	70.359	0	0	3
2	3	4	88.434	0	0	3
3	2	3	117.039	1	2	4
4	1	2	165.681	0	3	0

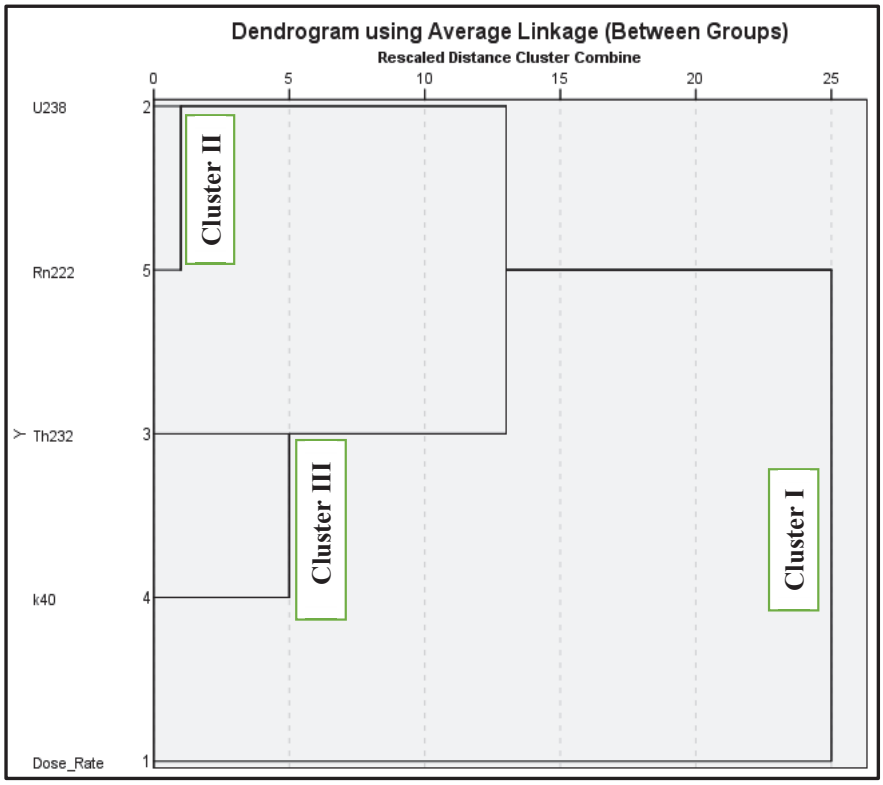

Figure (4.39) Dendrogram using Average linkage between groups.

Table (4.25) Cluster Membership

Case	3 Clusters
Dose_Rate	1
U-238	2
Th-232	3
K-40	3
Rn-222	2

4.10 Conclusions

According to the obtained results of background radiation, gamma emitters, and alpha emitters in the current research, the researcher has conclude the following points:

1. The results of background radiation levels and then radiological risk such as dose rate, AAED, and ELCR in all samples of the present study are within the acceptance of the permissible limit according to UNSCEAR 2008.
2. The specific activity of ^{238}U and ^{232}Th in all soil samples have been found to be within worldwide according to UNSEAR 2008, while the specific activity of ^{40}K for some samples are larger than worldwide according to UNSEAR 2008.
3. The results of the ten radiological hazard parameters due to ^{238}U, ^{232}Th and ^{40}K in most samples are less than the world average according to the radiation protection report UNSCEAR2000, UNSCEAR2008, OECD and ICRP1993.
4. The results of alpha emitters (C_{Rn}, C_{Ra} and C_U) as well as AED E_S and E_A in all soil samples are less than the average of global level.
5. The average values for the results of the dose rate, gamma and alpha emitter with all the risk parameters calculated in the present study for Kufa city have values lower than Najaf city.In the same time,results of Najaf city are less than the global limit.
6. Statistically, using software package SPSS version 26 has found a strong positive correlation and significant in all soil samples between ^{222}Rn concentrations and the specific activity ^{238}U, while the correlation between ^{222}Rn concentrations with other gamma emitters are weak correlation coefficient and no significant. Also, a positive correlation and significant in all soil samples have been found between the concentrations of dose rate and the specific activity of ^{40}K, while the correlation between dose rate with other gamma emitters as well as alpha emitters are no correlation coefficient and no significant.
7. Another statistically relation between CR-39 detector and RAD-7 detector for ^{222}Rn concentrations, shows a strong positive and a significant correlation have been found in 50 samples (20 samples in Kufa city and 30 samples in Najaf city).
8. The Arc GIS statistical geographic tools succeeded in analyzing the background radiation, gamma and alpha emitters in soil samples of Kufa and Najaf cities by mapping the elements.

9. The data obtained in this study has improved the suitability of the Alert Inspector Dosimeter, NaI(Tl), CR-39, and RAD-7 techniques for such samples.
10. As a result, background radiation, gamma-ray and alpha particles levels and radiological hazard index in most soil samples in the study area Iraq ,does not constitute a health hazard.

4.11 Recommendations

In order to protect the air and Public health from X to radiation,the following recommendations are introdiced to the responsible authorities such as the Ministry of Health, Ministry of Industry, Ministry of Environment, Local Government in Najaf and Geological Survey.

1. Forming a specialized work team to conduct a radiological survey of another regions of Al-Najaf governorate, planning an integrated radiological map, increasing the number of samples studied.
2. Providing a study in all governorates of the country to draw a radiological map.
3. Reducing the use of chemical fertilizers, which are used especially in agricultural areas
4. Conducting radiological surveys periodically to detect and monitor Radiation changes in the governorate.
5. Providing modern enough scientific and research institutions to conduct their own systems of radiological environmental studies.
6. Creating a radiation map that includes measurement of all concentrations of radioactivity that all living creatures, especially humans, are exposed to. As well as realizing the permissible limits locally for the purpose of comparison with the globe researches.

REFERENCES

[1] R. Kaser, A. S. Dizman, F.K. Görür, "Determination of radioactivity levels of soil samples and the excess of lifetime cancer risk in Rize province, Turkey," Int. J. Radiat. Res., vol. 14, no. 3, pp. 237–244, 2016.

[2] H. H. Nemah , "Assessment of Uranium Concentration and Physiochemical Parameter of Groundwater of Najaf and Kufa cities," M.Sc. thesis, Kufa University, 2017.

[3] United Nations Scientific Committee on the Effects of Atomic Radiation. (1996). Sources and Effects of Ionizing Radiation, United Nations Scientific Committee on the Effects of Atomic Radiation (UNSCEAR) 1996 Report: Report to the General Assembly, with Scientific Annexes. United Nations.

[4] ICRP, International Commission on Radiological Protection ICRP publication 65, annual of the ICRP 23(2).Pergamon Press,

[5] J. G. Morse, "Nuclear Methods in Mineral Exploration and Production.," p. 293, 1977.

[6] R. A. Fathi, L. Y. Matti, H. S. Al-Salih, and D. Godbold, "Environmental pollution by depleted uranium in Iraq with special reference to Mosul and possible effects on cancer and birth defect rates," *Med. Confl. Surviv.*, vol. 29, no. 1, pp. 7–25,2013.

[7] S. A. Dewji and N. E. Hertel, Advanced Radiation Protection Dosimetry. CRC Press, 2019.

[8] S. S. Nayif, "Measurement of Radon Concentration in some schools' air in the City of Karbala using CN-85 and LR-115 Detectors,"M.Sc. thesis, Karbala University, 2018.

[9] O. H. Adnan, "Studying The Radioactivity Of oil products in middle and south region fields using gamma spectroscopy," M.Sc. thesis, Al-Mustansiriyah University, 2016.

[10] D. J. Lawi, "Alpha Particles Emissions in Some Samples of Medical Drugs in Iraq," M.Sc. thesis, Kufa University, 2018.

[11] M. I. Ojovan, W. E. Lee, and S. N. Kalmykov, An introduction to nuclear waste immobilisation., Third Edit. Elsevier, 2019.

[12] A. A. Ridha, “Determination of Radionuclides Concentrations in Construction Materials Used in Iraq,” Ph.D. thesis, AL-Mustansiriyah University, 2013.

[13] M. Tufail, N. Akhtar, and M. Waqas, “Radioactive rock phosphate: the feed stock of phosphate fertilizers used in Pakistan,” Health Phys., vol. 90, no. 4, pp. 361–370, 2006.

[14] R. L. Mahler and A. Hamid, “Evaluation of water potential, fertilizer placement and incubation time on volatilization losses of urea in two northern Idaho soils,” Commun. Soil Sci. Plant Anal., vol. 25, no. 11–12, pp. 1991–2004, 2008.

[15] A. Abbas, “Risk Assessment from Natural and Anthropogenic Radionuclides in Locally and Imported for some Foodstuff,”M.Sc. thesis, University of Baghdad, 2015.

[16] United Nations Scientific Committee on the Effects of Atomic Radiation. (2009). Sources and Effects of Ionizing Radiation, United Nations Scientific Committee on the Effects of Atomic Radiation (UNSCEAR) 2008 Report: Report to the General Assembly, with Scientific Annexes. United Nations.

[17] S. Aközcan, “Natural and artificial radioactivity levels and hazards of soils in the Kücük Menderes Basin, Turkey,” Environ. Earth Sci., vol. 71, no. 10, pp. 4611–4614, 2014.

[18] E. F.Salman, M. K. Muttelab and J. K. Manii, “Radioactivity Natural Environmental Radiation in Middle of Iraq Governorates,” Adv. Tech. Biol. Med. open, vol. 8, no. 2, pp. 1–4, 2020.

[19] E. F.Salman, “Natural Radioactivity of Rocks and Soils in Middle Euphrates Governorates- Middle of Iraq,” Ph.D. thesis, Babel University, 2019.

[20] A.A.Abojassim and L. H. Rasheed, “Natural radioactivity of soil in the Baghdad governorate,” Environ. Earth Sci., vol. 80, no. 1, 2021.

[21] K. T. Chang, “Geographic Information System,” Int. Encycl. Geogr., pp. 1–10. 2019.

[22] M. Shin, J. Campbell, and S. Burkhart “Essentials of Geographic Information Systems v2.1, 2017.

[23] B. Bhatta, Remote sensing and GIS, 3rd Edition. Oxford Academic, 2021.

[24] H. Mutuk, H. Gümüş, and S. Turhan, “Measurement of the terrestrial and anthropogenic

radionuclide concentrations in Bafra Kizilirmak delta (bird sanctuary) in Turkey," Radiat. Prot. Dosimetry, vol. 158, no. 3, pp. 350–354, 2014.

[25] B. A. Almayahi, N. F. Makki, S. A. Kadhim and A. H. Alasadi, "Natural Radioactivity Measurements in different regions in Najaf city, Iraq," Int. J. Comput. Trends Technol., vol. 9, no. 6, 2014.

[26] L. A. Najam, S. A. Younis and N. F. Tawfiq, "A Comparative Study of the Results of Natural Radioactivity and the Associated Radiation Hazards of Na(Tl) and HPGe Detectors," Int. J. Recent Res. Rev., vol. VIII, no. 2, pp. 1–9, 2015.

[27] L. Sahin, N. Hafızoğlu, H. Çetinkaya and K. Manisa, "Assessment of radiological hazard parameters due to natural radioactivity in soils from granite-rich regions in Kütahya Province, Turkey Latife," Isotopes Environ. Health Stud., vol. 53, no. 2, pp. 1–12, 2016.

[28] R. L. Njinga and V. M. Tshivhase, "Lifetime cancer risk due to gamma radioactivity in soils from Tudor Shaft mine environs, South Africa," J. Radiat. Res. Appl. Sci., vol. 9, no. 3, pp. 310–315, 2016.

[29] I. H. Kadhim and M. K. Muttaleb, "Measurement of radioactive nuclides present in soil samples of district Touirij of Karbala province for radiation safety purposes," Int. J. ChemTech Res., vol. 9, no. 8, pp. 228–235, 2016.

[30] A. manjeet, A. Kumar, S. Kumar, J. Singh, P. Singh, and B. S. Bajwa, "Assessment of natural radioactivity levels and associated dose rates in soil samples from historical city Panipat, India," J. Radiat. Res. Appl. Sci., vol. 10, no. 3, pp. 283–288, 2017.

[31] E.F.Salman, M. K. Muttelab, and J. K. Manii, "Assessment of radioactivity levels and its associated radiological hazards in soil of Babylon governorate middle of Iraq," J. Phys. Conf. Ser., vol. 1234, no. 1, 2019.

[32] A. A. Ibraheem, A. El-Taher, and M. H. M. Alruwaili, "Assessment of natural radioactivity levels and radiation hazard indices for soil samples from Abha, Saudi Arabia," Results in Physics, vol. 11. pp. 325–330, 2018.

[33] B. Lyngkhoi, “Estimation of Radiation Hazard Indices and Excess Lifetime Cancer Risk in Soil Samples of East Khasi Hills District of Meghalaya using Gamma Ray Spectroscopy,” 2018.

[34] M. K. Muttaleb, I. H. Kadhim ,A. A. Shakir and Z. A. Abed “Study of Radioactivity of Selected Samples of Soil in Amarah City, Maysan Province, Iraq,” *Eng. Technol. J.*, vol. 36, no. 2, pp. 136–141, 2018.

[35] A. M. Al-Qararaha, A. H. Almahasneha, D.Altarawneha and A. Jaffal “Investigation of radioactivity levels and radiation hazards in soil samples collected from different sites in Tafila Governorate, Jordan,” Jordan J. Phys. Artic. Investig., vol. 12, no. 2, pp. 153–161, 2019.

[36] O.A. Oyebanjo , O. Sowole , O.O. Oyebanjo , F. Ayedun , T.A. Adagunodo and E.O. Falayi “Assessment of Environmental Impact in Soil Samples from Selected Market Dumpsites in Ikorodu Metropolis, Lagos State, South Western Nigeria,” 3rd International Conference on Science and Sustainable Development (ICSSD): Journal of Physics: Conf. Series 1299, 2019, pp. 1–13.

[37] S. R. Yousif, A.A.Abojassim and A. Hayder “Mapping of Natural Radioactivity in Soil Samples of Badra Oil Field Project Using GIS Program” Radiobiol. Radioecol., vol. 20, no. 1, pp. 060–069, 2019.

[38] N. Maden, E. Akaryali, and M. A. Gücer, “Excess lifetime cancer risk due to natural radioactivity in Gümüşhane Province, NE Turkey,” Turkish J. Earth Sci., vol. 29, no. 2, pp. 347–362, 2020.

[39] E. Pudjadi, N. Urokhim and Kusdiana “Assessment of natural radioactivity levels in soil sample from Botteng Utara Village, Mamuju Regency Indonesia,” Journal of Physics: Conference Series, pp. 1–9,2020.

[40] C. C. Mbonu and U. C. Ben, “Assessment of radiation hazard indices due to natural radioactivity in soil samples from Orlu, Imo State, Nigeria,” Heliyon, vol. 7, no. 8, 2021.

[41] M. Zubair and A. Shafiqullah, “Measurement of natural radioactivity in several sandy-loamy soil samples from Sijua, Dhanbad, India,” Heliyon, vol. 6, no. 3, 2020.

[42] L. A. Najam and Z. N. Hamoo, “Natural Radioactivity for Soil Samples of Different Sites of Ancient Mosul,” Technol. Reports Kansai Univ., vol. 62, no. 3, pp. 979–987, 2020.

[43] P. Lamichhane, B. Rijal, P. Shrestha, and B. R. Shah, “Assessment of Environmental Radioactivity in Soil Samples from Kathmandu Valley, Nepal,” J. Nepal Phys. Soc., vol. 7, no. 2, pp. 89–96, 2021.

[44] S. F. Alhous, L. A. Alasadi, S. A. Kadhim,H. H. Hussein and R. M. Alkhafaji “Calculation of Radioactivity Levels for Various Soil Samples of Neighborhood AL-Rahmah (Iraq),” EM Int. , Pollut. Res., vol. 40, no. 1, pp. 53–57, 2021.

[45] A. A. Ibrahim, A. K. Hashim, and A.A.Abojassim, “Comparing of the natural radioactivity in soil samples of university at al-husseineya and al-mothafeen sites of kerbala, Iraq,” Jordan J. Phys., vol. 14, no. 2, pp. 177–191, 2021.

[46] I. Akkurt, K. Gunoglu, O. Gunay and M. Sarıhan, “Natural radioactivity and radiological damage parameters for soil samples from Cekmekoy-İstanbul,” Arab. J. Geosci., vol. 15, no. 53, pp. 1–11, 2022.

[47] M.S. Karim, E.M. Mnawer , F.I.Abbas and M. H. Abdallah, “Determination of alpha particles concentrations in soil Samples taken from area situated in Anbar governorate by using nuclear track detector (CR-39),” Dayala J. pure Sci., vol. 8, no. 4, pp. 88–94, 2012.

[48] S. S. Shafik, A. H. Al-Mashhadani and M. A. Saeed, “Uranium Concentration in Soil of some Eastern Iraqi Regions using Nuclear Track Detector (CR-39),” Asian Journal of Applied Science and Engineering, vol. 3, no. 9. pp. 61–71, 2014.

[49] K. H. Abass, B. Y. Mohammed, A. N. Rehem, “Measurement of Soil-Gas Radon in Some Areas of Iraq Using Nuclear Track Detector CR-39,” Int. Lett. Chem. Phys. Astron., vol. 53, pp. 90–94, 2015.

[50] S. S. Fleifil and T. M. Salman, “Estimation of Boron Concentration in Soil Samples in Al-Zubair, Abu-khasib and Al-mdiana districts of Basrah governorates using SSNTDs Techniques,” Adv. Appl. Sci. Res.Libr., vol. 7, no. 4, pp. 42–46, 2016.

[51] A.A.Abojassim, “Alpha particles concentrations from some soil samples of al-najaf (Iraq),” Polish J. Soil Sci., vol. L/2, pp. 249–263, 2017.

[52] H. N. Azeez , M. H. Kheder, M. Y. Slewa and Y. Sleeman. “Radon Concentration Measurement in Ainkawa Region Using Solid State Nuclear Track Detector,” Iraqi J. Sci., vol. 59, no. 1B, pp. 482–488, 2018.

[53] K. M. Thabayneh, “Determination of radon exhalation rates in soil samples using sealed can technique and CR-39 detectors,” J Environ Health Sci Engineer ,vol. 16, no.2, pp. 121–128, 2018.

[54] A. Elzain, H. Idriss, Y. S. Mohammed, K. S. Mohamed, M. A. Ali, M. S. Elkhalig, I. Salih, A. K. Sam, M. H. Eisa, S. S. Mahmoud and M. K. Massoud, “Assessment of radioactivity from selected soil samples from Halfa Aljadida area, Sudan,” Radiochim. Acta, vol. 107, no. 6, pp. 489–502, 2019.

[55] M. H. Kheder, “Measurement of Radon Concentration Using SSNTD in Bartella Region,” Al-Mustansiriyah Journal of Science, vol. 29, no. 4. p. 110, 2019.

[56] M. H. Kheder, H. N. Azeez , M. Y. Slewa and T. A. Zaker “Determination of Uranium Contents in Soil Samples in Al-Hamdaniya Region Using Solid State Nuclear Track Detector CR-39,” Al-Mustansiriyah J. Sci., vol. 30, no. 1, pp. 194–201, 2019.

[57] W. M. Shakir, R. T. Mehdi and B. K. Rejah “Detecting the Possibility of Soil Pollution with Radon Emissions for an Area Located within Baghdad University Campus- AL-Jadiriyah,” Iraqi J. Sci., vol. 60, no. 9, pp. 1985–1996, 2019.

[58] D. A. Salim and S. A. Ebrahiem “Measurement of Radon concentration in College of Education, Measurement of Radon concentration in College of Education, Ibn Al-Haitham buildings using Rad-7 and CR-39 detector ", 15th International Symposium on District Heating and Cooling Ibn Al- Haith,” Energy Procedia, vol. 157, pp. 918–925, 2019.

[59] S. Ş. Bal and M. Doğru “Evaluation of Soil Radon Gas and Earthquake on the Fault Zone,” BEU J. Sci., vol. 9, no. 2, pp. 703–710, 2020.

[60] H. S. Mustafa , M. H. Kheder and S. G. Mahmood “Hermite Numerical Method to Estimate the Radon and Radium Effects of the Soil in Bartella Region,” Eureka Phys. Eng., no.2, 2020.

[61] M. G. Al-Gharabi and A. A. Al-Hamzawi “Measurement of Radon Concentrations and Surface Exhalation Rates using CR-39 detector in Soil Samples of Al-Diwaniyah Governorate, Iraq,” Iran. J. Med. Phys., vol. 17, no. 4, pp. 220–224, 2020.

[62] E. F. Salman, “Evaluation of Alpha Particles Concentration and Exhalation Rate in Soil Samples in Kifle City/Iraq,” Adv. Tech. Biol. Med. open, vol. 9, no. 2, pp. 1–4, 2021.

[63] A. K. Hasan, A. R. H. Subber “Measurement of Radon Concentration in Soil Gas using RAD7 in the Environs of Al-Najaf Al-Ashraf City-Iraq,” Pelagia Res. Libr. Adv. Appl. Sci. , vol. 2, no. 5, pp. 273–278, 2011.

[64] A.A.Abojassim, Q. S. Jabar, A. H. Al.Mashhadani and A. A. Al.Bayati "Measurement of radon and thoron concentrations of soil- gas in Al-Kufa city using RAD-7 detector,” Iraqi J. Phys., vol. 10, no. 19, pp. 110–116, 2012.

[65] R. Mehra and B. Pankaj, “Estimation of annual effective dose due to Radon level in indoor air and soil gas in Hamirpur district of Himachal Pradesh,” J. Geochemical Explor., vol. 142, pp. 16–20, 2014.

[66] R. Avikumar, D. Davis, S. Shekar, R.K and P. Rakash, “Measurement of radon activity in soil gas using RAD7 in the Environs of Chitradurga District, Karnataka, India,” Elixir Earth Sci., vol. 80, pp. 31078–31082, 2015.

[67] Y. M. Z. Al-bakhat, N. H. K. Al-Ani, B. F. Mohammed, N. H. Ameen and Z. A. Jabar, “Measurement of Radon Activity in Soil Gas and the Geogenic Radon Potential Mapping Using RAD7 at Al-Tuwaitha Nuclear Site and the Surrounding Areas Yousif,” Radiat. Sci. Technol., vol. 3, no. 3, pp. 29–34, 2017.

[68] M.A. Hassan and O. A. Ibrahim, “Measurements of radon gas concentration in surface soil in Baghdad city,” Iraqi J. Phys., vol. 16, no. 37, pp. 73–78, 2018.

[69] A. A. Sharrad and A. K. Farhood, “Radon Concentration Measurements in Soil Gas of Sawa Lake, Samawa City – South of Iraq,” Int. J. Adv. Res., vol. 7, no. 6, pp. 170–177, 2019.

[70] M. O. Isinkaye and Y. Ajiboye , “Correlations of ^{226}Ra and ^{222}Rn activity concentrations in surface soil and groundwater of basement complex geological area of southwest Nigeria,” SN Appl. Sci., vol. 2, no. 6, pp. 1–8, 2020.

[71] I. Yashodhara, N. Karunakara, K. S. Kumar, R. M. Tripathi, “Radiation levels and radionuclide distributions in soils of the gogi region, a proposed uranium mining region in north Karnataka,” Radiat. Prot. Environ., vol. 34, no. 4, pp. 267–269, 2011.

[72] S. Monica, A.K.V. Prasad, S.R. Soniya“Estimation of indoor and outdoor effective doses and lifetime cancer risk from gamma dose rates along the coastal regions of Kollam district, Kerala,” Radiat. Prot. Environ., vol. 39, no. 1, pp. 38–43, 2016.

[73] A. H. Alasadi, A. S. Alaboodi, L. A. Alasadi, and A.A. Abojassim, "Survey of Absorbed Dose Rates in air of Buildings Agriculture and Sciences in University of Kufa at Al-Najaf Governorate, Iraq", vol. 8, no. 4. pp. 1388–1392,2016.

[74] S. P. Gautam, A. Silwal, S. Acharya and B. Aryal “Annual Effective Dose from Natural Background Radiation in Pokhara, Nepal ,” Asian J. Res. Rev. Phys., vol. 3, no. 2, pp. 36–42, 2020.

[75] P. O. Olagbaju, I. C. Okeyode, O. O. Alatise, and B. S. Bada, “Background radiation level measurement using hand held dosimeter and gamma spectrometry in Ijebu-Ife, Ogun State Nigeria,” Int. J. Radiat. Res., vol. 19, no. 3, pp. 591–598,2021.

[76] L. A. Alasadi, Gamma Background Radiations and Measurements with Applications. IntechOpen, 2019.

[77] S. Turhan, E. Goeren, M. Karatasli, Z. Yegingil, and F. A. Ugur, “Study of the radioactivity in environmental soil samples from Eastern Anatolia Region of Turkey,” Radiochim. Acta, vol. 106, no. 2, pp. 161–168, 2018.

[78] M. B. H. Al-Bedri, H. A. Arar and W. O. Hameed , “Determination of Natural Radioactivity Levels in Surface Soils of Old Phosphate Mine at Russaifa of Jordan,”

Int. J. Phys. Res., vol. 4, no. 3, pp. 31–38, 2014.

[79] M. Hassan, Y. H. Ngadda and A. Adamu "Health Risk Assessment of Radionuclides in Soil and Sediments of some Selected Areas of Pindiga, Nigeria," J. Radiat. Nucl. Appl., vol. 5, no. 2, pp. 95–103, 2020.

[80] G. K. Skinner, "Practical gamma-ray spectrometry," Spectrochimica Acta Part A: Molecular and Biomolecular Spectroscopy, vol. 52, no. 3. p. 379, 1996.

[81] E. K. Abbas, "A study of Natural Radiation in the Soil of Najaf Province," M.Sc., University of Kufa, 2011.

[82] A. K. Ekal , "Measurement Of Natural Radiation Level In Some Local and Imported Building Materials,",M.Sc., University of kufa, 2011.

[83] O. C. Avwiri and G. Tutumeni, "Measurement of Natural Radioactivity and Evaluation of Radiation Hazards in Soil of Abua/Odual Districts Using Multivariate Statistical Approach," British Journal of Environmental Sciences, vol. 4, no. 35. pp. 35–48, 2016.

[84] V. S. Shirley, E. Browne, and C. M. (Charles M. Lederer, Table of isotopes. Wiley, 1978.

[85] C. Cremer and B. R. Masters, "Resolution enhancement techniques in microscopy," Eur. Phys. J. H 2013 383, vol. 38, no. 3, pp. 281–344, 2013.

[86] G. Gilmore, "Interactions of Gamma Radiation with Matter," in Practical Gamma-Ray Spectrometry, John Wiley& Sons, Ltd., 2011, pp. 24–38.

[87] G. S. Bineng, S. Tokonami, M. Hosoda, Y. F. T. Siaka, H. Issa, T. Suzuki and O. Bouba "The Importance of Direct Progeny Measurements for Correct Estimation of Effective Dose Due to Radon and Thoron," Front. Public Heal., vol. 8, no. 17, pp. 1–12, 2020.

[88] S. A. Durran and R. Ilic, Radon Measurements by Etched Track Detectors/Applications in Radiation Protection, Earth Sciences and the Environment. Engand, Slovenia: Default Book Series, 1997.

[89] J. E. Gingrich, "Radon as a geochemical exploration tool," J. Geochemical Explor., vol.

21, no. 1–3, pp. 19–39, 1984.

[90] E. J. Mohammed, “Radon Concentrations in some Soil and Air Samples of Dwellings in Karbala City and Influencing Factors on Lung Cancer Risks Using CR-39,”, M.Sc., Karbala University, 2016.

[91] S. S. Nayif, “Measurement of Radon Concentration in the air of some Schools in the City of Karbala using CN-85 and LR-115 Detectors,” M.Sc.,Karbala University, 2018.

[92] H. Zeeb, F. Shannoun, and W. H. Organization, WHO handbook on indoor radon: a public health perspective. World Health Organization, 2009.

[93] A. F. Nadir, N. H. Al-Hashimi and A. H. Subber, “Theoretical and Experimental Study To Evaluate Natural Radioactivity Applied on a Selected Area in Basrah Governorate (Zubair),” M.Sc., Basrah University, 2015.

[94] G. R. Choppin and P. J. Wong, “The Chemistry of Actinide Behavior in Marine Systems,” Aquat. Geochemistry, vol. 4, no. 1, pp. 77–101, 1998.

[95] E. Hodgson, P. E., Gadioli, E. and Gadioli-Erba, “Introductory Nuclear Physics Oxford Science Publications ,(1997).

[96] J. Edward and J. Turner, "Atoms, radiation, and radiation protection". Wiley-VCH, 2007.

[97] S. Lee, G. Tewolde, and J. Kwon, “Design and implementation of vehicle tracking system using GPS/GSM/GPRS technology and smartphone application,” 2014 IEEE World Forum Internet Things, pp. 353–358, 2014.

[98] S. Bhatt, “Biological Effects of ^{224}Ra,” UCMS, Delhi University,1978.

[99] C. E. Crouthamel, F. Adams, R. Dams, R. Belcher and H. Freiser, Applied Gamma-Ray Spectrometry (International series of monographs in analytical chemistry, v. 41), 2013.

[100] A.A.Abojassim, R. H. Hashim, and N. S. Mahdi, “Basics of Nuclear Radiation,” Basics Nucl. Radiat., pp. 1–86, 2021.

[101] T. Pochet, “Nuclear detectors. Physical principles of operation,” Tech. l’Ingenieur.

Genie Nucl., vol.2, no.188, pp. 1-13, 2005.

[102] C. Grupen, “Introduction to Radiation Detectors,” in In digital Encyclopedia of Applied Physics, Wiley, 2009, pp. 1–26.

[103] Wikimedia, “Detectors summary,” wikimedia.org. https://commons.wikimedia.org/wiki/File:Detectors_summary_3.png#file.

[104] J. Izewska and G. Rajan, “Review of Radiation Oncology Physics: A Handbook for Teachers and Students; Chapter 3 - Radiation Dosimeters,” International Atomic Energy Agency, 2012, pp. 71–99.

[105] “Radiation survey meter - Stock Image - C023/3924 - Science Photo Library.” https://www.sciencephoto.com/media/640792/view.

[106] N. Tsoulfanidis and S. Landsberger, “Measurement detection of radiation,” Measurement and Detection of Radiation, 4th edition , pp. 1–563, 2015.

[107] S. Durrani and R. Adomirilic, “Solid Statenuclear track Detectors,” Handbook of Radioactivity Analysis, Second Edition, Elsevier Science, 2003, p. 179.

[108] C. W. Fabjan, “Collider Detectors for Multi-TeV Particles,” Encyclopedia of Physical Science and Technology, Academic Press, 2003, pp. 253–268.

[109] K. P. Eappen and Y. S. Mayya, “Factors affecting the registration and counting of alpha tracks in solid state nuclear track detectors,” Indian J. Phys., vol. 83, no. 6, pp. 751–757, 2009.

[110] C. P. Bean, M. V. Doyle, and G. Entine, “Etching of submicron pores in irradiated mica,” J. Appl. Phys., vol. 41, 1970.

[111] Durridge Company Inc, “Durridge RAD7 User Manual,” 2015. https://www.manualslib.com/manual/1158422/Durridge-Rad7.html#manual.

[112] V. K. Fouad, F.A. Saffa and S. Issakian, “Geological Map of Iraq, Scale 1: 1000 000, 4th Edition, 2012,” Papers of the Scientific Geological Conference , part 2, 2015, vol. 11, no. 1, pp. 9–16.

[113] A. K. Hussein, N. A. Kadhim, A. S. Jaber, and A.A.Abojassim, "Water Quality Index for Surface Water Assessment by Using Gis Techniques, Alnajaf, Kufa, Iraq," Materials Science and Engineering,2nd International Scientific Conference of Al-Ayen University, 2020, vol. 928, no. 7.

[114] Z. A. Al-Taghlubi and S. I. Al-Hassen, "A Geographical Analysis of the Light Pollution in Residential Districts in Najaf City Sources and Registered Levels," Iraq Acad. Scintific Journal, vol. 1, no. 44, pp. 453–476, 2020.

[115] S. K. Lafta, A.A.Abojassim and H. A. Ali, "Monthly monitoring of physicochemical and radiation properties of Kufa River, Iraq," Pakistan J. Sci. Ind. Res. Ser. A Phys. Sci., vol. 61, no. 1, pp. 43–50, 2018.

[116] G. S. Abid and A.N. Rasheed, "Spatial Analysis of Urban Land Uses in Al - Kufa City," M.Sc. thesis, Kufa University, 2014.

[117] A. D. Miall, The geology of fluvial deposits: sedimentary facies, basin analysis, and petroleum geology, 4th edition, Spriger, 2013.

[118] Sander and Breur, "The performance of NaI(Tl) scintillation detectors," M.Sc. thesis, University of Amsterdam, 2013.

[119] B. A. Almayahi, A. A. Tajuddin, and M. S. Jaafar, "Radiation hazard indices of soil and water samples in Northern Malaysian Peninsula," Appl. Radiat. Isot., vol. 70, no. 11, pp. 2652–2660, 2012.

[120] B.U. Nwaka, H.U. Emelue and C. Nwokocha "Natural radiation levels and health hazard indices of soil in Owerri Nigeria," Int. J. Eng. Sci., vol. 3, no. 12, pp. 5–9, 2014.

[121] M. A. Kobeissi, O. El Samad, K. Zahraman, S. Milky, F. Bahsoun, and K. M. Abumurad, "Natural radioactivity measurements in building materials in Southern Lebanon," J. Environ. Radioact., vol. 99, no. 8, pp. 1279–1288, 2008.

[122] A.A.Abojassim, "Comparative study between active and passive techniques for measuring radon concentrations in groundwater of Al-Najaf city, Iraq," Groundw. Sustain. Dev., vol. 11, 2020.

[123] G. R. Moss, A. P. Fews, D. L. Henshaw, and M. F. Hansen, “A high sensitivity nvlap-accredited neutron dosimetry system.”

[124] A. A. Marza , M. A. Al-Shareefi, A. A. Abojassim, “Uranium Concentrations and Some Physicochemical Parameters of Water Samples at Marshes (Ahwar) in Dhi-Qar Governorate,” Water, Air, Soil Pollut. 2021 *2324*, vol. 232, no. 4, pp. 1–15, 2021.

[125] A. A. Abojassim, “Assessment of Radiation Hazard Indices and Excess Life time Cancer Risk due to Dust Storm for Al-Najaf, Iraq,” WSEAS Trans. Environ. Dev., vol. 10, pp. 312–319, 2014.

[126] A. A. Abojassim, “Estimation of Human Radiation Exposure from Natural Radioactivity and Radon Concentrations in Soil Samples at Green Zone in Al-Najaf, Iraq,” Iranian (Iranica) Journal of Energy & Environment, vol. 8, no. 3. pp. 239–248, 2017.

[127] K. Manai, C. Ferchichi, M. Oueslati, and A. Trabelsi, “Gamma Radiation Measurements in Tunisian Marbles,” World Journal of Nuclear Science and Technology, vol. 02, no. 03. pp. 80–84, 2012.

[128] A.A. Abojassim, M. H. Oleiwi, and M. Hassan, “Natural radioactivity and radiological effects in soil samples of the main electrical stations at Babylon Governorate,” Nuclear Physics and Atomic Energy, vol. 17, no. 3. pp. 308–315, 2016.

[129] A. A. Abojassim, “Evaluation of Radiation Hazard Indicesduo to Gamma Radiation in Hattin Complex at Babylon Government,” Middle East J. Sci. Res., vol. 24, no. 7, p. 2196, 2016.

[130] C. Okogbue and M. Nweke, “The ^{226}Ra, ^{232}Th and ^{40}K contents in the Abakaliki baked shale construction materials and their potential radiological risk to public health, southeastern Nigeria,” J. Environ. Geol., vol. 02, no. 01, 2018.

[131] A. M. Ali, A. A. Abojassim and F. A.Majeed, “Radiological risk due to naturally occurring radioactive materials in the soil of Al-Samawah desert, Al-Muthanna Governorate, Iraq,” Iran. J. Med. Phys., vol. 16, no. 5, pp. 323–328, 2019.

[132] A. A. Abojassim, A. R. Shltake, L. A. Najam and I. R. Merza “Radiological parameters

due to radon-222 in soil samples at Baghdad Governorate (Karakh), Iraq.," Pakistan J. Sci. Ind. Res. A Phys. Sci., vol. 60, no. 2, pp. 72–78, 2017.

[133] A. A. Mowlavi, M. R. Fornasier, A. Binesh, and M. De Denaro, "Indoor radon measurement and effective dose assessment of 150 apartments in Mashhad, Iran," Environ. Monit. Assess. 2011 1842, vol. 184, no. 2, pp. 1085–1088, 2011.

[134] N. F. Tawfiq, N. O. Rasheed, and A. A. Aziz, "Measurement of Indoor Radon Concentration in Various Dwellings of Baghdad Iraq," Int. J. Phys., vol. 3, no. 5, pp. 202–207, 2015.

[135] D. S. Azam, A.Naqvi and A. H. Srivastava, "Radium concentration and radon exhalation measurements using LR-115 type II plastic track detectors," Nucl. Geophys., vol. 9, no. 6, pp. 653–657, 1995.

[136] M. S. Khan, M. Zubair, D. Verma, A. H. Naqvi, A. Azam, and M. K. Bhardwaj, "The study of indoor radon in the urban dwellings using plastic track detectors," Environ. Earth Sci., vol. 63, no. 2, pp. 279–282, 2011.

[137] M. S. Khokhar, R. S. Kher, V. B. Rathore, S. Pandey, and T. V. Ramachandran, "Comparison of indoor radon and thoron concentrations in the urban and rural dwellings of Chhattisgarh state of India," Radiat. Meas., vol. 43, no.1, 2008.

[138] M. P. Campo and E. W. Martins, "Calibration of solid state nuclear track detector CR-39 for radon measurements," Int. Nuclear Atlantic Conf. - inac. Santos, SP, Brazil, 2007 Vol.39, no.40.

[139] A. J. Khan, A. K. Varshney, R. Prasad, R. K. Tyagi, and T. V. Ramachandran, "Calibration of a CR-39 plastic track detector for the measurement of radon and its daughters in dwellings," Int. J. Radiat. Appl. Instrumentation. Part D. Nucl. Tracks Radiat. Meas., vol. 17, no. 4, pp. 497–502, 1990.

[140] R. L. Grasty, "Radon emanation and soil moisture effects on airborne gamma-ray measurements," Geophys. J., vol. 62, no. 5, pp. 1379–1385, 2012.

[141] A. K. Hashim, L. A. Najam, F. M. Aljomaly, "Contribution of soil in the annual effective dose due to radon in the air of some dwellings in the city of Karbala, Iraq,"

Pol. J. Med. Phys. Eng.vol.27, no.3,pp.233-239,2021.

[142] A. .H. Subber, N. H. Al-Hashmi, A. F. Nader, J. H. Jebur and M. K. Khodier "Constructasa simple radon chamber for measurement of radon detectors calibration factors," Pelagia Res. Libr. Appl. Sci. Res., vol. 6, no. 2, pp. 128–131, 2015.

[143] A. Al-bayati and A. A. Abojassim, Radon and Thoron Concentrations Measurement in Al-Najaf and Al-Kufa Area, Lambert, 2014.

[144] UNSCEAR. (2009). Sources and Effects of Ionizing Radiation, United Nations Scientific Committee on the Effects of Atomic Radiation (UNSCEAR) 2008 Report: Report to the General Assembly, with Scientific Annexes. Vol. I: sources, vol II: Effects, New York, 1-17.

[145] B. Eke and H. Emelue, "Measurement of background ionizing radiation in the federal university of technology owerri, Nigeria using calibrated digital geiger counter," Int. J. Phys. Res. Appl., vol. 3, no. 1, pp. 070–074, 2020.

[146] P. C. Okoye and G. O. Avwiri, "Evaluation of background ionising radiation levels of braithwaite memorial specialist hospital Port Harcourt, Rivers State," Am. J. Sci. Ind. Res, vol. 4, no. 4. pp. 359–365, 2013.

[147] "Radiological protection principles concerning the natural radioactivity of building materials."Eropean Commission, 2000.

[148] Nuclear Energy Agency, "Exposure to radiation from the natural radioactivity in building materials," 1979.

[149] "ICRP, International Commission on Radiological Protection publication 65, Annual of the ICRP 23(2). Pergamon Press, Oxford. 1993.

[150] H. Zeeb and F. Shannoun. Who Handbook on Indoor Radon a Public Health Perspective, Department of Public Health and Environment, 2009.

[151] United Nations. Scientific Committee on the Effects of Atomic Radiation., "Sources,

effects and risks of ionizing radiation : UNSCEAR 2016 report to the General Assembly, with scientific annexes."

[152] United Nations. Scientific Committee on the Effects of Atomic Radiation., "Sources, effects and risks of ionizing radiation : UNSCEAR 1 report to the General Assembly, with scientific annexes."

[153] J. M. Samet ,National Academies of Sciences, Engineering, and Medicine. 1999. "Health Effects of Exposure to Radon": BEIR VI. Washington, DC: The National Academies Press, Washington, D.C.1999.

[154] S. Zwillinger and D. Kokoska, Standard Probability and Statistics Tables and Formulae, 3rd edition. Boca Raton : Chapman & Hall/CRC, 2019.

[155] J. S. Kim and R. Dailey, Biostatistics for oral healthcare. Blackwell Munksgaard, 2008.

Competing Interests

The authors have declared that no competing interests exist.

Biography of editors

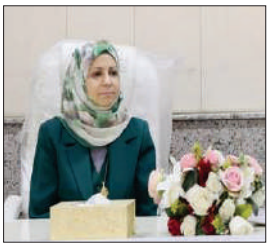

Prof. Dr. Lubna Abdulrasool Mahdi AlAsadi
University of Kufa, Faculty of Science, Department of Physics, Al-Najaf, Iraq.

She has been working at the Department of Physics at the University of Kufa since 2006. She completed B.SC in Physics from the University of Kufa College, Science Department of Physics (2004), M.SC in Nuclear Physics from the University of Kufa College, Science Department of Physics (2011), and got a scholarship to Dalhousie University in Canada, and a PhD in Nuclear Physics from the University of Kufa College of Education for Girls, Department of Physics (2022). Her research interests focus on natural and anthropogenic nuclear radiation emitted from natural sources such as soil, water, and air, as well as various foods that enter the human body through ingestion or inhalation. She also had many published papers in Local and international journals, and reviewed many papers.

Prof. Dr. Ali Abid Abojassim
University of Kufa, Faculty of Science, Department of Physics, Al-Najaf, Iraq.

He has been working at the University of Kufa, Department of Physics, since 2006. He completed a B.Sc. in Physics from the University of Kufa, College of Science, Department of Physics (2003), an M.Sc. in Nuclear Physics from the University of Babylon, College of Science, Department of Physics (2006), and PhD in Nuclear Physics and Environmental Science from Baghdad College, College of Science, Department of Physics (2013). His research areas include nuclear physics and the Environment. He is the best reviewer in many world conferences and journals. He is the editor of many local and international scientific journals. He has published 180 Papers in the national and international journals.